Title
Modulating the local microenvironment around type 1 diabetes implants

Author
Chendke, Gauree Shriram

Publication Date
2023

Peer reviewed|Thesis/dissertation

Modulating the local microenvironment around type 1 diabetes implants

by

Gauree Shriram Chendke

DISSERTATION

Submitted in partial satisfaction of the requirements for degree of

DOCTOR OF PHILOSOPHY

in

Bioengineering

in the

GRADUATE DIVISION

of the

UNIVERSITY OF CALIFORNIA, SAN FRANCISCO
AND
UNIVERSITY OF CALIFORNIA, BERKELEY

Approved:

DocuSigned by:
Tejal A. Desai
5D917BC35F4B4A0...

Tejal A. Desai

Chair

DocuSigned by:
Julie B. Sneddon

Julie B. Sneddon

DocuSigned by:
Phillip B. Messersmith
DC0BCACA0AAD459...

Phillip B. Messersmith

Committee Members

Dedication and Acknowledgements

I would not have been able to earn my Ph.D. without the endless support of my mentors, friends, and family. I'm sincerely grateful for each one of you and for the faith you've had in me.

First and foremost, I would like to express my heartfelt gratitude to my advisor, Dr. Tejal Desai, for her invaluable guidance and support throughout my PhD. Since I first met her in 2016, she has been an inspiration and role model to me. I am particularly grateful to Tejal for providing me with countless opportunities to develop my research skills and showing confidence in my abilities, especially when I didn't have confidence in myself. In addition to her mentorship, Tejal has also been a compassionate and understanding advisor. She has provided me with emotional support and guidance during difficult times and has helped me with my professional and personal growth. I am grateful for her kindness and generosity and feel privileged to have had her as my advisor.

I sincerely appreciate my qualifying exam committee members, Dr. Shuvo Roy, Dr. Kevin Healy, Dr. Todd McDevitt, Dr. Julie Sneddon, and my thesis committee, Dr. Phil Messersmith and Dr. Julie Sneddon. Their guidance, support, and expert feedback have significantly contributed to my research and academic development throughout this journey. A special thank you goes to Julie, who has consistently believed in me over the past six years, provided invaluable advice, and genuinely cared about my well-being.

Being a part of the Desai lab for the past 6 years has been an unforgettable experience. I'm thankful for the friendships I made when I first joined the lab as a lab manager. Thank you, Long Le, for being a great teacher and fantastic friend, bringing me containers filled with homemade frosting (especially the pumpkin one), and continuing to

host Priya and me for random dinners. Liz Levy, thank you for being an amazing friend, for always reaching out and checking in on me, helping me, and for peer-pressuring me to face my fear of dogs by making me hang out with Leia. You are the reason I can comfortably walk past dogs (sort of). Karen Samy, I'm grateful for my friendship with you, your positive outlook, your infectious laughter, and my nickname "GaurGaur," which you and Liz still use after all these years. I thank Joel Finbloom for being a mentor and a close friend. I truly appreciate your time mentoring me, advising me on my professional and personal problems, making that amazing banana ice cream to celebrate my quals, and our happy hours. Will Lykins, I will finally say: Nothing sucks right now. Thank you for always encouraging me and being incredibly kind. I'm thankful to mentors like Joel, Dan Bernards, Jean Kim, and Xiao Huang for their guidance in planning and troubleshooting experiments. Thank you to all these "old Desai lab" members for cultivating a positive, happy, and fun lab environment and motivating me to pursue a PhD and join the Desai lab as a graduate student.

From the "new Desai lab," i.e., Desai lab after I joined as a graduate student, I would like to thank Darnell Cuylear. Thank you for being an incredibly supportive friend, a great listener and advice-giver for science and non-science issues, sending me good music and TV show recommendations, and genuinely caring about me and our friendship. Thank you also for always being down to get coffee, boba, drinks, or dessert, even when it's raining hard and we don't have umbrellas. I promise I will watch the TV show Dark one day. Preethi Raghavan, also known as my twin, thank you for joining the lab and becoming one of my closest friends in a short period of time. It's crazy how similar we are, looks and personality-wise, and I'm extremely thankful for your sense of humor,

kindness, support, TV choices, and gifting me homemade ghee and 1lb of frosting. I'll miss doing a double take every time I see you in lab because I thought you were me. I can't wait to watch you grow and celebrate your accomplishments. Justin Zhong, thank you for your help with science, for being a great listener, for teaching me how to make green Thai curry, and for setting a great example of discipline, especially regarding physical activity. Cynthia Perez, thank you so much for being a great friend and empathetic listener. I truly admire your resilience and strength and genuinely hope there are no more difficulties that come your way. Lastly, I would like to thank Bhushan Kharbikar for his support, kindness, willingness to help everyone, and passion for science. I'm genuinely grateful to be a part of the Desai lab and to have the opportunity to meet such inspiring scientists and create lifelong friendships.

I also want to thank Priya Mohindra, my biggest advocate, who is practically like a sister to me. It's not an exaggeration to say I would not receive my PhD had it not been for Priya. From reading my personal statements for graduate school applications to celebrating my PhD graduation to consoling me after rough days, Priya has supported and encouraged me at every turn. I cannot thank you enough for selflessly helping me achieve my goals, believing in me, and paving the path. You are an amazing scientist, a loyal friend, and one of the kindest humans I've met. I will cherish all the great memories we created and our good laughs, from sneaking out to go to Tartine, walking across SF to get Halal Guys, crying in Café 24, and spending hours FaceTiming and just hanging out. Your friendship means the world to me, and I cannot wait for our future life adventures.

Most importantly, I would also like to thank and dedicate my PhD to my parents and sister. Everything I do and will do is to make the three of you proud. Even though my parents had no family or friends in the US, my parents made the brave decision to move here so that my sister and I get the best education. Their sacrifice, unconditional love, and unwavering support are why I am who I am today. Baba, thank you for setting the best example and instilling the importance of education. Even when I'm worked up about things not going my way in lab, you've always been there to calm me down and help me see things logically. Your hard work, your determination, your sincerity, your passion for learning, and your love for your family are qualities I strive for. Mama, words cannot describe how grateful I am to you. You've experienced all the ups and downs of my entire PhD journey through my constant complaints and venting sessions. Thank you for somehow always knowing precisely what I need, even when I don't know it myself. You've taught me to be strong, kind, stand up for myself and others, forgive, and love and care for others and myself. Tai, I'm thankful you are my role model and biggest protector. I've always tried to be an intelligent, caring, self-sufficient, sociable, and strong person like you, and I'm glad we have a lifetime together for me to learn from you. Thank you for paving the path, for being the first person in our family to take big risks, for allowing me to learn from your mistakes, for guiding me in the right direction, and for protecting me from everything (including my parents). I know I have nothing to worry about as long as I have you.

Lastly, I would like to thank Abhinav Vadrevu, my partner and best friend, for being my constant source of support and the reason behind my happiness. Your encouragement after the rough lab days, unwavering patience even after I make you wait

for at least 45 minutes because of lab mishaps, and love have shown me that you will always be in my corner, no matter what. Thank you for believing in me and for always being there when I needed you the most. You've selflessly devoted hours to helping me with everything – from crafting delicate emails to driving me home from Parnassus to editing my resume and meal prepping for me because I was busy (or sometimes just lazy). I am incredibly fortunate to have you by my side. I'm thankful for your parents, who have always been incredibly kind and supportive of my research, and for Amulya and Akshay, with whom we have created so many fun memories during our various trips. You have made my grad school experience unforgettable, and I can't wait to spend the rest of our lives together.

Contributions

Chapter 1 was adapted from “Modulating the Foreign Body Response of Implants for Diabetes Treatment,” a work published in Advance Drug Delivery Reviews in 2021 and authored by Bhushan N. Kharbikar, Gauree S. Chendke, and Tejal A. Desai. Chapter 2 was modified from “Supporting Survival of Transplanted Stem-Cell-Derived Insulin-Producing Cells in an Encapsulation Device Augmented with Controlled Release of Amino Acids,” published in Advanced Biosystems in 2019 and authored by Gauree S. Chendke, Gaetano Faleo, Charity Juang, Audrey V. Parent, Daniel A. Bernards, Matthias Hebrok, Qizhi Tang, and Tejal A. Desai. Chapter 3 is modified from “Replenishable Prevascularized Cell Encapsulation Devices Increase Graft Survival and Function in the Subcutaneous Space,” published in Bioengineering and Translational Medicine in 2022 and authored by Gauree S. Chendke, Bhushan N. Kharbikar, Sudipta Ashe, Gaetano Faleo, Julie B. Sneddon, Qizhi Tang, Matthias Hebrok, and Tejal A. Desai.

Modulating the local microenvironment around type 1 diabetes implants

Gauree S. Chendke

Abstract

Type 1 diabetes (T1D) is an autoimmune disease characterized by destroying insulin-producing beta cells within the pancreas, leading to high blood glucose levels and various complications. Cell encapsulation devices offer a promising approach to treating T1D by protecting insulin-producing cells from immune attack while restoring endogenous insulin production. However, their effectiveness is limited by inadequate cell survival due to the foreign body response that results in insufficient vasculature and inflammation at the implantation site. This thesis aims to improve the performance of cell encapsulation devices by addressing these challenges.

Chapter 1 discusses the foreign body response and fibrosis in response to implantable devices for diabetes treatment, providing insights into molecular mechanisms, cellular interactions, and strategies for long-term success. The thesis then examines techniques to optimize cell encapsulation devices for T1D. Chapter 2 focuses on developing an innovative encapsulation device designed to improve the survival of encapsulated stem cell-derived insulin-producing cells within the poorly vascularized subcutaneous space. The device features an internal compartment that steadily releases the essential nutrients alanine and glutamine over several weeks, increasing post-transplantation cell survival by 30% in the subcutaneous space.

Chapter 3 presents a novel, replenishable, pre-vascularized implantation methodology (RPVIM) aimed at promoting vascular integration around the implant and enhancing nutrient supply to encapsulated cells. The findings reveal that over 75% of

RPVIM devices containing insulin-producing cells survive after 28 days of implantation in the subcutaneous space. Importantly, RPVIM devices outperform other implantation methodologies in terms of survivability and maintain the functionality of encapsulated insulin-producing beta cell clusters, which is a critical factor in successful T1D management.

Lastly, Chapter 4 explores the impact of surface topography on macrophage polarization in response to biomaterials used for cell encapsulation in T1D. Adjusting the surface topography of polycaprolactone (PCL)-based biomaterials can polarize macrophages towards the reparative phenotype, thus modulating the immune response and accelerating device engraftment. This study evaluates gene expression of the M1 inflammatory phenotype and M2 reparative phenotype in macrophages cultured on mineralized PCL thin films with nanoscale topography and micron-scaled topographic PCL thin films. These results offer valuable insights into tailoring biomaterial properties to improve cell encapsulation device success in treating T1D.

In conclusion, this thesis delves into the challenges cell encapsulation devices face for T1D treatment due to the foreign body response. Through the development of nutrient-supplementing devices, pre-vascularization techniques, and tailoring of biomaterial properties, this body of work aims to enhance the performance and long-term success of cell encapsulation devices in treating T1D.

Table of Contents

List of Figures

List of Tables

Chapter 1. Modulating the Foreign Body Response of Implants for Diabetes Treatment

1.1 Introduction

Diabetes mellitus (DM) is a group of common metabolic syndromes with a typical hyperglycemic phenotype, caused by decreased insulin sensitivity, reduced insulin secretion, increased glucose production, and decreased glucose utilization.[1–9] The two most common categories of DM are type 1 diabetes mellitus (T1D) and type 2 diabetes mellitus (T2D). T1D is the result of insulin deficiency due to immune-mediated or idiopathic β-cell destruction. Although the precise mechanism of β-cell directed autoimmunity is still ambiguous, it has been shown that β-cells are more susceptible to cytokines, such as tumor necrosis factor-α (TNFα), interleukin 1-β (IL-1β) and interferon-γ (INFγ).[10–14] T2D, on the other hand, results from varying degrees of insulin resistance, impaired insulin secretion, and relative insulin deficiency. In the early stages of T2D, β-cells become hyperinsulinemic to compensate for insulin resistance and maintain standard glucose tolerance. However, as the disease progresses, islets are unable to sustain the hyperinsulinemic state, leading to development of overt diabetes, which further causes a decline in insulin secretion. Over time, an increase in hepatic glucose and lipid production can lead to the failure of β-cells.[5–7,15–17]

Although the exact causes for both T1D and T2D are unknown, numerous factors have been implicated, including metabolic disorders of late pregnancy, genetic defects of β-cells, genetic defects in insulin action, diseases of exocrine and endocrine pancreas, specific drugs/chemicals, infections, and other idiopathic syndromes.[11,17–20] DM is diagnosed with tests of fasting plasma glucose level and oral glucose tolerance, as

determined by the American Diabetes Association. The diagnostic criteria for DM vary depending on the type of diabetes. For Type 1 diabetes, the diagnosis is made if the patient has symptoms of hyperglycemia along with a random plasma glucose level of 200 mg/dL (11.1 mmol/L) or higher, or a fasting plasma glucose level of 126 mg/dL (7.0 mmol/L) or higher, or a 2-hour plasma glucose level of 200 mg/dL (11.1 mmol/L) or higher during an oral glucose tolerance test (OGTT). For Type 2 diabetes, the diagnosis is made if the patient has a fasting plasma glucose level of 126 mg/dL (7.0 mmol/L) or higher, or a 2-hour plasma glucose level of 200 mg/dL (11.1 mmol/L) or higher during an OGTT, or a hemoglobin A1c (HbA1c) level of 6.5% (48 mmol/mol) or higher, or in a patient with classic symptoms of hyperglycemia or hyperglycemic crisis, a random plasma glucose level of 200 mg/dL (11.1 mmol/L) or higher is sufficient for diagnosis.[1–11, 14–24] The 2020 National Diabetes Statistics Report, released by the Center for Disease Control and Prevention (CDC), has identified that 34.2 million (10.5% of the US population) have DM.[21] According to the International Diabetes Federation in 2019, the global prevalence of DM was 463 million (9.3% of the world population), and this number is expected to rise to 700 million by 2040.[22–24]

Despite the high prevalence of this disease, currently there is no cure for DM.[3,6,26–29] The cornerstone for management of diabetes is rigorous monitoring of blood glucose levels using finger pricking and administrating exogenous insulin to help regulate blood glucose levels. Current technologies used for insulin administration include syringes, injection aids such as pens or injection ports, and insulin pumps for continuous open-loop subcutaneous infusion or intraperitoneal infusion. Despite technological advances, these strategies are expensive, painful, require high patient compliance, entailing insulin

dependence, and do not provide accurate glycemic control, resulting in frequent hypoglycemic episodes.[30–35]

Many groups have been developing alternative strategies to achieve effective blood glucose homeostasis that require low patient attention. The two broad categories for these therapies are closed-loop insulin delivery systems and pancreas or β-cell replacement therapies (Table 1).[36–45]

Also known as artificial pancreases, closed-loop insulin delivery systems offer great promise as these systems can detect transient hyper and hypoglycemic events and project future blood glucose dynamics. Continuous blood glucose monitoring (CGM) is one such example of a closed-loop insulin delivery system that has brought a monumental change in exogenous insulin administration. CGM is considered the ideal tool for self-management of diabetes as it can permit measurement of interstitial glucose using a subcutaneous sensor and continuous reporting of real-time glucose levels and trends, while also detecting and predicting the hypo- and hyper-glycemic events. The closed loop insulin delivery system integrates a CGM with an insulin delivery pump to administer the right amount of insulin based on CGM-predicted real-time blood glucose levels. This intelligent sensor-augmented insulin pump uses CGM with a feedback loop to implement timely and optimal insulin dosing, maintaining long-term euglycemia.[32,34,36–38,40,41,46–53]

Pancreas or β-cell replacement is another promising therapy, especially for T1D, that has progressed immensely in the last decade. Islet transplantation has shown great potential in achieving insulin independence in more than 50% – 85% of patients for approximately 2 – 5 years.[54–59] Unfortunately, the limited supply of donor tissue and need for life-long immunosuppression severely limit the application of this therapy.[60–62] To

address the issue of donor tissue shortage, efforts have been directed at developing stem cell-derived insulin-producing cells or a xenogeneic source of islets.[60,62–70] Other groups have been focusing on eliminating the need for immunosuppressive drugs by developing an immuno-isolation technology that will allow for successful encapsulation and transplantation of islets or insulin-producing cells.[60,61,65,71–78] The success of these devices depends primarily on the ability of a semipermeable yet immuno-isolating membrane to allow sufficient exchange of nutrients, oxygen, and insulin, while preventing immune cell infiltration. The two broad categories of immune-isolation modalities that are under investigation are extravascular devices and intravascular devices.[74,79] Extravascular micro- or macro-capsules containing islets are transplanted in extravascular spaces, such as peritoneal cavity or subcutaneous cavity.[74–76,79–83] On the other hand, intravascular devices are directly anastomosed to blood vessels.[79,84–86] Such immune-isolation technologies, combined with a replenishable islet source, have enormous potential in the successful treatment of DM.[87–90]

Despite advances, these state-of-the-art technologies remain in their experimental stage. The limitations are not inherent to the sensors or immuno-isolation devices but rather to their performance *in vivo*. The technologies have demonstrated excellent performance *in vitro* in terms of graft survival and function, but in the *in vivo* environment, there is a drastic decline in the performance of the glucose sensors and immuno-isolation devices.[71–73,79,81–83,88,91–93] The decline in function is largely attributed to the multifaceted and dynamic foreign body response (FBR) that occurs upon activation of the host immune response.[79,88,94–101] The various stages of FBR include inflammation, degradation,

biofouling, loss of host microvasculature, and complete fibrous encapsulation and isolation of the implant, which leads to implant failure.[97,102–109]

Continuous glucose monitors (CGMs) and vascular perfusion devices rely on glucose and oxygen diffusion through a membrane for sensor function and cell survival. However, fibrotic capsule formation around these implants creates a barrier, hindering the diffusion of oxygen, glucose, and nutrients. This obstruction severely reduces CGM sensor performance and can lead to graft loss in immuno-isolation devices due to β-cell starvation and hypoxia.[74,79,103,110–113] Moreover, fibrous tissue around the implant can also prevent diffusion of insulin out of the implant, rendering the implant ineffective.[114–119] Therefore, it is imperative to develop efficient strategies that can target and modulate the FBR.

In this chapter, we will detail the host-material immune and foreign body responses that occur post-implant, particularly in the context of implants used for the management and treatment of DM. Next, we will discuss the various biomaterial properties and cellular microenvironment that are at play and dictate the progression of FBR. We also discuss general strategies that have traditionally been used to mitigate fibrosis. Lastly, we highlight different modification techniques that have been applied to suppress fibrotic overgrowth and enhance the subsequent function of diabetes implants.

1.2 Activation of Immune Cascade and Subsequent Cellular Interactions at the Implant – Tissue Interface

The immune system is comprised of both the innate and adaptive arms. The innate immune system elicits a non-specific immune response immediately after recognition of

foreign material, while the adaptive immune system, typically activated by the innate immune response, elicits an antigen-specific immune response. Cross-talk between both of these systems, mediated through soluble factors, determines the host response to implants.[14,107]

During implantation, nicked blood vessels around the implant cause accumulation of platelets and biomolecules that initiate the coagulation cascade, leading to the formation of a provisional matrix. This fibrin-dominant provisional matrix is linked with protein adsorption that occurs on the implant's surface and is considered key in subsequent leukocyte adhesion interactions.[120,121] Moreover, activation of the complement system synergistically supports matrix formation and activation of the immune system (**Figure 1.1a**). There are separate pathways in the complement system that lead to the production of anaphylatoxins, C3a and C5a. The released C3a and C5a induce the innate inflammatory response around implants by increasing vascular permeability, activating monocytes and neutrophils through the release of chemokines and chemo-attractants, and stimulating the release of reactive oxygen species (ROS) from granulocytes. Other pathways that also initiate the cellular inflammatory response include recognition and uptake of biomaterial associated pathogen-associated molecular patterns (PAMPs) or injured host tissue associated damage-associated molecular patterns (DAMPs) and alarmins. PAMPs and DAMPs are recognized by pattern recognition receptors (PRRs) such as Toll-like receptors (TLRs) and C-type lectins that are present on the surface of innate immune cells.[102,120–127] (**Figure 1.1b**)

1.2.1 Innate immune response

Nicked blood vessels lead to focal hemorrhage and edema at the implant site, causing migration and adsorption of biomolecules on to the surface of the implant and the formation of plasma protein-enriched interstitial matrix around the implant. Immune cells such as neutrophils, monocytes, and macrophages recognize proteins with damaged conformations and are activated to release a barrage of cytokines and chemokines. These cells govern the acute inflammatory response and release proteolytic enzymes that degrade the implant while clearing cellular debris. Additionally, the phagocytes (macrophages) engulf and present the antigens to the thymocytes or T cells.

1.2.2 Adaptive immune response

Macrophage and dendritic cells are antigen-presenting cells (APCs) that can internalize foreign antigens, i.e. ions from CGMs and antigens from encapsulated islets, and present them to T cells via major histocompatibility complex (MHC) molecules. The allogenic and xenogenic antigen or cell debris exacerbate the T cell response. CD4+ helper T cells get activated to display pro-inflammatory Th 1 mode and secrete pro-inflammatory cytokines and chemokines such as Interleukin-1β (IL-1β), IL-6, TNFα, and iNOS. An excessive pro-inflammatory response can lead to uncontrolled damage and loss of implanted islets. Over time, inflammation resolves, and the reparative macrophages dominate the environment around the implant. These macrophages mediate the anti-inflammatory Th2 secretory profile, including IL-4, IL-5, IL-13, and IL-10, which increases tolerance of implants and delays FBR. The reparative macrophages extenuate a pro-inflammatory state with parallel immune-regulation and positive remodeling to achieve tissue homeostasis.

Successful remodeling at the implant site happens when the innate immune response shifts from pro-inflammatory to the reparative environment and facilitates the development of site-specific functional tissue and tolerates the implant (**Figure 1.2a**).[128–131] Due to the intricate nature of this immune cascade, slight variations could lead to the development of a foreign body response, as seen with diabetes implants (**Figure 1.2b**).[141–145] Next, we will outline the activation of FBR and key determinants of fibrosis.

1.2.3 Dysfunctional immune system, autoimmunity crossover and implants in T1 and T2D

Immune system activation is a common predisposition for T1D and T2D. Independent of etiopathogenetic causes, inflammation seems to be a common mechanism among different types of diabetes.[17–19,132–134] The central and peripheral immune tolerance failure contribute to the presence (or activation) of auto reactive T cells. Regulatory T cells (Tregs) are defective in phenotypic autoimmune T1D, while several islet auto-antigens and peptide epitopes are targeted by effector T cells (Teffs).[10,19] During DM progression the immune cells such as B cells, macrophages, dendritic cells, and natural killer cells mediate the inflammation. The disruption in regulation and control of local inflammatory cytokines production are also a critical factor in progression of DM.[135,136] T2D is mostly considered as metabolic disorder characterized by dyslipidemia, hyperinsulinemia, and obesity, but with the credible hypothesis that pathogenesis and progression of T2D is credibly linked with inflammation.[137–139] Inflammation contributes to the promotion of metabolic abnormalities such as dyslipidemia, hyperinsulinemia and obesity, which in turn regulate immune cell functions to establish systemic low-grade inflammation (LGI).[16,137]

The metabolism and immune system share a bidirectional relationship. Chronic low-grade inflammation (LGI), immune cell infiltration, and oxidative stress exacerbate metabolic impairments in insulin-sensitive tissues, promoting insulin resistance. Stressed islets further stimulate local inflammation, resulting in abnormal innate and adaptive immunity. This involves alterations in the proliferation and function of T cells, macrophages, B cells, and NK cells, as well as the release of inflammatory mediators that contribute to systemic insulin resistance, β-cell damage, and the significant role of autoimmunity in type 2 diabetes (T2D) pathogenesis.[138,140,141] Consequently, both type 1 and T2D are characterized by the coexistence of insulin resistance and auto- and allo-reactivity against islet antigens, creating a vicious cycle where initial cytokine stress leads to further metabolic stress and additional loss of β-cell function.[18,142]

The overlapping etiology and pathophysiology of type 1 and type 2 diabetes lead to comparable immunological reactions to the implants utilized for monitoring and treating diabetes. The active or memory autoimmune response to islets is presented to the islet implants. The fast-tracked inflammatory islet infiltrations and selective toxicity to the β-cells in transplanted implants lowers the success of allo-islet transplants in autoimmune patients compared with non-autoimmune patients. Despite the use of immunosuppressive drugs, many transplant recipients have shown marked increases in antibodies to glutamic acid decarboxylase (GAD) and islet antigen 2 (IA-2), representing indirect or direct re-exposure to autoantibodies.[143] The likelihood of graft rejection is closely linked to differences in pre-transplant islet autoantibody levels, autoantibody titer, and post-transplant cytotoxic T cell responses. The relative contribution of islet autoimmunity to graft survival, however, remains unclear. Presence of HLA class and I

class II specific antibodies in addition to GAD, IA-2 autoantibodies also indicated the autoreactive may be independent of allo-rejection.[143,144] Growing evidence shows that regardless of the use of immunosuppression to enhance islet graft survival, chronic islet autoimmunity may eventually lead to graft rejection and recurrent diabetes. The autoimmunity may accelerate the inflammatory response toward implants but follows similar mechanistic processes towards regeneration or fibrosis depending on the cue presented at the implant-tissue interface.[143,145–148]

Alongside the progression of diabetes mellitus (DM), a decline in cellular response leads to a decrease in overall immunity against opportunistic infections. This decline is characterized by low complement factors and a diminished cytokine response upon stimulation, which results in progressively dysfunctional humoral immunity. Additionally, long-term DM patients exhibit reduced functional efficiency of polymorphonuclear cells and macrophages.[132,149,150] Though this aspect is out of the scope for this chapter, it is a crucial aspect of immune dysfunction leading to increased prevalence of infectious and non-infectious diseases in patients with T1 and T2D.

1.3 Development of Foreign Body Response and Fibrosis – A Multifront War

Fibrosis is defined as the formation of fibrotic capsule around the implant and occurs due to the activation of the immune cascade. If the innate immune response is not resolved (marked by the unsuccessful elimination of the foreign material and transition into the reparative environment), macrophages fuse together to form foreign body giant cells (FBGCs). FBGCs, considered the hallmark of chronic inflammation and FBR, are multi-nucleated cells that adhere onto the surface of the implant and have increased

inflammatory and phagocytic capacity, further amplifying the immune response. The inflammatory signals produced further promote proliferation of vascular endothelial cells and fibroblasts, which secrete proteoglycans and collagen for the organization of extracellular matrix. Due to excess inflammatory signals, there is superfluous secretion/production of collagen III, resulting in the formation of granulated tissue and fibrous tissue around the implant. This process eventually leads to implant isolation from host tissue, rendering it ineffective. Additionally, fibrous encapsulation formation also depends on the regenerative capacity of the tissue surrounding the implant. When composed primarily of the dormant cells, the tissue usually experiences greater inflammatory cascade and leads to fibrosis.

The root of the FBR lies in the first step – the nature of protein interaction with the implant's surface. The protein-surface interaction is a complex phenomenon influenced by the protein quantity, composition, conformational changes, diffusion coefficient, size, and surface affinity. Protein characteristics are dictated by the physicochemical properties of the implant such as surface chemistry, energy, charge, geometry, porosity, topography.[120,151–154] Additionally, implant-tissue biomechanics is another crucial factor that heavily contributes to the FBR. The implants impose chronic mechanical loading and disrupt the tissue, which induces tissue remodeling and elicits FBR. Lastly, the immune cascade is an orchestra of cells, with each cell type interacting through soluble factors or direct activation. It is widely accepted that sequential transition between cell activation states and cell types is crucial in resolving the immune response. The next section will describe these three components and factors of these components that can alter the implant – tissue response.

1.4 Areas for control at the implant – tissue Interface

1.4.1 Protein adsorption and interaction

Protein adsorption on the implant's surface is based on concentration gradient and surface affinity of the proteins, as many proteins are competing for surface binding sites. Protein adsorption is principally driven by the accumulation of considerable noncovalent bonds, protein conformations, and the redistribution of charged groups at the interface.[154,155] However, the hydrophobic interactions, the composition of biomaterial, charge, and topography at the tissue-implant interface are also of vital importance.

1.4.1.1 Hydrophobic interactions

Protein adsorption is a thermodynamically driven interaction between proteins and implant surfaces. The strong interactions between a hydrophobic implant surface and neighboring polar water molecules lower the overall entropy. Unfolding of proteins compensates for the energetically unfavorable loss in entropy at the hydrophobic surface. The hydrophobic moieties on proteins form weak noncovalent interactions with the surface to exclude water molecules and favorably increase the entropy of water while driving protein adsorption. These weak noncovalent interactions collectively contribute to proteins' total adsorption on the implants with hydrophobic and weak hydrophilic surfaces. The displacement of water on hydrophilic surfaces present a large energy barrier, making it unfavorable for protein adsorption.[154–158] For instance, fibrinogen loses its compact secondary structure and expose sequestered moieties for enhance cellular binding on the residential biomaterial surface based on its hydrophobicity.

1.4.1.2. Charge-charge interactions and protein conformational change

The favorable charge interactions and conformational changes in protein structure help overcome the energy barrier and displace the water molecules that drive protein adsorption on the hydrophilic and hydrophobic surfaces. The pH around implant alters the electrostatically driven charge-charge interaction between implant surface and proteins. In aqueous environments, pH alters the charges on the material surface and proteins. Especially at the isoelectric point of protein, small ionic interactions and formation of hydration bonds can favor adsorption. Conformational changes of proteins increase the overall entropy and enhance adsorption kinetics. Proteins with favored structure overcome comprehensive charge barriers to form noncovalent bonds with the implant surface irrespective of hydrophobicity. The variability in the structural conformation of proteins across implant interface varies with the quantity of protein present and the surface chemistry of implant. Depending on concentration and extent of conformational changes, these proteins may expose the integral binding motifs that are usually unavailable in their native state.[152,153,155,156,159] For example, fibrinogen at very low concentration preferentially adopts a β-sheet conformation while unraveling integral platelet binding motif, which favors high concentration of platelet adsorption on the hydrophobic surface. Fibrinogen forms a spectrum of conformations while adsorbing at different rates based on concentration and surface chemistry. Bioactivity of exhibited motifs preferentially enhances pro-inflammatory cell phenotype, contributing to FBR.

1.4.1.3. Surface energy and charge

Hydrophobicity or hydrophilicity of the implant's biomaterial defines the surface energy, which is critical in adsorption of proteins. Conformational change in proteins

allows greater protein adsorption on hydrophilic implant surfaces, whereas proteins adsorbed on hydrophobic surfaces that did not undergo structural modification preserve their native biological activity. The protein's flexibility, reversibility, and the extent of conformational modification play a vital role in a subsequent inflammatory cascade involving immune cells and surface interactions. The overall high binding strength of noncovalent interactions at the hydrophobic implant surface interface impairs the anti-inflammatory cellular interaction and reorganization. Different ratios of fibronectin and vitronectins are observed with increases in positive charge surface.[152,153,156,160–163]

Additionally, the polarity of implant surface also plays a role in protein adsorption and subsequent cellular interactions. Surface charge modulates the distribution and composition of adsorbed proteins, and differential and preferential protein binding to the polar region on a charged implant surface interface influences downstream inflammatory cellular responses, leading to FBR.

1.4.1.4. Surface topographies

Topographic features on ECM modulate cell behavior, and imprinting these ECM patterns on surface of implants may mimic the ECM topography induced changes in cell behavior. Surface topography modulates protein adsorption, which sequentially alters macrophage adhesion, proliferation, cytokine secretion, and FBR. Changing the scale, shape, and spatial arrangement of topographical features also alters protein adsorption and subsequent cellular response. Nano-scaled topographies offer relatively higher surface area than micron-scaled topographies, thus allowing more protein adsorption. Addition of topography also alters surface energy and charge density of the material,

further influencing the variable protein adsorption profile, conformational change, and cellular response.

Topographical structures induce complex physical stresses at the cellular level, generating differential cytoskeletal tensions, which activate mechanotransduction and gene expression cascades. Fibroblast and macrophages, which play a vital role in FBR, are sensitive to topographical features, and the downstream cellular response of these cells is the result of topographically induced cell behavior, which include contact guidance, cell selection, cell differentiation, and cell-mediated matrix organization. Discontinuous features and topographical roughness lead to preferential cell selection, accumulation, and interaction around the implant, while in some cases, selective cell proliferation and differentiation are also achieved.[102,103,107,127,164–174] The degree of spatial arrangement of topographies also regulates cell behavior. Ordered topographic features reduce cell adhesion compared to random arrangement of the topographic features or planar surface.[103,107,174–180] However, the multiple responses to topographical features makes it challenging to isolate the effectors.

1.4.1.5 Surface chemistry

Modulating surface properties of biomaterials to make them nonimmunogenic or hypoimmunogenic can limit macrophage adhesion, activation, and formation of FBGCs. The terminal chemistry on implant surface commands the conformation of adsorbed protein, which provides a binding site for protein-specific receptors on leukocytes and phagocytes. For example, ionic chemistry on the surface affects protein composition and conformation as counterions in the local microenvironment can stabilize the protein structure, altering protein adsorption dynamics.[106,108,155,164,171,181–184]

1.4.1.6. Surface coating

The implant surface can be coated to generate a barrier that masks the nonspecific protein adsorption and subsequent leukocyte adhesion. A pre-adsorbed coating of known noninflammatory or less inflammatory protein can alter the receptor-ligand binding, leading to minimal fibrosis. Coating the implant surface with lower immunogenic biomaterial also masks the immune reaction leading to FBR with a similar mechanism.[107,118,156,170,180]

1.4.2 Cellular and tissue level biomechanics

Biomechanics and cell interaction with the material plays an important role in the development of fibrotic overgrowth.[104,108,185,186] Cells interact with ECM and implants through proteins known as integrins that physically couple the ECM or implant surface to the cell cytoskeleton. Integrins act as mechanotransducers that transmit signals across the membrane through cytoplasmic-domain-associated focal adhesion molecules. Force-dependent focal adhesion complexes grow larger and mature as integrin clustering increases, leading to force-dependent cytoskeletal changes that ultimately lead to activation of transcription factors.[187–191] Mechanical cues provided by the ECM or implant surface, along with chemical and topographical cues, dictate cellular processes such as cell adhesion, migration, proliferation, gene expression, and apoptosis. Other mediators that function similarly to integrins and alter cellular activity are G proteins, receptor tyrosine kinase (RTK), mitogen-activated protein kinase (MAPK), c-Jun N-terminal kinases (JNK), extracellular signal-regulated kinases (ERK), and calcium ions.[192–196]

Mechanical changes in the cell cytoskeleton ultimately change the biochemical molecules secreted by cells. The cytoskeleton is made up of microfilaments (α-actinin,

filamin A, talin, vinculin), microtubules, and intermediate filaments, and all these components work together to provide mechanical properties that maintain cell shape and tensegrity in the presence of external stress. The external mechanical forces can lead to gene regulation and protein synthesis through pathways such as MAPK phosphorylation by activating the transcription regulatory proteins in the cytoplasm and nucleus. Moreover, mechanosensitive ion channels can also control cellular processes through intracellular calcium ion levels that are altered by mechanical force on the cells.

In terms of tissue-level biomechanics, the external mechanical forces generate motion and pressure at the tissue implant interface. The magnitude, duration, and transmission of each force varies based on the implants' apparent relative motion and source of each force. These forces are widely classified as normal forces, transverse force, torsional force, hydrostatic pressure, stiffness, elasticity, and viscoelasticity.[192,195,197–200] Normal forces, i.e., tensile force, arise from pushing or pulling the implant, while compressive force is the force the implant and tissue apply to each other. Shear stress occurs due to transverse and torsional loading and determines implant sliding. Acute shear stress arises from pulling and brushing against the implant, while chronic shear stress results from repeated abuse due to walking, running, or any cyclical activity. Fluid surrounding the implant exerts nondeforming, random hydrostatic pressure, which thermodynamically affects stability of the implant. Once external force has been applied, this resistance to deformation depends on the inherent stiffness, elasticity, and viscoelastic properties of implant biomaterial or ECM.[201]

Thus, biomechanics play a crucial role at the macroscale level (where implant and tissue interact), microscale level (cells are affected), and nanoscale level (protein

adsorption is affected). Mechanical properties of biomaterial affects all cell types, especially immune cells and fibroblasts, and cyclic mechanical loading on these cells promotes secretion of the autocrine and paracrine soluble factors that regulate ECM protein production along with inflammatory cytokines such as IL-1β, IL-6, TNFα, and oxidative stress markers such as cyclooxygenase-2, nitric oxide, prostaglandins E2.[187,202–206] The cellular response to the biomechanical forces has a self-perpetuating and deleterious response leading to FBR and fibrous capsule formation.

1.4.3 Cellular interactions

Immune cells and their interaction with the environment and with each other play a key role in determining the resolution of the immune response.

1.4.3.1 Innate immune response

Polymorphonuclear leukocytes (PMNs) such as neutrophils, eosinophils, and basophils provide the first line of host defense as they migrate quickly to the implantation site. TGF-β, platelet-derived growth factor (PDGF), and histamine are chemoattractants that guide PMNs to activate enzymatic degradation of implanted material by stimulating release of proteolytic enzymes and ROS. These cells also secrete cytokines including TNFα, IL-1β, IFNγ along with other signals such as monocyte chemotactic protein-1, chemokines, and macrophage inflammatory protein-1β. Together these cytokines and proteins help PMNs remove cellular debris around the implant while also further amplifying the immune response by activating monocytes, tissue-resident macrophages, immature dendritic cells, and lymphocytes. Neutrophils, in particular, release neutrophil extracellular traps (NETs) to trap pathogens in place, and sustained release of these traps have been linked with fibrosis and excessive production of the dense fibrotic matrix.

Chemoattractants such as CCL2, CCL3, and CCL4 have been implicated in recruiting monocytes to the implantation site. The β2 integrin receptors of recruited monocytes bind to IgG, fibronectin, fibrinogen, and complement fragment iC3b on the implant surface, causing monocyte to differentiate into inflammatory macrophages (typically known as classically activated M1 macrophages).[102,120–127] These macrophages secrete pro-inflammatory cytokines such as IL-1β, IL-6, TNFα that recruit other immune cells, along with chemokines, ROS, and proteolytic enzymes that help phagocytose apoptotic PMNs, clear debris, and attempt to degrade the implanted biomaterial. The accumulation of cytokines and chemokines also activates tissue-resident macrophages near the implant. Within 48 to 96 hours of implantation, macrophages are considered the predominant cell type that orchestrates and determines the subsequent immune response based on the chemical and physical properties of the biomaterial. Since most implants, especially for the treatment of diabetes, are larger than macrophages, adherent macrophages will be unable to phagocytose the material, at which point they enter the "frustrated phagocytosis" zone. However, specific cues or properties of the biomaterial can promote macrophages to shift to other activation states (typically known as alternatively activated M2 macrophages), in which they produce anti-inflammatory cytokines that promote tissue remodeling and angiogenesis. Together, the soluble factors released by M2 macrophages lead to recruitment of fibroblasts and endothelial cells, promoting angiogenesis and the integration of the implant.[103,128,131,207–209]

1.4.3.2 Adaptive immune response

The adaptive immune system can be activated through antigen presentation by macrophages and dendritic cells (DCs) (**Figure 1.3**). These antigen-presenting cells

(APCs) activate T cells by presenting MHC and costimulatory molecules that activate naïve T cells. Some examples of DAMPs in diabetes implants include ions from CGMs and antigens from encapsulated islets. The DAMPs are recognized by PRRs, and depending on which PRRs, DCs can mature and upregulate specific T cell activation. Local cytokines and growth factors such as IL-10, TGF-β, hepatocyte growth factor, and granulocyte colony stimulating factor produced by other immune cells around the implant have been shown to inhibit DC maturation, demonstrating the importance of biomaterial properties in directing maturation of DCs.

Maturation of DC has been associated with activation of various T cells, including CD 4 helper Th1, Th2, Th17, and regulatory T cells (Tregs). Typically, especially in cases of chronic inflammation, Th1 and Th2 cells are primarily responsible in modulating the local inflammatory response around the implant as these cells produce large quantities of cytokines that activate local macrophages to their different phenotypes. The role of these T lymphocytes has also been linked with innate lymphoid cells (ILCs), which lack T and B cell receptors. ILC2, especially, have been associated with inhibiting Th1 and promoting Th2 polarization of CD4 helper T cells, indicating the potential role of ILCs in regulating implant induced fibrosis as well. Additionally, activation of Tregs could influence wound healing as these cells regulate the activation of CD8 cytotoxic T cells and produced IL-10, a cytokine that can activate the anti-inflammatory responses of macrophages and CD4 helper T cells. Tregs also produce growth factors that promote differentiation of local stem cells along with fibroblasts. Recently, a different T lymphocyte subset, Th17 cells, has been linked with fibrosis due to their ability to produce IL-17, a cytokine that promotes the pro-fibrotic phenotype of macrophages and fibroblasts.

Depletion of γδ T cells can also prevent wound healing, suggesting their possible involvement in implant induced fibrosis. Despite this information, the role and activation of T cells by implants has not been fully elucidated, and research on the crosstalk between T lymphocytes and macrophages could serve as a powerful and unique tool in modulating local inflammation and subsequent fibrosis of implants.[102,125,179,180,208,210–214]

1.4.3.3 Other cell types

Apart from immune cells, other cell types, including fibroblasts and mesenchymal stem cells (MSCs), play a critical role in biomaterial-mediated fibrosis.[211,215–217] Fibroblasts are highly dynamic, extracellular matrix depositing mesenchymal cells that are recruited by macrophages during inflammation. Once recruited, local cytokines such as PDGF, VEGF, and TGF-β activate the fibrotic phenotype of fibroblasts. These cells are typically known as myofibroblasts, which deposit type I and III collagen around the implant until there are no local inflammatory cytokines present or until the ECM provides physical cues that promote release of the weak focal adhesions formed between myofibroblasts and the ECM. If the myofibroblasts cannot detect these local changes and continue secreting excessive collagen, fibrotic tissue can encapsulate the implant, cause a fibrotic scar formation, and prevent implant function.[211–217]

MSCs are also present at the implant site and have regenerative and immunomodulatory properties that can activate the innate and adaptive system and determine the fate of the implant. MSCs activate macrophage polarization to its anti-inflammatory by secreting factors such as prostaglandin E2, which increases the production of IL-10 while reducing the secretion of TNFα and IL-12. Since anti-inflammatory macrophages are associated with Tregs, it is assumed that MSCs also lead

to the induction of Tregs. Moreover, secretion of these factors leads to a decrease in dendritic cell maturation and a decrease in T lymphocyte and natural killer cell proliferation. Due to these multi-functional properties, MSCs are typically used for wound-healing purposes; however, their exact role and mechanism in preventing biomaterial induced fibrosis has not been fully explored.[103,183,211,215–218]

Knowing the three critical determinants of fibrosis, we can apply various strategies to biomaterials to modulate either protein adsorption, biomechanics of material and tissue, and manipulate surrounding immune cells to control the local microenvironment post-implant (**Figure 1.4**). In the next section, we have outlined the general strategies that have been used to regulate FBR and fibrosis.

1.5 Biomaterial Strategies to Regulate the FBR and fibrosis

FBR and fibrous encapsulation are common problems associated with implantable CGMs or islet encapsulation devices. At the implant – tissue interface, the adverse host immune response leading to FBR/fibrosis can be minimized with two practical approaches: immune evasive strategies and immune-interactive strategies.[190,219,220] Immune evasive strategies involve use of intrinsically inert biomaterials that are recognized as foreign material but do not directly activate a specific immune response. Immune-interactive strategies, on the other hand, engage and elicit the controlled cellular responses, favorably modulating it to minimize the FBR.[190,219,221]

1.5.1 Immune evasive strategies

Immune evasive biomaterials used for implants are inert and elicit minimal host response. An extensive array of biomaterials has been investigated, including natural biomaterials and synthetic biomaterials.

1.5.1.1. Natural biomaterials

A wide range of natural biomaterials with boundless functionalities is available. These materials are usually derived from materials present in the living system through the process of physical, chemical, or enzymatic decellularization.[104,107,130,222,223] These biomaterials are usually biocompatible and may display specific protein binding sites and biochemical signals, driving downstream cellular response towards regeneration and away from FBR and fibrosis. The downsides of natural biomaterials are premature biodegradation and unpredictable mechanical failure. Moreover, xenogeneic natural biomaterials have very high immunogenicity. Examples include gelatin, which is one of the commonly used natural biomaterials in pancreatic islet encapsulation. It has a triple helical structure with a repetitive sequence of glycine–proline/hydroxyproline–proline/hydroxyproline. Due to the structure, gelatin can immobilize water and make the implant surface hydrophilic, leading to low binding of FBR specific proteins.[127,164,184,222,224–226] Another natural polymer, chitosan, is obtained by the alkaline hydrolysis of chitin derived from the fungal cell wall, insects, and shrimp's exoskeleton. It is a polysaccharide with repeated D-glucosamine and N-acetyl-D-glucosamine units and carries a positive charge due to the cationic amine group. It exhibits, both, pro- and anti-inflammatory responses, depending on the degree of deacetylation of chitin, molecular weight, ionic charge, and solubility. Lower molecular weight chitosan shows upregulation

of pro-inflammatory cytokines such as TNFα, IL-6, IFNγ, while higher molecular weight shows downregulation of these cytokines. Moreover, downregulation of pro-inflammatory cytokines is also observed at increased polymer solubility and in its zwitterionic state.[110,211,225,227–229] Hyaluronic acid is also a non-immunogenic biopolymer derived from the ECM of connective and epithelial tissues. It is a negatively charged polysaccharide with repeated units of D-glucuronic acids and N-acetyl glucosamine. At lower molecular weight, it is pro-inflammatory as it induces upregulation of TNFα and IL-1β, but at higher molecular weight, it becomes less immunogenic as it increases secretion of IL-10, an anti-inflammatory cytokine.[103,222,225,228,229] Heparin, used widely for intravascular implants in DM, is a linear glycosaminoglycan with a negative charge due to the high content of sulfonic and carboxyl groups in its D-glucuronic and D-glucosamine repeating units. Heparin and its derivative inhibit inflammatory cytokines such as TNFα, IL-6, IL-8, IL-1β at lower molecular weight in a dose-dependent manner.[81,170,211,229,230] Agarose is another natural polysaccharide composed of linear chains of D-galactose and 3,6-anhydro-L-galactopyranose. It is a thermosetting polymer with very low immunogenicity as it can locally inhibit the complement system, thus reducing the immune response leading to FBR.[230–233] Alginate is a widely used biopolymer, especially for islet encapsulation for the treatment of T1D. It is a negatively charged biopolymer with the repeated units of mannuronic and guluronic acids and has excellent gelation property in the presence of divalent cations. Its immunogenic property depends on the ratio of mannuronic and guluronic acid. Unsaturated oligomers upregulate TNFα and induce a greater pro-inflammatory response as compared to saturated oligomers.[222,230,234–236] Another polymer that has extensively improved islet transplantation outcomes is collagen. It has numerous

subtypes that are present in connective tissues, with the most prominent subtypes being collagen type I, II, and III. It has a triple helical structure with a repeated unit of glycine, proline, and hydroxyproline sequence, and the immunological profile of collagen depends on this helical structure as well as the fibril's amino acid sequence.[167,180,186,237–240] Lastly, silk is a natural polymer with a core structural protein, fibroin, that is surrounded by sericin, which is responsible for the immunogenicity of silk.[107,230,232,241,242] Isolated fibroin has very low immunogenicity, controllable biodegradability, and excellent mechanical properties, making it an excellent candidate for improving islet encapsulation efficiency and long-term graft function with limited FBR.

1.5.1.2. Synthetic biomaterials

Synthetic biomaterials are easy to synthesize, inexpensive to produce, and have predictable and tunable functional properties. Though they have excellent physicochemical, mechanical, and degradation properties, they are more prone to induce a pro-inflammatory response, causing difficulty in integrating with host tissues.[221,223,243] An example of synthetic biomaterial is polycaprolactone (PCL), which is used widely with implants as it is an inert, biodegradable, linear aliphatic polyester. It is a hydrophobic, biocompatible polymer with a prolonged degradation rate that can be easily modified by changing the molecular weight.[106,107,202,219,230,244] Polyethylene glycol (PEG) is another inert, non-immunogenic, flexible, biocompatible hydrophilic polymer of ethylene oxide. It is resistant to protein adsorption and is known to minimize the protein corona formation. It has a linear and branched structure that can be easily modified to covalently attach a variety of functional groups.[81,126,229,233,245–247] Polyvinyl alcohol (PVA) is yet another synthetic polymer that has been successfully used as a biomaterial for implants. It is

derived from hydroxylation of polyvinyl acetate and has varying chemical properties based on the percentage of hydrolysis. It is highly non-immunogenic due to its hydrophilicity, low protein adsorption, and high-water solubility.[110,167,211,248,249] Polyurethane (PU) is composed of aliphatic or aromatic units derived from polyether or polyester monomers. Its immunogenicity mostly depends on the ratio of polyoxyethylene (PEO) to polytetramethylene oxide (PTMO). Water absorption and hydrophilicity of PU depends on the quantity of PEO present as PEO has low interfacial free energy with water and high surface mobility.[126,170,184,223,229,250,251] Polytetrafluoroethylene (PTFE), commonly known as Teflon, is a highly crystalline fluoropolymer of tetrafluoroethylene. It has a hydrophobic, electronegative, and low-friction surface that is suitable for most blood-contacting implants but does induce a mild inflammatory response.[217,223,229,248,252] Polyglycolic acid (PGA) is a polyester with a high degradation rate and a linear aliphatic structure that is synthesized using ring-opening polymerization of glycolic acid. There is no standard agreement on the immunological profile of PGA as it prevents initiation of lymphocyte DNA synthesis but also promotes the pro-inflammatory response by activating MHC-II and IL-2 receptor.[180,223,229,253] Polylactic acid (PLA) is a linear, aliphatic polymer of lactic acid with slow degradation rate and excellent mechanical properties. It is used in blood-contacting implants and causes no thrombosis and minimum stenosis. However, acidic degradation products of the polymer are reported to provoke a pro-inflammatory response.[230,254–256] Lastly, polylactic-co-glycolic acid (PLGA) is a blend of PLA to PGA, with varying ratios resulting in different immune responses in terms of immune cell infiltration and FBR.[228,249,257–259]

1.5.2 Immune engaging strategies

Biomaterials can also provide structural, biochemical, and biomechanical cues that will activate the immune system at the implant-tissue interface. Some properties of biomaterials make them inherently immune-engaging;[190,219,223,260,261] one such example is decellularized extracellular matrices.[216,229,239,262–264] These large, structural, protein-based matrices derived from native tissue are lipid and cell-free, making them highly immune-privileged biomaterial that can modulate and downregulate a myriad of immune responses. Another example of an inherently immune engaging material is fibrin,[204,225,254] a filament-forming soft network formed by an enzymatic reaction between fibrinogen and thrombin. Presence of fibrin ligands in several integrin receptors downregulates pro-inflammatory cellular response leading to FBR.

Other immune engaging strategies include local delivery of pro-inflammatory and anti-inflammatory molecules. Examples of these molecules include antibodies, cytokines, chemokines, prostaglandins, leukotrienes, proteolytic enzymes, free oxygen radicals, and nitric oxide.[82,107,130,211,212,215,219,228,265] Pro-inflammatory molecules such as heat shock protein 70 (HSP-70), lipopeptide-2, cytosine-phosphorothioate-guanine oligodeoxynucleotides (CpG) target the immune system through TLR pathways to help initiate acute inflammation that eventually leads to the reparative response.[14,126–128,211,266] A significant acute and chronic anti-inflammatory response with inhibition of FBGC and fibrosis is obtained using glucocorticoids, superoxide dismutase, and nonsteroidal anti-inflammatory molecules. Other anti-inflammatory factors such as IL-4, IL-10, anti-TNFα also play a significant role in promoting tissue repair and regeneration.[126,211–213,228,267–269] Local delivery of these pro-resolvin mediators end the acute inflammatory response by

inducing macrophage polarization to its reparative M2 phenotype, which begins the process of tissue granulation and regeneration.[126,179,270] Promoting integrin clustering, activating immune cells, and providing growth factors can also induce tissue regeneration while suppressing FBR. Immune cells, such as macrophages and MSCs can be used as a biological source to produce immune-modulatory molecules.[211,215,271] Epidermal growth factor (EGF),[103,106,272] vascular endothelial growth factor (VEGF),[108,211,273] fibroblast growth factor (FGF),[81,211,274,275] granulocyte-macrophage colony-stimulating factor (GM-CSF), PDGF, and TGF-β together form a complex signaling network, which helps guide cross-talk between the immune cells, tissue cells, and leukocytes to successfully modulate the reparative immune response.[103,126,211,228,276–278] Additionally, hydrophilic biomaterials[156,157,186] induce a lower local immune response as compared to hydrophobic polymers[167,202,279] as hydrophilic polymers have significantly lower monocyte adhesion and formation of FBGCs. Surface topographies on commonly used biomaterials for implants, such as polycaprolactone (PCL),[106,178,280] polylactic acid (PLA),[183,186,224] poly-dimethyl-siloxane (PDMS),[80,107,224] promote macrophage polarization and also reduce FBR. Lastly, surface coating reduces non-specific adhesion of proteins on the implant-tissue interface and prevents biofouling. Polymer coatings of PEG, PAA, polyethyleneglycol-block-poly l-lysine hydrochloride (PEG-b-PLL),[81,233,281] polyethylene glycol diacrylate (PEGDA),[282,283] poly N-isopropyl acrylamide, and poly 2-hydroxyethyl methacrylate (PHEMA)[80,107,211] have demonstrated minimal protein adsorption.

1.6 Engineering Immune Engaging Biomaterials

Immune-engaging biomaterials have shown great potential in modulating FBR and fibrosis, as these materials can induce specific immune cell response that promotes implant integration and function. Essential strategies for designing such biomaterials include altering surface chemistry through biofunctionalization, changing surface topography, and emphasizing the role of biomechanics in implant design.

1.6.1 Surface chemistry

The bio-functionality of the material depends on how surface chemistry influences protein adsorption.[155,178,284] Immune-modulating surface chemistries are engineered by modifying the original implant surface through non-covalent deposition and adsorption of biomolecules and through covalent cross-linking of functional groups such as thiols,[183] silanes,[166,233] or biomolecules[110,207,211] on the material surface. Ion-beam implantation,[285,286] chemical conjugation, silanization,[166,233,284] self-assembly of monomers,[80,110,252,287,288] and plasma-assisted techniques[164,289,290] are a few of the most critical processes used to modify surface chemistry. Ion-beam implantation injects accelerated ions (cations and anions) into a material to alter its surface charge, energy, and chemistry, directly affecting implant-protein interaction. Surface coating can also be added to materials containing functional groups, such as -OH, -COOH, -NH_2, via electron beams as high energy ionizing radiations, upon exposure to the reactive groups, can react to form a functional coating on the biomaterial surface. Silanization is another technique in which silane molecule reacts with a hydroxylated substrate, which, upon polymerization, produces a covalently linked surface coating. This technique is commonly used on implant surfaces to alter chemical properties such as surface energy. Self-

assembly monolayers (SAMs)[166,272] are highly ordered surfactants that spontaneously assemble by covalently anchoring on the biomaterial surface. Alkanethiols[291] is a well-known SAM facilitating in hydrophilic, hydrophobic, non-fouling short chain, and polysaccharide terminal modification. Some of the molecules with no functional alkyl groups such as proteins, porphyrins, nucleotide bases, and hydrocarbons with aromatic rings can also form SAMs. Plasma assisted techniques, such as radiofrequency glow discharge plasma-induced surface ablation, etching, and coating using low pressure suitable ionized gas, are used to modulate the cell-material interactions by tuning the density of the functional group deposition on biomaterials.[106,166,275,292]

1.6.2 Biofunctionalization, coating, and patterning

Bioactive molecules can be covalently coupled to functional groups on the surface of a biomaterial. Favorable modulation of downstream immune response is proportional to the density of immobilized ligands, spatial distribution, colocalization with agonistic or synergistic ligands, and steric hindrance. The practical approach is to mimic properties of the ECM onto biomaterial surface to accelerate tissue regeneration. Material surface can be functionalized with peptides, proteins, growth factors, and endothelial cells to alter protein adhesion, improve blood compatibility, inhibit foreign body response, and increase the patency of implants. Small oligopeptide sequences such as arginine-glycine-aspartic acid (RGD)[106,257,293] and proline-histidine-serine-arginine-asparagine (PHSRN)[127,294] contain receptor binding domains for macrophage-specific adhesive proteins that can regulate macrophage phenotype. PEGylation (PEG coating or brush layers on the implant surface) prevents protein adsorption, and its non-biofouling activity depends on its molecular weight, chain length, chain density, and conformation and is directly

proportional to the degree of polymerization and the density of surface brush bristles.[110,127,295–297] To further contain the pro-inflammatory immune response, rapamycin and other active biomolecules can be doped in the PEG coating and slowly released into the microenvironment to inhibit non-specific binding and proliferation of inflammatory macrophages.[107,298,299] Di block PEG copolymer, such as PEG-b-PLL and VEGF/bFGF linked PEGDA, support neovascularization with minimal fibroblast adhesion while simultaneously masking pro-inflammatory entity with an outer anti-fouling layer to ameliorate the FBR. Examples of notable anticoagulants and anti-fouling agents that successfully prevent the pro-inflammatory response are warfarin,[167,233] heparin,[170,211,300] hirudin,[272,301] argatroban,[301] chlorothalonil,[302] phosphorylcholine-PDMS,[303–305] PEG-fluoropolymer,[166] ethisorb,[229,306] zwitterionic polymers such as phosphorylcholine, sulfobetaine (SB), carboxybetaine (CB),[110,166,233,307] and many more. Materials can also be modified using biochemical patterning to spatially control cell organization, attachment, and differentiation. These well-defined and ordered colocalization of synergist, agonist, or even antagonist molecules can be achieved using microcontact printing and other Lithographie, Galvanoformung, Abformung (LIGA) processes.[308–312]

1.6.3 Surface topography

Topographies are precisely engineered geometric features that can be nano- or micron-scaled. The size of the features, shape, geometry, spatial arrangement, frequency, geometry, randomness, and roughness can influence protein adsorption, cell differentiation, and the overall FBR.[107,174,180,182] Several techniques can be used to install surface topography. For example, photolithography, limited to the sub-micron scale, uses ultraviolet exposure to transfer topographical features on photosensitive material through

a patterned mask. For nanoscale features ranging above 4 nm, electron beam lithography (EBL) uses high energy focused electron beam, in the range of 15 – 30 kV, to transfer nanotopography on substrate coated with photosensitive material.[178,290,313] Additionally, soft lithography can used to replicate and transfer these features on the biomaterial substrate. Similar to EBL, high energy reactive focused ion beam (FIB) can also be used to fabricate nanoscale topographies using etch masks consisting of self-assembled nano colloids.[178,290] This technique, known as colloidal lithography, is used to make nanocolumns, nanosphere, and nanocones on material surface. Polymer demixing uses spontaneous phase separation of blended polymer to fabricate random, disordered, sub-micrometric to micrometric scale, co-localized features, such as pores, pits, islands, and ribbons.[164,172,183,290] Electrospinning can also be used to fabricate nanoscale, fiber-like topography. In this method, high voltage, typically in the range of 25 – 50 kV, is used to draw charged polymer solution or eject polymer melt at a controlled rate to yield nanoscale fibers. The topographical arrangement of these fibers depends on the collection methods used; aligned fibers are obtained if collected on the rotating drum collector while random fibers are obtained if collected on the planar collector.[184,282,314–317] Similarly, electrospraying uses electrohydrodynamic process and high voltage electric field to spray a charged polymer solution at low concentration to obtain self-dispersed nanoscale particle topography on substrates.[313,318,319] Additionally, techniques such as dip coating,[108,183,265] laser machining, embossing,[170,178,183,291] acid etching,[170,287,320] dry etching,[256,287,321,322] sandblasting,[164,203] grinding,[287,323] etc., can also be used to successfully install surface topography.

1.6.4 Biomechanics at the implant level

Mechanical properties of implant that can induce FBR include several metrics such as implant location, relative motion, force intensity, shape, size, thickness, and bulk material mechanical properties of the biomaterial.[104,108,206,324] Implant location affects biomechanics of the implant as different external forces are at play, which, ultimately, limits the functionality, performance, and lifetime of the implant. For example, percutaneous implants are subjected to micromotions, exterior pressures, and forces that propagate along the implant and impact cells at the interface.[108,206,324] On the contrary, subcutaneous or intravascular devices experience less direct forces.[80,206,233,325] Moreover, implant shape significantly affects the distribution of the interfacial forces as well. Higher stress concentrates at sharp angles, curves, and edges, inducing strong FBR with thicker fibrous encapsulation.[104,199,206,326] Implant size is also another crucial factor in determining development of fibrotic overgrowth, as it has been demonstrated that smaller implants cause less tissue trauma, with reduced acute inflammatory response, and can sometimes evade the FBR completely. The induced pro-inflammatory response is less dependent on the length of the implant, as compared to the height, as there is lower disruption in collagen fibers that are parallel to the implant. On the other hand, thicker implants (higher heights) create a separation between the parallel running collagen fibers, triggering the ECM to fill the voids, resulting in a thicker fibrous capsule. For example, paper-thin polyvinyl chloride/polyacrylonitrile (PVC/PAN)[227,253,281] and silicone-coated PVC/PAN[107,127,174,265,327] implants showed lower fibrosis as compared to thicker implants. Lastly, differences in the modulus of the material and surrounding tissue can lead to accumulation of stress at the implant interface, resulting in fibrosis.[102,104,186,206]

In fact, it has been demonstrated that implants with modulus similar to that of the surrounding have reduced interfacial stress, which downregulates the pro-inflammatory response leading to FBR.

In the next section, the application of these aforementioned strategies in the development of implants for DM will be evaluated.

1.7 Strategies Used to Modulate Fibrosis for Diabetes Implants

Treatments for DM include closed-loop insulin delivery systems, also known as artificial pancreas, along with glucose sensors that detect blood glucose levels and secrete the appropriate amount of insulin based on the detected glucose levels.[38,247,328,329] Islets or β cell replacement using intravascular or extravascular encapsulation devices can also serve as long-term treatment for DM, specifically for T1D.[91,248,314] Though these technologies have their own inherent challenges, the issue of FBR and fibrosis remains unresolved.[81,91,230,330]

1.7.1 Continuous glucose monitoring systems

The implantable glucose sensor is a highly valuable, clinical technology that improves the quality of life of DM patients through real-time monitoring of glycemic variability. It notifies the user of hypoglycemic and hyperglycemic events with early predictions and makes maintaining euglycemia an achievable goal when combined with closed-loop insulin administration technologies.[52,247,328] However, contemporary CGMs lose their lifespan, reliability, and accuracy approximately one week after implantation. This loss occurs due to FBR that results in avascular collagenous tissue encapsulation

of the CGM and due to the metabolically active inflammatory cells around the implant that change local pH and glucose concentration.[47,52,247,331]

Numerous strategies for improving longevity of CGMs have been evaluated. Traditionally, platinum-iridium (Pt/Ir)[332,333], silver/silver chloride (Ag/AgCl)[184,224,334] based amperometric electrode, isotonic fluid perfused microdialysis fibers, and other enzyme-based electrochemical sensors were used for glucose sensing.[335–337] However, these materials have limited biocompatibility, which is why tremendous progress has been made in developing new materials, such as carbon nanomaterials,[338,339] polymer microgels,[340–342] and semiconductor quantum dots (QDs),[343,344] that enhance the glucose-sensing capabilities and biocompatibility of the sensors. Carbon nanotubes (CNTs),[247,338] graphene-based electrodes,[247,338,345] PAA hydrogel with reduced graphene and lutetium phthalocyanine,[346] and other non-enzymatic sensors,[336,338,345] have shown excellent glucose sensitivity with relatively greater biocompatibility in vitro. Moreover, boronic acid-functionalized glucose-responsive polymer gels, metal nanoparticles infused with phenylboronic acid (PBA)[342] functionalized microgels, poly(amidoamine) (PAMAM)[342] functionalized microgel, photoluminescent cadmium selenide/zinc sulfide (CdS/ZnS)[342], have also shown great promise in providing excellent glucose sensitivity and higher biocompatibility.

Though the new materials have outstanding glucose sensitivity, their biocompatibility and success as implantable CGMs rely heavily on favorable immunological response at the interface. Polymer coatings can be applied as they can potentially mitigate fibrosis without changing implant function. Several inorganic, organic, and bio-functional polymers with anti-fouling properties have been assessed. For

example, a nafion-coated CGM probe showed greater function for more than a week, even though it eventually failed due to mineralization.[347–349] Polyether-based aliphatic PU, PU with silicone, and polyethylene oxide (PU-S-PEO) coated sensors significantly inhibit leukocyte adhesion, FBGC formation, and reduce downstream inflammatory cascade up to 2 months.[350–352] PEG-modified hydrogels,[339,351,352] copolymers of 2-hydroxyethyl methacrylate (HEMA),[353–355] and ethylene di-methacrylate[356,357] coated implants have also shown lesser fibrous encapsulation compared to PU control. Zwitterionic polymer coating can also be used as an anti-fouling coating for CGMs as its net neutral charge and high hydrophilicity can resist protein adsorption and subsequent cell adhesion.[107,166,351,358] In fact, zwitterionic pSBAA[359–361] and pCBAA[362,363] coated surfaces suppress leukocyte attachment significantly better than PEG-coated surfaces. Moreover, inorganic composites, such as sol-gel derived silicates and silica-based material, and naturally occurring materials, such as alginate and collagen, have shown minimal inflammatory response when coated on biosensors.

Topographical and biomechanical properties of the CGMs can also influence the inflammatory response. For example, PLLA foam coated implantable glucose sensor reduced the thickness of the fibrous capsule with a better capillary density.[352,364] Glucose sensor with a porous expanded PTFE membrane demonstrated better integration of implant with the surrounding tissue for more than 5 months.[184,365] High precision PMMA templated porous PHEMA hydrogel, silicone, and fibrin coated implant developed only a very thin fibrous capsule, increased vascularization, and reduced pro-inflammatory macrophage phenotype.[365,366] Electrospun, aligned, single and coaxial PU and gelatin fibers of different diameters have also been used to coat glucose sensors, in which

monodispersed fiber diameter, permeability, and orientation influences the host response. The coaxial PU-gelatin electrospun fibers effectively prevent formation of fibrous capsule as compared to their counterpart.[366–368] Also, since mechanical properties of fibers or other coating materials play a crucial role in modulating FBR, coating materials with modulus that is similar to that of the surrounding tissue induces lower pro-inflammatory response.[369,370] An implants' perceived modulus can also be modulated with a brush-like coating of an interpenetrating polymer network that can reduce the FBR. Additionally, polymer coating of double network N-isopropyl acrylamide and 2-methylpropane sulfonic acid membrane (NIPAAm: AMPS) with characteristic thermoresponsive cyclic swelling-deswelling inhibits protein adsorption and subsequent leukocyte attachment.[369–373]

To enhance the sensor integration capability further, the delivery of active small or large molecules can be downregulated. Sensors coated with dexamethasone, a glucocorticoid, have decreased vascular permeability and leukocyte extravasation. It also prevents leukocyte adhesion and recruitment by reducing the production of proteolytic enzymes and cytokines.[374–377] PLGA particles releasing tyrosine kinase inhibitor (masitinib) from CGMs modulate macrophage polarization and decrease the FBR.[378–381] Extended local delivery of VEGF from HEMA, PEG hydrogels, and PLGA microspheres can also modulate the pro-inflammatory response. PLGA particle coated on the sensor has been used for dual delivery of dexamethasone and VEGF with no significant synergistic effect. Nitric oxide (NO) has also been used to mitigate fibrotic overgrowth as it upregulates VEGF production and vascularization while downregulating pro-inflammatory cytokine secretion.[382–384] A variety of delivery systems are developed for

localized long-term NO delivery from CGMs sensors. S-nitrosothiol and N-diazonium diolates are used as a source for NO generation and are incorporated in various polymer-based delivery vehicles coated on glucose sensors. S-nitrosothiol surface-functionalized silica nanoparticle and xerogels doped surface coating led to NO release from the sensor surface, resulting in decreased inflammatory cells, thin fibrous capsule formation, and long-term sensor function.[350,351]

1.7.2 Microencapsulation and PEGylation of islets

Microencapsulation for islet transplantation is a widely used strategy in which islets are entrapped within a polymeric membrane that provides three-dimensional architecture to the cells while also providing a high surface area to volume ratio for increased access to nutrients and oxygen. Despite normalizing blood glucose levels in diabetic animals, microcapsules have not achieved clinical outcomes due to the formation of fibrosis around the capsules. This section of the review outlines strategies used for commonly used T1D microencapsulation materials to prevent fibrotic overgrowth.

1.7.2.1 Alginate microcapsules

Microencapsulation of islets in alginate hydrogel is a conventional approach for treatment of T1D. Alginate is a natural, hydrophilic copolymer that exists as calcium, magnesium, or sodium salts of alginic acid in cell walls of brown seaweed. It is a non-toxic, low-cost unbranched polysaccharide composed of D-mannuronic and L-guluronic acid residues joined by glycoside linkages. The monomeric composition of alginate hydrogels affects the biodegradability, porosity, and mechanical integrity, making it an easily modifiable hydrogel. Moreover, divalent cations such as calcium (Ca^{2+}) are typically used to gel the hydrogel under mild conditions. Despite the success of these

microcapsules in T1D, due to batch-to-batch variability as well as the presence of endotoxins, cellular fibrotic overgrowth is still an issue that has prevented successful clinical advances of the material. Approaches to preventing the fibrotic overgrowth for alginate hydrogel include changes in monomeric composition, increasing size of microcapsules, surface modification, co-delivery of anti-inflammatory drugs, and co-encapsulation.[385,386]

One of the major components that can be controlled to prevent fibrosis in alginate microcapsules is material purity. Although alginate is a natural polymer, it contains endotoxins such as liposaccharides that can activate host inflammatory response through TLRs. Many studies have been conducted that show that alginate purity is a key component in reducing capsular overgrowth.[385,386] Moreover, alginate composition as well as its molecular weight can also affect the biocompatibility of the microcapsules. However, there are many conflicting reports regarding what ratio of repeating units of guluronic (G) and mannuronic (M) acid in alginate leads to higher biocompatibility.[387,388] Also, using a low molecular weight, lower viscosity alginate induce a greater fibrotic response as compared to intermediate and high molecular weight alginate capsules.[389]

Size of the microcapsules can also determine activation of FBR. Typically, microencapsulation spheres are 0.8-1.5 mm in diameter, however, this size range creates a large diffusion barrier for encapsulated cells, leading to necrosis and accelerated fibrotic encapsulation. Smaller, 0.25-0.35 mm in diameter alginate-polylysine-alginate microcapsules, on the other hand, were more biocompatible and showed prolong graft survival.[390] However, a recent study has shown contradictory results and also demonstrated that device geometry also plays a key role in modulating FBR and fibrosis

in rodents and non-human primates. The study showed that spherical materials of 1.5 mm diameter or greater caused lower fibrosis than smaller spheres or disc shaped hydrogels. This remains true across materials of different stiffnesses such as alginate, glass, polycaprolactone, polystyrene and stainless steel. Moreover, encapsulation of rat pancreatic islet cells in 1.5-mm alginate capsules were able to control blood-glucose levels for up to 180 days in a diabetic mouse. This was particularly significant as the widely accepted 0.5-mm alginate capsules have shown control of blood-glucose levels for approximately only 30 days. The increased graft survival and functionality was largely dictated by the reduced cellular deposition and fibrosis formation observed on alginate spheres of larger diameters.[307]

Additionally, many groups have modified the surface of alginate microcapsules to increase the biocompatibility. Alginate beads with alternating layers of polyethyleneimine, polyacrylacid, or carboxymethylcellulose were tested, and the use of any of these multilayer-membrane had no adverse fibrotic effects on the grafts. Results also showed high insulin secretion, indicating increased survival of islets.[391] Additionally, coating rapamycin-containing polyethylene glycol significantly reduced fibrosis around the implant by decreasing macrophage cell proliferation.[102,228,299,392,393] However, this biocompatibility of PEG coated alginate microspheres depends greatly on the transplant site.[81,388] Chemical conjugation of triazole-thiomorpholine dioxide to alginate demonstrated lower fibrosis around empty alginate microspheres transplanted in rodents and non-human primates.[211,394–396] Encapsulation of islet stem cell clusters in these chemically modified microspheres also showed little evidence of fibrotic overgrowth after 6 months and excellent glucose control when transplanted into diabetic rodents.[395,397–399]

Similarly, chemically modified alginate using corline heparin conjugate had no negative effects on the encapsulated islets and helped reduce fibrotic overgrowth in syngeneic and allogeneic rat transplantation model by ~65% and 43%, respectively.[102,400] Coating alginate microcapsules with chitosan also had significantly lower fibrosis around the implant after 1 year of, both, xenogeneic and allogeneic transplant.[81,236,401,402]

Moreover, a large library of amines, alcohols, azides, and alkynes have been covalently conjugated to alginate to modify the latent functionalities and properties of the polymeric alginate backbone. Barium alginate microspheres of 300-350 μm size modified with Z2-Y12, Z1-Y15, and Z1-Y19 showed lower fibrotic overgrowth after 28 days of implantation in the subcutaneous space and almost no fibrous deposition after 14 days of implantation in the intraperitoneal space of C57BL/6J mice. These modified materials contained triazole functionality and showed little to no presence of macrophages, myofibroblasts, or general cellular deposition around the microcapsules. Although the mechanism of how triazole-containing materials mitigate foreign body responses is still unknown, there is strong evidence that triazole derivatives may prevent activation of macrophages and other immune cells, thus, disrupting the process of fibrosis.[403] Allogenic transplantation of islets encapsulated Z1-Y15 modified alginate microspheres in non-human primate animal model showed no pericapsular fibrotic capsule in 6 out of 7 animals and 90.0% islet cell viability was retained after 4-months of implant. Additionally, when glucose-stimulated insulin secretion of the encapsulated islets was measured, these islets secreted significantly higher levels of insulin compared to non-modified alginate microspheres.[404]

More recently, zwitterionic polymers bearing CB, SB, and phosphorylcholine have shown ultra-low-fouling properties due to their high resistance to nonspecific protein adsorption and cell attachment. SB-conjugated alginate microcapsules were implanted in the intraperitoneal space of C57BL/6J mice, intraperitoneal space of dogs, and omental pouch of pigs for up to 6 months. SB-alginate microcapsules in mice showed significantly less cellular overgrowth than unmodified alginate microspheres. Similar results were also seen in large animals, including dogs and pigs, indicating the effectiveness of this strategy in various species. Moreover, after encapsulating rat islets, SB-coated microcapsules also showed significantly better long-term glycemic control for up to 200 days in streptozotocin (STZ)-induced diabetic mice.[405] Although zwitterionic hydrogels have great anti-fouling properties, these hydrogels lack mechanical properties. Therefore, triazole moieties have been integrated into a hydrogel monomer to create a more mechanically robust hydrogel that has greater compressive strain and tensile strain. Despite the addition of triazole, the biocompatibility of the hydrogel was unaffected. In fact, encapsulation of islets in triazole-zwitterionic alginate hydrogels showed correction of glycemic levels in diabetic mice and subcutaneous implantation of the hydrogels also showed significantly lower foreign body response as compared to control.[406]

Instead of surface conjugation, co-encapsulation of anti-fibrotic drugs is also a possible strategy for mitigating fibrosis. Co-encapsulated GW2580, a colony stimulating factor 1 receptor (CSIF1R) inhibitor, with β cells in diabetic mice showed lower fibrosis in microcapsules containing the drug. GW2580 targets CSIF1R, which is has been shown to play a key role in targeting monocyte/macrophage phenotype polarization and mediating the FBR against implants. Moreover, subcutaneous and intraperitoneal

transplantation of rat islets in 0.5 mm alginate microcapsules with and without drug in STZ-induced diabetic C57BL/6 mice showed promising results. After 72 days in the subcutaneous space, control capsules had a collagen-encapsulated sack around the graft while the drug loaded capsules were fibrosis free. Moreover, there was also a difference between encapsulating amorphous and crystalline GW2580-loaded capsules. The study showed that, after ~1.3 years, crystalline drug capsules had higher islet viability, as indicated by ~30-fold higher Pdx1 expression, and lower myofibroblast and fibrosis response, as indicated by 74% lower α-smooth muscle actin expression.[393] Additionally, incorporation of CXCL12, an immunomodulatory cytokine, in sodium alginate microcapsules containing stem cell derived β cells prevented pericapsular fibrotic response, leading to long-term (>150 day) glycemic correction in mice. The presence of CXCL12 also enhanced the glucose-stimulated insulin secretion of the stem cell derived β cells, which helped the treated mice correct hyperglycemia faster than the control group.[107,398] Co-delivery of other drugs, such as dexamethasone and curcumin, can effectively minimize fibrotic cellular overgrowth as these drugs inhibit activities of inflammatory proteases and reactive oxygen species. When curcumin was co-encapsulated with rat islets in alginate microcapsules, there was reduced fibrosis around the implant and promoted greater glycemic control in the diabetic mice.[102,307,407]

Lastly, co-encapsulation of different cell types with islets can help mitigate fibrotic overgrowth induced by alginate microcapsules as well. Co-encapsulation and co-transplantation of mesenchymal stem cells (MSCs) with islets resulted in significantly lower perivascular fibrotic overgrowth along with improved graft survival and functionality. Additionally, MSCs pre-stimulated with IFN-γ and TNF-α secreted higher quantity of

immunomodulatory cytokines and showed slightly lower fibrosis around the graft. Data also suggested that the observed decrease in fibrosis could be attributed to the upregulation of IL-10 and G-CSF, which directly inhibit TNF-α.[408] Sertoli cells are another set of companion cells that have shown higher engraftment and function of islets when co-encapsulated in alginate microcapsules as these cells inhibit T-cell and B-cell proliferation while increasing local IL-12 production. Co-microencapsulation of these Sertoli cells with islets increased local immunosuppressive factors and showed higher islet β cell mitotic function that produced significantly higher insulin release upon glucose stimulation. However, the effect of these cells in directly preventing fibrosis has not been studied yet.[248,409]

1.7.2.2 Other microcapsules

Microcapsules fabricated from other natural and synthetic polymers have also shown promise in preventing fibrosis of grafts fabricated for T1D. For example, islets encapsulated in 5% agarose hydrogels were able to maintain euglycemia in diabetic mice for more than 100 days.[410–412] Moreover, histological analysis showed that implantation of these hydrogels for 100, 150, 200, 300, and 400 days induced little to no immune response.[211,410–412] Collagen microcapsules have also shown minimal fibrosis, however, their high degradation and low mechanical stability limit their application for long-term treatment of T1D.[413] Additionally, bio-composite silica ceramic microcapsules did not induce fibrosis and the encapsulated islets demonstrated high insulin secretion after one month of implantation in the subcutaneous space of diabetic mice.[414] Hyaluronic acid hydrogel have also been used to encapsulate islets, and after 80 days *in vivo*, not only were the mice non-diabetic due to the functioning encapsulated islets, histological

analysis showed little to no cellular overgrowth around the implant.[415] Lastly, although various polymers can also be combined to modulate the immune response, there is a narrow window in chemistry and capsule processing that may limit successful use of multi-polymer microcapsules. One study showed that subtle changes in the concentration of any of the components in a multi-component polymer capsule fabricated from the combination of sodium alginate, cellulose sulfate, poly (methylene-co-guanidine) hydrochloride, calcium chloride, and sodium chloride can lead to severe biocompatibility issues.[314,416]

1.7.2.3 PEGylation

Polyethylene glycol (PEG) is used for a variety of drug delivery and nanotechnology applications due to its high biocompatibility. Coating the surface of proteins or drugs with PEG molecules, or "PEGylation" is a widely used technique that allows particles to evade the immune system and prolong their circulation time. Addition of the PEG brush layer creates an impermeable layer on the surface of the attached polymer, causing steric hindrance that prevents protein adsorption along with the subsequent immune cell response. This protein resistance depends on PEG brush layer density, length, and conformation.[417–419] Recently, there have been many advances in using this technique for nanoencapsulation of cells, particularly islets.

Successful covalent attachment of PEG to primary rat islets has been demonstrated by several groups, demonstrating that single polymer grafting approach can be used with islets to successful modulate local transplant environment without adversely affecting cell survival or function.[82,420] PEGylated islets have also showed a 90% decrease in antibody binding, making them antigenically silent. Moreover, these

islets decreased lymphocyte proliferation when cultured in the presence of lymphocytes in vitro. Thin conformal coating of islets with PEG-alginate using microfluidics is also another PEGylation that can be used to minimize graft size and volume, while preventing fibrosis.[82,233,421,422] However, in most cases, results showed that PEGylation only delays the rejection of allogeneic and xenogeneic grafts in rodent models, indicating that further enhancement of this therapy is necessary to completely prevent the post-transplant immune reaction.[423] A study showed that transplantation of PEGylated islets led to 60% normoglycemia in diabetic mice for more than 100 days, while local delivery of anti-LFA-1 antibody alone resulted in 50% euglycemia in diabetic mice. The combination of these two strategies, in which PEGylated islets were transplanted along with anti-LFA-1 antibody, however, showed synergistic effects, with 78% of the grafts exhibiting euglycemia at 100 days.[418] Co-transplantation of PEGylated islets with combination therapy of cyclosporine A (CsA) and anti-CD4 monoclonal antibody (OX-38), also again showed synergistic effects after 30 days *in vivo*.[417,424] In fact, the combinatorial approach of sub-therapeutic dosage of CsA and PEGylated islets provided a semi-permanent effective therapy for at least 1 year. The non-fasting blood glucose levels of mice treated with the combinatorial approach showed no significant change at day 100, day 200, and 1 year. Although the insulin production levels decreased after 1-year, further refinement of this therapy can offer great promise in long-term protection of islets.[417] Moreover, a recently published study included rapamycin monotherapy alongside allotransplantation of PEGylated islets in non-human primate model. Even at the lowest islet dosage (4160 IEQ/kg), animals with PEGylated islets had significantly higher glycemic function, higher

fasting C-peptide levels, and required no exogenous insulin supply as compared to the untreated controls.[419]

A potential method to enhance islet protection through PEGylation is by increasing PEGylation layers. Increasing the amount of PEG conjugated to islet surfaces through multiple PEGylation or by amplifying PEGylation using poly-l-lysine, poly(allylamine), or poly(ethyleneimne) can completely shield islets. Although increased PEGylation with these molecules caused greater islet cell toxicity, the overall cell viability and function were unaffected. In fact, 100 days after allotransplant, 3 out of the 7 mice showed survival of triple PEGylated islets in diabetic mice. The 4 transplants that were rejected still showed immune cell protection at day 20, while the control, naked islet grafts, did not even survive 1 week.[425] Another method to enhance PEGylation involves attaching nanoparticles to PEGylated islets. A group showed that long-term (>100 days) euglycemia in 30% of PEGylated grafts, 43% of PEGylated grafts with empty nanoparticles, and 57% of PEGylated grafts with leukemia inhibitory factor (a factor that promotes adaptive immune tolerance and regulated pancreatic β cell mass). The addition of nanoparticles on the PEGylated islets expand the potential of this therapy as they allow for local, sustained delivery of immunomodulatory drugs.[82,426]

1.7.3. Macroencapsulation

Macroencapsulation is another promising strategy for islet replacement as it allows encapsulation of large number of islets in a retrievable and replenishable device. These larger, micron-scaled, semi-permeable devices may allow greater selectivity through manipulation of membrane properties. However, due to larger device size, macroencapsulation devices tend to be limited by oxygen and nutrient diffusion that leads

a greater loss in cell mass. Currently, there is not a universally accepted macroencaspulation device design, size, or material that has shown to provide maximum cell viability and function while preventing immune cell infiltration. Therefore, many research groups have developed their own encapsulation devices, with carefully chosen materials, pore sizes, and surface coatings to increase the device's function as a cell encapsulation technology for T1D. However, regardless of these differences, an issue that still remains chemical and mechanical properties of the device can induce a foreign body response post-implant, which eventually leads to implant failure.[74,427,428]

The need to modulate fibrosis for macroencapsulation devices was demonstrated through the outcomes of the commercially available TheraCyte device produced by Baxter Healthcare. The device was a planar pouch fabricated from PTFE, designed to promote vasculature around the device while still isolating the encapsulated cells. This was done through the double membranes, in which the outer membrane was 15 μm thick with 5 μm pore size that allowed for angiogenesis and the inner membrane was 30 μm thick with 0.4 μm pore size that allowed for immune protection. After 6 months of implant in rats, severe fibrosis had developed inside the device, although no inflammatory cells were observed in close proximity to the outer membranes of the device. However, due to the likelihood of fibrosis, graft survival time post-transplant was shortened and limits the use of this device for clinical applications. This result of fibrosis is attributed to the material itself (PTFE), which has been associated with inducing inflammatory reactions that activate FBR and fibrosis.[427,429]

To avoid the results seen from the TheraCyte device, inert synthetic polymers such as polycaprolactone (PCL) can be used to fabricate islet macroencapsulation devices.

Indeed, porous, thin-film PCL devices can support the survival and function of stem-cell derived insulin producing cells for 6 months *in vivo*. One of the key factors that contributes to the success of these devices is the material itself. PCL is a nontoxic polymer that has been used in numerous FDA-approved medical devices. Compared to other polyesters, it has a lower ratio of esters to carbon, allowing it to have longer degradation times. Moreover, when the ester bonds are degraded through hydrolytic cleavage, the resulting byproduct is caproic acid, which is well tolerated by the body. Histological results show that when implanted in the subcutaneous space for four months, porous PCL shows no deposition of fibrotic tissue along the graft. This contrasts greatly from polypropylene films, which showed collagen deposition around the graft and greater immune cell infiltration. Immunostaining after one month of implant also showed that, overall, porous PCL had increased blood vessel formation and reduced fibrosis and macrophage recruitment when the device was transplanted near the liver and the subcutaneous space.[430–433]

A recently published study also reported a new retrievable and scalable cell encapsulation device that can be used for islet transplantation.[434] The body of the device was made of PDMS, and the internal structure, fabricated using photolithography, contained chambers designed specifically for holding encapsulated cells along with an injection port for loading cells. Porous PCTE membrane was chemically bonded to the PDMS chips, allowing for controlled release of small molecules while protecting encapsulated cells from immune attack.[434] To address the issue of biocompatibility, zwitterionic polymers were coated onto the surface of the PCTE membranes through surface-initiated atom transfer radical polymerization, allowing growth of dense brush

layers on the surface of the membrane. Their studies found that membranes coated with small molecule tetrahydropyran phenyl triazole (THPT) showed 70% reduction in collagen buildup after 4 weeks of implantation. Gene expression analysis showed that THPT coating suppressed expression of CD146, a marker for neovascularization, as well as TNFα and IL-1β, which are inflammatory cytokines.[434] Overall, there was significantly lower cellular overgrowth and total DNA content around the device compared to non-coated membranes. Moreover, rat islets in alginate solution were loaded in the uncoated and THPT-coated devices, and results showed that, upon implantation in diabetic mice, the encapsulated device was able to restore euglycemia in mice for over 75 days.[434] Although the devices failed during the late phase of the study, this failure in devices was not due to fibrosis as minimal fibrotic deposition was observed around the device. Additionally, human embryonic kidney cells were also encapsulated in these THPT-coated devices, and even after 130 days, the coated devices provided protection against fibrosis.[434]

Instead of using a sturdy, polymeric encapsulation device, efforts have also been focused on increasing the mechanical properties of hydrogels so that they can serve as retrievable encapsulation devices. A group has developed a technique to fabricate nanofiber-enabled encapsulation devices (NEEDs) by impregnating Nylon 6 tubular or planar electrospun nanofiber membranes with hydrogel precursor solution using capillary action.[435] After the hydrogel had completely infiltrated the electrospun nanofiber membranes, the hydrogel precursor solution was crosslinked, resulting in hydrogels of various sizes, porosities, and greater mechanical properties. Not only were these devices able to encapsulate various cell types, but they also retained the biocompatible properties

of the hydrogels. Moreover, primary islets suspended in Matrigel were encapsulated into NEEDs and transplanted into the peritoneal cavity of diabetic mice. After 8 weeks, the mice showed corrected blood glucose levels with minimal fibrosis around the graft. This strategy allows for the use of versatile polymers such as polycaprolactone (PCL) and polyacrylonitrile (PAN) that can be electrospun into various shapes and sizes as well as various hydrogels such as PEG and collagen that can be impregnated with cells to provide greater survival.[435]

Some groups have also shown that natural polymers can be used to enhance islet transplantation as well as mitigate fibrosis in macroencapsulation devices. Engagement with ECM components such as collagen is critical for islets as it has been shown that in vitro culture of islets with collagen promotes islet differentiation, survival,[436,437] and reorganization of pancreatic endocrine cell monolayers into islet-like organoids.[433,438,439] Using this knowledge, a group explored the use of type I oligomeric collagen scaffolds for encapsulating islets. This group used an oligomer, instead of monomeric collagen, because oligomers can retain their natural intermolecular crosslinks that result in interconnected, fibrillar scaffolds of high stiffness and longer degradation times. When islets were encapsulated in these type I oligomeric collagen devices/scaffolds and implanted in the subcutaneous space for 14 days, results showed high biocompatibility with no inflammatory reaction around the implant along with preservation of islet morphology. These qualities of the scaffolds heavily contributed in the ability of the encapsulated islets to correct and maintain low blood glucose levels of diabetic mice for up to 90 days in vivo.[440] Another similar approach of promoting formation of extracellular matrix by developing a fibroblast populated type-I collagen matrix scaffold has been

successful as well. This approach showed a significant increase in insulin secretion and reduced the critical islet mass required to reverse diabetes from 200 to 100 islets per recipient. Moreover, due to the fibroblasts embedded in the scaffold, higher production of growth factors and increased cell proliferation was observed. This increase in cell proliferation, however, did not lead to fibroblast over-growth, demonstrating the fabrication of a device that enhances engraftment with controlled fibrotic response.[433]

Additionally, the combined use of natural and synthetic materials has also been explored. A group has fabricated alginate hydrogel capsule that is surrounded and bound to a nanoporous, wettable, Ca^{2+} releasing nylon polymer thread, resulting in *in situ* crosslinking of the alginate hydrogel. This thread-reinforced alginate fiber for islet encapsulation (TRAFFIC) device provides facile mass transfer while still providing the mechanical stability needed for easy implantation and retrieval. The therapeutic potential of this device for treating T1D was also demonstrated when rat islets were encapsulated and implanted into diabetic C57BL/6 mice and human islets were encapsulated and implanted into SCID-Beige mice. Both the models demonstrated diabetes correction for several months, and additionally, the scaling up of the device in dogs was also proven. Additionally, changing the thickness of the alginate devices so that they have a diameter of ~1.3 mm lowered cellular overgrowth than thinner devices with diameter of 500 μm after 7-month of implantation in the intraperitoneal space. Even implantation in dogs showed no fibrosis or histological evidence of inflammation in the tissue, further confirming the biocompatibility of the device.[396]

Lastly, a new technology that incorporates microencapsulation of islets in a three-dimensional structure to promote a microenvironment that is conducive to survival of islets

also shows great potential in providing long term treatment for T1D. Islets in PEG hydrogel were casted into a PDMS mold, and after 12 days of implantation in the epididymal fat, encapsulated islets were able to promote euglycemia. Moreover, after 8 weeks of implantation, histological staining showed a thin layer of connective tissue around the hydrogel, demonstrating that these devices were integrated in the body and did not result in a foreign body response.[441]

1.7.4 Vascular perfusion devices

The challenges of inadequate supply of nutrients, hypoxia, and central necrosis in extravascular devices (micro and macro encapsulation) impelled the development of vascular perfusion devices (such as intravascular diffusion chamber and intravascular ultrafiltration chamber).[233,399] Intravascular bioartificial pancreas device (iBAP) is anastomosed to blood vessels, allowing blood perfusion through the device.[442] Unlike extravascular devices, iBAPs do not rely on passive diffusion and instead rely on connective mass transfer of glucose and insulin across the immune isolation barrier membrane. This intravascular approach, however, interposes normal blood flow and results in acute implant rejection due to immediate blood mediated inflammation reaction (IBMIR).[82,233,248,399] Consequently, activation of the coagulation cascade and complement system leads to thrombosis, which reduces the membrane permeability and eventually leading to islet necrosis.[82,233,248] Additionally, this approach requires more intensive and invasive surgical procedures that result in significant vessel injuries and tissue trauma, which further exacerbate the immune response to iBAPs.

For vascular perfusion devices, traditionally, a two-prong approach is used to manage immune response to both IBMIR and FBR.[103,443] The two strategies are to, first, select an immune evasive, inert, synthetic, non-degradable biomaterial for fabricating both the immune isolation membrane and shell of the iBAP, and second, to immobilize active immune modulators, such as small molecules and other biologics. With these devices, there is a greater risk of coagulation and hemorrhage complications, and this limits the choice of biomaterials used to fabricate the immune isolation membrane of iBAPs. An example of iBAP material that has achieved partial feat is a silicon nanopore membrane.[84,86] This membrane emerged as a preferred choice due to its established bioinert and biocompatible nature. Another example of such a material is alumina, however, complete understanding of its in vivo biocompatibility is still unknown.[233,444–446] Although, titania nanopores membranes for intravascular device can also be used as titania has been already approved for a few other implants, but more studies need to be conducted on the use of titania nanopores in terms of its immune-isolation properties, pore characteristics, and compatibility with implanted islets.[170,180,183,444–446] Negative photoresist SU-8 2025 and 2075,[258,444,446,447] along with polycarbonate (PC), ePTFE, Dacron, PU, and nylon, have also been evaluated,[443,444,446,448,449] but all these materials have sown minimal success as fluid exchange through the nanopore membranes eventually slowed, leading to thrombosis, clotting, and fibrosis.

Due to the limited choices of biomaterials for vascular perfusion devices, more efforts have been placed in developing approaches to modulate the immune system therapeutically. Typically, before encapsulation, islets can be cultured in the presence of small molecules, such as L-arginine,[330,450,451] cyclosporine A,[82,248] enalapril,[452,453]

nicotinamide,[454–456] vitamin B derivative, that will suppress the initial inflammatory reaction caused by islet associated tissue factors and other chemotactic factors, such as MCP-1, MIF, IL-8. Monoclonal antibodies, siRNA, and other active site inhibitors are also used to attenuate IBMIR.[457]

Inhibition of the coagulation system can also increase long term efficacy of iBAPs. Anticoagulants and antiapoptotic molecules, such as activated protein C (APC),[458–460] thrombin inhibitors (such as melagatran, N-acetylcysteine),[461–464] and platelet inhibitors (anti-GP IIb/IIIa),[465,466] significantly reduce pro-inflammatory cytokines and inhibit IBMIR. Thrombomodulin and human recombinant antithrombin (ATryn)[467–470] can limit thrombosis and reduce deposition of fibrin, infiltration of PMN leukocytes, expression of pro-inflammatory cytokines, and thrombin-antithrombin (TAT) complex.[82] Withaferin-A, an anti-NFκB molecule, can also suppress the inflammatory response to implanted islets and IBMIR.[471–475]

Additionally, antibodies from islets and the coagulation process also trigger the complement system, which initiates recruitment of immune cells. Complement inhibitor (compstatin) and anaphylatoxin inhibitory peptide (C5aIP) can effectively manage complement system-induced inflammatory response.[471,476,477] Low molecular weight dextran sulfate (LMW-DS) can also successfully inhibit the coagulation and complement cascade. CD39 and soluble form of CR1 can serve as attractive targets to ameliorate the IBMIR and FBR.[92,478,479]

Surface coating is one of the most widely used immune engaging strategies in the context of vascular perfusion devices in which the immune isolation membrane or encapsulated islets are coated with an immune-passivation material. For example, silicon

nanopore membranes have been modified with PEG to minimize protein fouling, which prevents IBMIR and FBR.[84,233,442,480] Also, coating poly(sulfobetaine methacrylate) (pSBMA), a zwitterionic polymer, on silane treated silicon-nanopore immune isolation membrane has also demonstrated effective suppression of the immune reaction. Other zwitterionic polymers, such as poly(2-methacryloyloxyethyl phosphorylcholine) (pMPC) and poly oligo(ethylene glycol) methyl ether methacrylate (pOMEGA), can also be coated on silicon nanopore membranes to form brush-like structures change surface hydrophilicity such that steric repulsion prevents protein and cell adhesion, leading to attenuation of FBR.[166,272,360,361,448]

Lastly, cell surface modification or islet-endothelial cells (EC) co-graft have also been effective in modulating the immune response. The amine group on the surface of islets cans be used to covalently attach an ultrathin heparin-PEG film, which can successfully suppress IBMIR and modulate immune cell response.[300,444,448] IBMIR and FBR can also be downregulated by reducing complement and coagulation activation with a coating of biomolecules, such as thrombomodulin, urokinase, APC, and sCR1.[233,468] These biomolecules can be linked onto the islet surface using maleimide/thiol bonding or DNA hybridization.[82,110] ECs or colony-forming ECs can also be co-transplanted with islets as ECs are neutral to blood exposure, lower the C3a level and TAT complex formation, preventing IBMIR and FBR.[110,408,481–483]

1.7.5. Ancillary strategies

In addition to the work predominantly focused on mitigating the FBR accompanying implantable CGMs, intravascular and extravascular islets encapsulation devices, many

independent efforts are also being made in the field. Efforts to address fibrosis and associated challenges in various domains can be effectively expanded to enhance the range of available strategies for implants used in diabetes mellitus management.

We have discussed crucial role of biomechanics in FBR and fibrosis, and several biomechanical design aspects for the implant to resist the FBR.[199,206,324] Recently published work on an actuatable soft reservoir for modulating host FBR uses a milli-scale dynamic soft reservoir (DSR) to mechanically oscillate and, subsequently, modulate the implant-tissue interface's biomechanics for downregulating pro-inflammatory response. The induced oscillatory motion at the biotic-abiotic interface perturbs fluid flow along with cellular activity in the peri-implant tissue, promoting an anti-inflammatory response and reducing the fibrotic capsule while preserving its coherency and collagen maturity. This is a highly versatile and tunable DSR platform that can be integrated with implantable devices to manage diabetes mellitus, specifically for continuous glucose sensors and cell encapsulation devices, for which rapid diffusion of glucose, insulin, oxygen, and other small molecules are required to improve medical outcomes.[484]

On a similar principle, using magnetoelastic resonator can also modulate FBR at the biotic-abiotic interface. This exciting work describes a passive, wireless, resonant magnetoelastic actuator to manipulate the fluid flow on the surface of implantable Ahmed glaucoma drainage devices. The magnetic field, generated by external coils, remotely excites the actuator to resonate, generating perturbations that limit FBR and significantly augment glaucoma drainage devices' efficacy for lowering intraocular pressure. The ability of the magnetoelastic actuators can be appropriated for fibrosis mitigation in the implants for diabetes treatment.[485]

Likewise, the mechanical mismatch, in terms of topography, surface geometry, surface chemistry, between the implant and peri-implant tissue is a driver of FBR. Matching the implant stiffnesses with host tissue and providing surface properties that resist non-specific protein and cell binding significantly reduce pro-inflammatory response. A study exploited these key drivers and incorporated them while designing the sheath for the cardiac implantable electronic device (CIED). Scientists micro-engineered a non-resorbable, biosynthesized cellulose (BC) membrane that can be conformally wrapped around CIED implants. The mechanical properties of BC membrane, along with the rendered surface topography and spatial arrangement, synergistically minimized the adhesion and differentiation of the cellular mediators responsible for FBR. This BC conformal sheathing can be effectively borrowed and employed for CGMs, intravascular and extravascular cell encapsulation strategies to extenuate FBR.[174,484,486]

Additionally, in terms of local delivery of FBR mitigating molecules, the effect of an active modulation of immune response using small and large biomolecules wear off with the depletion of the drug and/or changes in release rate. An exciting study addressed this issue by fabricating crystallized concentrated drug depots of the various anti-inflammatory drugs within implants' (such as micro, macro extravascular cell-encapsulation devices, and implantable CGMs) material. These concentrated drug depots offer long-term, sustained release of the active immune modulators, which extends the overall lifespan (more than 12 months) of the implant and functional performance by reducing the fibrosis.[393]

1.8 Concluding Remarks

All current and future treatments for DM require the use of implants or cellular grafts that can detect blood glucose levels and secrete insulin for correction of the detected blood glucose levels. Technologies like CGMs (percutaneous or subcutaneous electrochemical sensors), artificial pancreas, intravascular, extravascular immuno-isolation, and cell encapsulation not only improve the outcome, but also have the potential to be a cure for DM. The long-term function and efficacy of these grafts depends on the activation and regulation of the immune cascade, which consists of two phases: the inflammatory phase and reparative phase. In the inflammatory phase, cellular debris is cleared through the secretion of proteolytic enzymes, degradation enzymes, inflammatory cytokines, etc. Once the debris has been cleared, the reparative phase dominates, in which cytokines and chemokines that promote angiogenesis and integration of the implant are secreted. After cells such as fibroblasts have completed the tissue repair process through deposition of collagen, the implant has successfully integrated within the body. However, if there are inflammatory cues present that prevent the resolution of the immune cascade, foreign body giant cells form, leading to excessive collagen deposition (fibrosis) and device failure. Therefore, it is essential to develop biomaterials that will not trigger a strong, inflammatory immune response that leads to fibrotic overgrowth and rejection of implant.

The body's immune response to an implanted biomaterial can be regulated by protein adsorption, biomechanics of the implant material and tissue, and cellular activation. Protein adsorption on the implant surface occurs almost instantaneously and plays a key role in the immune cell – implant interaction. Biomechanics of the biomaterial

as well as the tissue also affect the immune response, as mechanical loading and stress at implant site can directly promote secretion of soluble factors by immune cells. Both protein adsorption and biomechanics affect the activation of the immune cascade, in which various cell types are involved. Secretion of soluble factors or expression of surface markers can activate multiple cell types from both the innate and the adaptive immune system.

Knowing the factors that play a key role in the activation and progression of foreign body response, biomaterials can be modified such that the foreign body response can be minimized. Immune evasive strategies involve the use of natural biomaterials or relatively inert synthetic materials. Immune-engaging strategies, on the other hand, involve changing material surface properties by changing surface chemistry, biofunctionalizing the surface, applying surface coating, adding surface patterning or topography, and changing the materials' mechanical properties. All these strategies have been applied to implants, particularly those used for diabetes. Many groups have demonstrated the effectiveness of these strategies in mitigating fibrosis. However, due to the intricate nature of the immune response, no strategy has had complete long-term success *in vivo*.

A potential way to further increase efficacy of implant materials in mitigating fibrosis could be through combinations of the various stand-alone solutions that have been used in the past. By combining different strategies, a greater synergistic effect may be induced. Moreover, the mechanisms by which the immune cells interact with biomaterials have not been completely elucidated. Key details about which factors are contributing to this immune cell activation are crucial for successful design of an anti-fouling implant. More insights on macrophage polarization would also be beneficial for designing biomaterials

that promote the reparative M2 macrophage phenotype and subsequent integration of implant.

Increasing knowledge and insight on how the biological events can be modulated by changing chemical and physical properties of implant material, along with recent advances, will introduce highly biocompatible implants that have greater longevity *in vivo*. The future of the field of diabetes relies on this advancement as more sophisticated implant designs will allow implantable technology for diabetes to reach its full potential.

Table 1.1. Summary of the four different types of implants used to treat T1D and T2D

Treatment	Disease Type	Purpose
Continuous Glucose Monitors (CGMs)	T1D, T2D	Allows diabetes management through continuous measurement of glucose concentration in interstitial fluid. Can be connected to insulin pumps that can release insulin once high glucose levels are detected by CGM
Vascular Perfusion Devices	T1D	Intravascular bioartificial pancreas (iBAP) are semi-permeable islet encapsulation devices that are anastomosed to blood vessels, allowing blood perfusion through the device. Rely on connective mass transfer of glucose and insulin across the membrane instead of passive diffusion.
Islet Microencapsulation	T1D, T2D	Provides insulin delivery without the need for patient compliance by replacing islets/ β cells. Islets or stem-cell derived β cells are encapsulated in micron-sized semi-permeable encapsulation devices, which can be implanted in various parts of the body. Provides high surface area to volume ratio for increased access to nutrients and oxygen, thereby increasing encapsulated cell viability.
Islet Macroencapsulation	T1D, T2D	Provides insulin delivery without the need for patient compliance by replacing islets/ β cells. Islets or stem-cell derived β cells are encapsulated in macro-scale sized semi-permeable encapsulation devices. Allows transfer of larger number of islets.

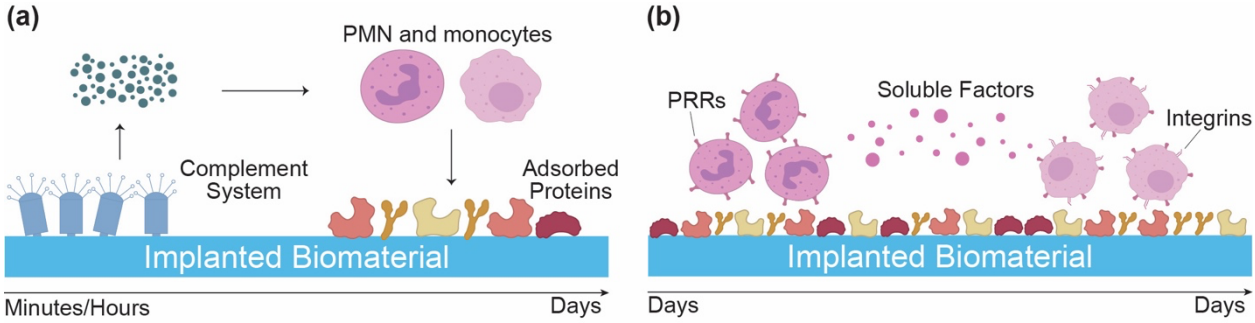

Figure 1.1. Multiple interrelated pathways activate the immune cascade post-implantation. **(a)** Soluble factors released from the activation of complement system (C3a, C5a), prime polymorphonuclear leukocytes (PMN) and macrophages. **(b)** The primed immune cells interact with adsorbed proteins through pattern recognition receptors (PRRs) that recognize pattern associated molecular patterns (PAMPs) on biomaterial. Soluble factors released from PMNs further activate monocytes, which use both PRR and integrins to interact with the implanted biomaterial. Monocytes differentiate into macrophages and control the subsequent immune response.

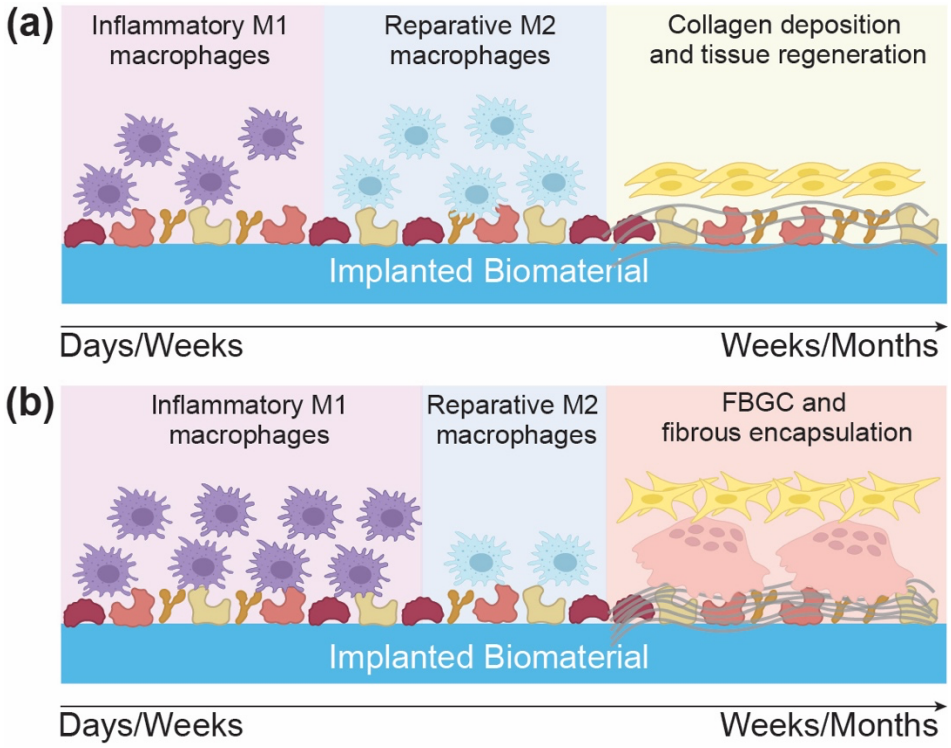

Figure 1.2. The fate of the implant depends on the resolution of the inflammatory immune cascade. **(a)** If macrophages can polarize from the inflammatory stage (M1) to their reparative stage (M2), they release soluble factors that promote fibroblasts to

secrete collagen and promote integration of the implant. **(b)** If macrophages are unable to successfully transition from M1 to M2 phenotype, foreign body giant cells (FBGC) form and adhere to the implant surface. FBGC secrete more inflammatory soluble factors that activate myofibroblasts (fibrotic phenotype of fibroblasts), which secrete excessive amounts of collagen, leading to fibrous encapsulation of implant.

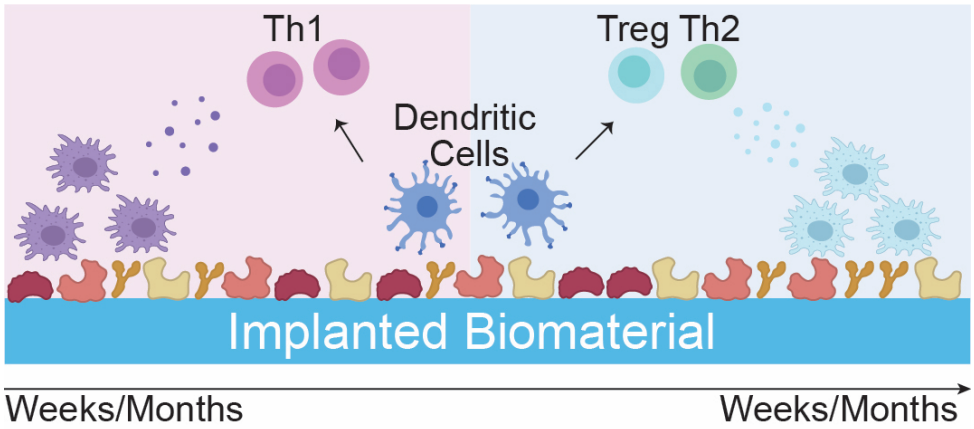

Figure 1.3. Macrophages and dendritic cells work together to activate the adaptive immune system. Dendritic cells and sometimes, macrophages present antigens to T cells that stimulate activation of different T cell subtypes. These subtypes are influenced by the soluble factors present in the local microenvironment. If pro-inflammatory macrophages are present, the secreted soluble factors activate the inflammatory Th1 CD4 cells. Meanwhile, if reparative macrophages are present, they secrete factors that activate the reparative Th2 CD4 cells along with regulatory CD4 (Treg) cells.

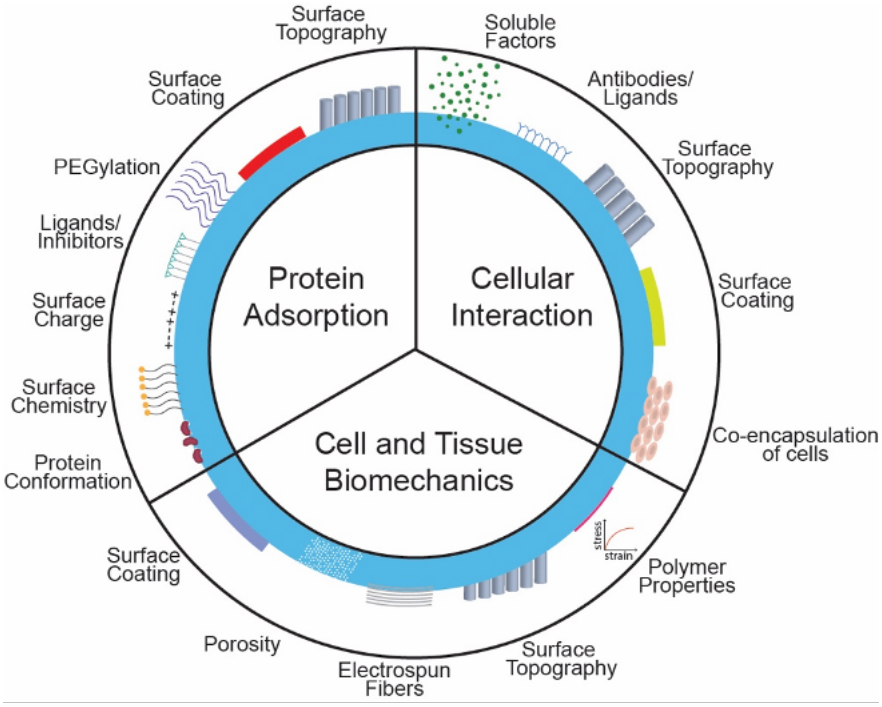

Figure 1.4. Several strategies can be used to mitigate the FBR and resulting fibrotic overgrowth. The three major categories that are affected by changes in material properties are protein adsorption, cell and tissue biomechanics, and cellular interaction. Changes in any of these three categories can induce a favorable immune response towards implants and increase their longevity as well as function in vivo.

1.9 References

1. Jiménez PG, Martín-Carmona J, Hernández EL. Diabetes mellitus. Med Spain. Published online 2020. doi:10.1016/j.med.2020.09.010
2. Atkinson MA, Eisenbarth GS, Michels AW. Type 1 diabetes. The Lancet. Published online 2014. doi:10.1016/S0140-6736(13)60591-7
3. Katsarou A, Gudbjörnsdottir S, Rawshani A, et al. Type 1 diabetes mellitus. Nat Rev Dis Primer. Published online 2017. doi:10.1038/nrdp.2017.16
4. Paschou SA, Papadopoulou-Marketou N, Chrousos GP, Kanaka-Gantenbein C. On type 1 diabetes mellitus pathogenesis. Endocr Connect. Published online 2018. doi:10.1530/EC-17-0347
5. Samson SL, Garber AJ. Type 2 diabetes. In: Encyclopedia of Endocrine Diseases. ; 2018. doi:10.1016/B978-0-12-801238-3.95795-7
6. DeFronzo RA, Ferrannini E, Groop L, et al. Type 2 diabetes mellitus. Nat Rev Dis Primer. Published online 2015. doi:10.1038/nrdp.2015.19
7. Chatterjee S, Khunti K, Davies MJ. Type 2 diabetes. The Lancet. Published online 2017. doi:10.1016/S0140-6736(17)30058-2
8. Schwartz SS, Epstein S, Corkey BE, Grant SFA, Gavin JR, Aguilar RB. The Time Is Right for a New Classification System for Diabetes: Rationale and Implications of the β-Cell–Centric Classification Schema. Diabetes Care. 2016;39(2):179-186. doi:10.2337/dc15-1585
9. Classification and diagnosis of diabetes. Diabetes Care. Published online 2017. doi:10.2337/dc17-S005

10. Usmani-Brown S, Perdigoto AL, Lavoie N, et al. β cell responses to inflammation. Mol Metab. Published online 2019. doi:10.1016/j.molmet.2019.06.013
11. Wilcox NS, Rui J, Hebrok M, Herold KC. Life and death of β cells in Type 1 diabetes: A comprehensive review. J Autoimmun. Published online 2016. doi:10.1016/j.jaut.2016.02.001
12. Burrack AL, Martinov T, Fife BT. T cell-mediated beta cell destruction: Autoimmunity and alloimmunity in the context of type 1 diabetes. Front Endocrinol. Published online 2017. doi:10.3389/fendo.2017.00343
13. Oram RA, Sims EK, Evans-Molina C. Beta cells in type 1 diabetes: mass and function; sleeping or dead? Diabetologia. Published online 2019. doi:10.1007/s00125-019-4822-4
14. Stabler CL, Li Y, Stewart JM, Keselowsky BG. Engineering immunomodulatory biomaterials for type 1 diabetes. Nat Rev Mater. Published online 2019. doi:10.1038/s41578-019-0112-5
15. Fernández-Real JM, Pickup JC. Innate immunity, insulin resistance and type 2 diabetes. Diabetologia. Published online 2012. doi:10.1007/s00125-011-2387-y
16. Pickup JC. Inflammation and Activated Innate Immunity in the Pathogenesis of Type 2 Diabletes. Diabetes Care. Published online 2004. doi:10.2337/diacare.27.3.813
17. Velloso LA, Eizirik DL, Cnop M. Type 2 diabetes mellitus - An autoimmune disease? Nat Rev Endocrinol. Published online 2013. doi:10.1038/nrendo.2013.131

18. Odegaard JI, Chawla A. Connecting type 1 and type 2 diabetes through innate immunity. Cold Spring Harb Perspect Med. Published online 2012. doi:10.1101/cshperspect.a007724
19. Tsalamandris S, Antonopoulos AS, Oikonomou E, et al. The role of inflammation in diabetes: Current concepts and future perspectives. Eur Cardiol Rev. Published online 2019. doi:10.15420/ecr.2018.33.1
20. Piñero-Piloña A, Raskin P. Idiopathic Type 1 diabetes. J Diabetes Complications. Published online 2001. doi:10.1016/S1056-8727(01)00172-6
21. Report NDS. National Diabetes Statistics Report, 2020. Natl Diabetes Stat Rep. Published online 2020.
22. WHO. Non-Communicable Diseases Fact Sheet. Public Health Action Guide Improv Health. Published online 2018.
23. WHO. Global action plan for the prevention and control of noncommunicable diseases 2013-2020. World Health Organ. Published online 2013. doi:978 92 4 1506236
24. WHO. Diabetes Programme. World Health Organ. Published online 2018.
25. Internation Diabetes Federation. IDF Diabetes Atlas Ninth.; 2019.
26. Nathan DM. Diabetes: Advances in diagnosis and treatment. JAMA - J Am Med Assoc. Published online 2015. doi:10.1001/jama.2015.9536
27. Bansal N. Prediabetes diagnosis and treatment: A review. World J Diabetes. Published online 2015. doi:10.4239/wjd.v6.i2.296
28. American Diabetes Association. Diagnosing Diabetes and Learning About Prediabetes. WwwDiabetesOrgDiabetes-BasicsDiagnosis. Published online 2015.

29. Classification and diagnosis of diabetes: Standards of Medical Care in Diabetes-2020. Diabetes Care. Published online 2020. doi:10.2337/dc20-S002
30. Frid AH, Kreugel G, Grassi G, et al. New Insulin Delivery Recommendations. Mayo Clin Proc. 2016;91(9):1231-1255. doi:10.1016/j.mayocp.2016.06.010
31. Malik FS, Taplin CE. Insulin therapy in children and adolescents with type 1 diabetes. Pediatr Drugs. Published online 2014. doi:10.1007/s40272-014-0064-6
32. Farrar D, Tuffnell DJ, West J, West HM. Continuous subcutaneous insulin infusion versus multiple daily injections of insulin for pregnant women with diabetes. Cochrane Database Syst Rev. Published online 2016. doi:10.1002/14651858.CD005542.pub3
33. Silver B, Ramaiya K, Andrew SB, et al. EADSG Guidelines: Insulin Therapy in Diabetes. Diabetes Ther. Published online 2018. doi:10.1007/s13300-018-0384-6
34. Brown J, Grzeskowiak L, Williamson K, Downie MR, Crowther CA. Insulin for the treatment of women with gestational diabetes. Cochrane Database Syst Rev. Published online 2017. doi:10.1002/14651858.CD012037.pub2
35. Pharmacologic approaches to glycemic treatment. Diabetes Care. Published online 2017. doi:10.2337/dc17-S011
36. Boughton CK, Hovorka R. The artificial pancreas. Curr Opin Organ Transplant. Published online 2020. doi:10.1097/MOT.0000000000000786
37. Boughton CK, Hovorka R. Advances in artificial pancreas systems. Sci Transl Med. Published online 2019. doi:10.1126/scitranslmed.aaw4949
38. Brooker G. The artificial pancreas. In: Handbook of Biomechatronics. ; 2018. doi:10.1016/B978-0-12-812539-7.00015-5

39. Bekiari E, Kitsios K, Thabit H, et al. Artificial pancreas treatment for outpatients with type 1 diabetes: Systematic review and meta-Analysis. BMJ Online. Published online 2018. doi:10.1136/bmj.k1310
40. Blauw H, van Bon AC, Koops R, DeVries JH. Performance and safety of an integrated bihormonal artificial pancreas for fully automated glucose control at home. Diabetes Obes Metab. Published online 2016. doi:10.1111/dom.12663
41. Thabit H, Hovorka R. Coming of age: the artificial pancreas for type 1 diabetes. Diabetologia. Published online 2016. doi:10.1007/s00125-016-4022-4
42. Haidar A, Legault L, Messier V, Mitre TM, Leroux C, Rabasa-Lhoret R. Comparison of dual-hormone artificial pancreas, single-hormone artificial pancreas, and conventional insulin pump therapy for glycaemic control in patients with type 1 diabetes: An open-label randomised controlled crossover trial. Lancet Diabetes Endocrinol. Published online 2015. doi:10.1016/S2213-8587(14)70226-8
43. Peyser T, Dassau E, Breton M, Skyler JS. The artificial pancreas: Current status and future prospects in the management of diabetes. Ann N Y Acad Sci. Published online 2014. doi:10.1111/nyas.12431
44. Hovorka R. Closed-loop insulin delivery: From bench to clinical practice. Nat Rev Endocrinol. Published online 2011. doi:10.1038/nrendo.2011.32
45. Cobelli C, Renard E, Kovatchev B. Artificial pancreas: Past, present, future. Diabetes. Published online 2011. doi:10.2337/db11-0654
46. Nimri R, Nir J, Phillip M. Insulin Pump Therapy. Am J Ther. Published online 2020. doi:10.1097/MJT.0000000000001097

47. Van Enter BJ, Von Hauff E. Challenges and perspectives in continuous glucose monitoring. Chem Commun. Published online 2018. doi:10.1039/c8cc01678j
48. Relative effectiveness of insulin pump treatment over multiple daily injections and structured education during flexible intensive insulin treatment for type 1 diabetes: cluster randomised trial (REPOSE). BMJ. Published online March 30, 2017:j1285. doi:10.1136/bmj.j1285
49. Karges B, Schwandt A, Heidtmann B, et al. Association of insulin pump therapy vs insulin injection therapy with severe hypoglycemia, ketoacidosis, and glycemic control among children, adolescents, and young adults with type 1 diabetes. JAMA - J Am Med Assoc. Published online 2017. doi:10.1001/jama.2017.13994
50. Bruen D, Delaney C, Florea L, Diamond D. Glucose sensing for diabetes monitoring: Recent developments. Sens Switz. Published online 2017. doi:10.3390/s17081866
51. Klonoff DC, Ahn D, Drincic A. Continuous glucose monitoring: A review of the technology and clinical use. Diabetes Res Clin Pract. Published online 2017. doi:10.1016/j.diabres.2017.08.005
52. Rodbard D. Continuous Glucose Monitoring: A Review of Successes, Challenges, and Opportunities. Diabetes Technol Ther. Published online 2016. doi:10.1089/dia.2015.0417
53. Steineck I, Cederholm J, Eliasson B, et al. Insulin pump therapy, multiple daily injections, and cardiovascular mortality in 18 168 people with type 1 diabetes: Observational study. BMJ Online. Published online 2015. doi:10.1136/bmj.h3234

54. Brennan DC, Kopetskie HA, Sayre PH, et al. Long-Term Follow-Up of the Edmonton Protocol of Islet Transplantation in the United States. Am J Transplant. 2016;16(2):509-517. doi:10.1111/ajt.13458
55. Tekin Z, Garfinkel MR, Chon WJ, et al. Outcomes of Pancreatic Islet Allotransplantation Using the Edmonton Protocol at the University of Chicago. Transplant Direct. Published online 2016. doi:10.1097/txd.0000000000000609
56. Rickels MR, Liu C, Shlansky-Goldberg RD, et al. Improvement in β-Cell secretory capacity after human islet transplantation according to the CIT07 protocol. Diabetes. Published online 2013. doi:10.2337/db12-1802
57. Langer RM. Islet Transplantation: Lessons Learned Since the Edmonton Breakthrough. Transplant Proc. Published online 2010. doi:10.1016/j.transproceed.2010.04.021
58. Shapiro AMJ, Ricordi C, Hering BJ, et al. International Trial of the Edmonton Protocol for Islet Transplantation. N Engl J Med. Published online 2006. doi:10.1056/nejmoa061267
59. Ryan EA, Lakey JRT, Rajotte R V., et al. Clinical outcomes and insulin secretion after islet transplantation with the edmonton protocol. Diabetes. Published online 2001. doi:10.2337/diabetes.50.4.710
60. Odorico J, Markmann J, Melton D, et al. Report of the Key Opinion Leaders Meeting on Stem Cell-derived Beta Cells. Transplantation. Published online 2018. doi:10.1097/TP.0000000000002217

61. Dimitrioglou N, Kanelli M, Papageorgiou E, Karatzas T, Hatziavramidis D. Paving the way for successful islet encapsulation. Drug Discov Today. Published online 2019. doi:10.1016/j.drudis.2019.01.020
62. Anazawa T, Okajima H, Masui T, Uemoto S. Current state and future evolution of pancreatic islet transplantation. Ann Gastroenterol Surg. Published online 2019. doi:10.1002/ags3.12214
63. Matsumoto S, Shimoda M. Current situation of clinical islet transplantation from allogeneic toward xenogeneic. J Diabetes. 2020;12(10):733-741. doi:10.1111/1753-0407.13041
64. Takaki T, Shimoda M. Pancreatic islet transplantation: toward definitive treatment for diabetes mellitus. Glob Health Med. 2020;2(4):200-211. doi:10.35772/ghm.2020.01057
65. Rickels MR, Paul Robertson R. Pancreatic islet transplantation in humans: Recent progress and future directions. Endocr Rev. Published online 2019. doi:10.1210/er.2018-00154
66. Graham ML, Schuurman HJ. Pancreatic islet xenotransplantation. Drug Discov Today Dis Models. Published online 2017. doi:10.1016/j.ddmod.2017.11.004
67. Reichart B, Niemann H, Chavakis T, et al. Xenotransplantation of porcine islet cells as a potential option for the treatment of type 1 diabetes in the future. Horm Metab Res. Published online 2015. doi:10.1055/s-0034-1395518
68. Samy KP, Martin BM, Turgeon NA, Kirk AD. Islet cell xenotransplantation: A serious look toward the clinic. Xenotransplantation. Published online 2014. doi:10.1111/xen.12095

69. Meier RPH, Seebach JD, Morel P, et al. Survival of free and encapsulated human and rat islet xenografts transplanted into the mouse bone marrow. PLoS ONE. Published online 2014. doi:10.1371/journal.pone.0091268
70. Marigliano M, Bertera S, Grupillo M, Trucco M, Bottino R. Pig-to-nonhuman primates pancreatic islet xenotransplantation: An overview. Curr Diab Rep. Published online 2011. doi:10.1007/s11892-011-0213-z
71. Ernst AU, Wang LH, Ma M. Islet encapsulation. J Mater Chem B. Published online 2018. doi:10.1039/c8tb02020e
72. Sneddon JB, Tang Q, Stock P, et al. Stem Cell Therapies for Treating Diabetes: Progress and Remaining Challenges. Cell Stem Cell. Published online 2018. doi:10.1016/j.stem.2018.05.016
73. Korsgren O. Islet encapsulation: Physiological possibilities and limitations. Diabetes. Published online 2017. doi:10.2337/db17-0065
74. Desai T, Shea LD. Advances in islet encapsulation technologies. Nat Rev Drug Discov. Published online 2017. doi:10.1038/nrd.2016.232
75. Steele JAM, Hallé JP, Poncelet D, Neufeld RJ. Therapeutic cell encapsulation techniques and applications in diabetes. Adv Drug Deliv Rev. Published online 2014. doi:10.1016/j.addr.2013.09.015
76. Kang AR, Park JS, Ju J, Jeong GS, Lee SH. Cell encapsulation via microtechnologies. Biomaterials. Published online 2014. doi:10.1016/j.biomaterials.2013.12.073
77. Weir GC. Islet encapsulation: Advances and obstacles. Diabetologia. Published online 2013. doi:10.1007/s00125-013-2921-1

78. Orive G, Hernández RM, Gascón AR, et al. Cell encapsulation: Promise and progress. Nat Med. Published online 2003. doi:10.1038/nm0103-104
79. Farina M, Alexander JF, Thekkedath U, Ferrari M, Grattoni A. Cell encapsulation: Overcoming barriers in cell transplantation in diabetes and beyond. Adv Drug Deliv Rev. 2019;139:92-115. doi:10.1016/j.addr.2018.04.018
80. Ernst AU, Wang LH, Ma M. Islet encapsulation. J Mater Chem B. 2018;6(42):6705-6722. doi:10.1039/c8tb02020e
81. Hwang PTJ, Shah DK, Garcia JA, et al. Progress and challenges of the bioartificial pancreas. Nano Converg. 2016;3(1):1-11. doi:10.1186/s40580-016-0088-4
82. Scharp DW, Marchetti P. Encapsulated islets for diabetes therapy: History, current progress, and critical issues requiring solution. Adv Drug Deliv Rev. 2014;67-68:35-73. doi:10.1016/j.addr.2013.07.018
83. Krishnan R, Alexander M, Robles L, Foster CE, Lakey JRT. Islet and stem cell encapsulation for clinical transplantation. Rev Diabet Stud. 2014;11(1):84-101. doi:10.1900/RDS.2014.11.84
84. Song S, Yeung R, Park J, et al. Glucose-Stimulated Insulin Response of Silicon Nanopore-Immunoprotected Islets under Convective Transport. ACS Biomater Sci Eng. Published online 2017. doi:10.1021/acsbiomaterials.6b00814
85. Song S, Blaha C, Moses W, et al. An intravascular bioartificial pancreas device (iBAP) with silicon nanopore membranes (SNM) for islet encapsulation under convective mass transport. Lab Chip. Published online 2017. doi:10.1039/c7lc00096k

86. Song S, Faleo G, Yeung R, et al. Silicon nanopore membrane (SNM) for islet encapsulation and immunoisolation under convective transport. Sci Rep. Published online 2016. doi:10.1038/srep23679
87. Zhou Q, Melton DA. Pancreas regeneration. Nature. Published online 2018. doi:10.1038/s41586-018-0088-0
88. Gamble A, Pepper AR, Bruni A, Shapiro AMJ. The journey of islet cell transplantation and future development. Islets. Published online 2018. doi:10.1080/19382014.2018.1428511
89. Kieffer TJ, Woltjen K, Osafune K, Yabe D, Inagaki N. Beta-cell replacement strategies for diabetes. J Diabetes Investig. Published online 2018. doi:10.1111/jdi.12758
90. Rezania A, Bruin JE, Riedel MJ, et al. Maturation of human embryonic stem cell-derived pancreatic progenitors into functional islets capable of treating pre-existing diabetes in mice. Diabetes. Published online 2012. doi:10.2337/db11-1711
91. Colton CK. Challenges in the Development of Immunoisolation Devices. In: Principles of Tissue Engineering: Fourth Edition. ; 2013. doi:10.1016/B978-0-12-398358-9.00028-8
92. Song S, Roy S. Progress and challenges in macroencapsulation approaches for type 1 diabetes (T1D) treatment: Cells, biomaterials, and devices. Biotechnol Bioeng. Published online 2016. doi:10.1002/bit.25895
93. Farney AC, Sutherland DER, Opara EC. Evolution of Islet Transplantation for the Last 30 Years. Pancreas. Published online 2016. doi:10.1097/MPA.0000000000000391

94. Wang Y, Vaddiraju S, Gu B, Papadimitrakopoulos F, Burgess DJ. Foreign Body Reaction to Implantable Biosensors. J Diabetes Sci Technol. Published online 2015. doi:10.1177/1932296815601869
95. Rigla M, Pons B, Rebasa P, et al. Human Subcutaneous Tissue Response to Glucose Sensors: Macrophages Accumulation Impact on Sensor Accuracy. Diabetes Technol Ther. Published online 2018. doi:10.1089/dia.2017.0321
96. Keselowsky BG, Bridges AW, Burns KL, et al. Role of plasma fibronectin in the foreign body response to biomaterials. Biomaterials. Published online 2007. doi:10.1016/j.biomaterials.2007.04.035
97. Kastellorizios M, Tipnis N, Burgess DJ. Foreign body reaction to subcutaneous implants. Adv Exp Med Biol. Published online 2015. doi:10.1007/978-3-319-18603-0_6
98. Major MR, Wong VW, Nelson ER, Longaker MT, Gurtner GC. The Foreign Body Response: At the Interface of Surgery and Bioengineering. Plast Reconstr Surg. Published online 2015. doi:10.1097/PRS.0000000000001193
99. Wang Y, Vaddiraju S, Gu B, Papadimitrakopoulos F, Burgess DJ. Foreign body reaction to implantable biosensors: Effects of tissue trauma and implant size. J Diabetes Sci Technol. Published online 2015. doi:10.1177/1932296815601869
100. De Groot M, Schuurs TA, Van Schilfgaarde R. Causes of limited survival of microencapsulated pancreatic islet grafts. J Surg Res. Published online 2004. doi:10.1016/j.jss.2004.02.018
101. Gifford R. Continuous glucose monitoring: 40 years, what we've learned and what's next. ChemPhysChem. Published online 2013. doi:10.1002/cphc.201300172

102. Jones K. Fibrotic Response to Biomaterials and all Associated Sequence of Fibrosis. In: Host Response to Biomaterials: The Impact of Host Response on Biomaterial Selection. ; 2015. doi:10.1016/B978-0-12-800196-7.00009-8
103. Corradetti B, Impact T. The Immune Response to Implanted Materials and Devices.; 2017. doi:10.1007/978-3-319-45433-7
104. Ratner BD. The Biocompatibility of Implant Materials. Elsevier Inc.; 2015. doi:10.1016/B978-0-12-800196-7.00003-7
105. Klopfleisch R. Macrophage reaction against biomaterials in the mouse model – Phenotypes, functions and markers. Acta Biomater. Published online 2016. doi:10.1016/j.actbio.2016.07.003
106. Chung L, Maestas DR, Housseau F, Elisseeff JH. Key players in the immune response to biomaterial scaffolds for regenerative medicine. Adv Drug Deliv Rev. 2017;114:184-192. doi:10.1016/j.addr.2017.07.006
107. Veiseh O, Vegas AJ. Domesticating the foreign body response: Recent advances and applications. Adv Drug Deliv Rev. 2019;144. doi:10.1016/j.addr.2019.08.010
108. Wang Y, Vaddiraju S, Gu B, Papadimitrakopoulos F, Burgess DJ. Foreign body reaction to implantable biosensors: Effects of tissue trauma and implant size. J Diabetes Sci Technol. 2015;9(5):966-977. doi:10.1177/1932296815601869
109. Kyriakides TR. Molecular Events at Tissue-Biomaterial Interface. Elsevier Inc.; 2015. doi:10.1016/B978-0-12-800196-7.00005-0
110. Chen W, Yung BC, Qian Z, Chen X. Improving long-term subcutaneous drug delivery by regulating material-bioenvironment interaction. Adv Drug Deliv Rev. Published online 2018. doi:10.1016/j.addr.2018.01.016

111. Desai TA, Tang Q. Islet encapsulation therapy — racing towards the finish line? Nat Rev Endocrinol. 2018;14(11):630-632. doi:10.1038/s41574-018-0100-7
112. Desai T, Shea LD. Advances in islet encapsulation technologies. Nat Rev Drug Discov. 2017;16(5):338-350. doi:10.1038/nrd.2016.232
113. Dolgin E. Encapsulating the problem. Nature. 2016;540(8 Dec):S60-62.
114. Gray M, Meehan J, Ward C, et al. Implantable biosensors and their contribution to the future of precision medicine. Vet J. Published online 2018. doi:10.1016/j.tvjl.2018.07.011
115. Mason McClatchey P, McClain ES, Williams IM, et al. Fibrotic encapsulation is the dominant source of continuous glucose monitor delays. Diabetes. Published online 2019. doi:10.2337/db19-0229
116. Wood A, O'Neal D, Furler J, Ekinci EI. Continuous glucose monitoring: a review of the evidence, opportunities for future use and ongoing challenges. Intern Med J. Published online 2018. doi:10.1111/imj.13770
117. Li J, Liang JY, Laken SJ, Langer R, Traverso G. Clinical Opportunities for Continuous Biosensing and Closed-Loop Therapies. Trends Chem. Published online 2020. doi:10.1016/j.trechm.2020.02.009
118. Teymourian H, Barfidokht A, Wang J. Electrochemical glucose sensors in diabetes management: an updated review (2010–2020). Chem Soc Rev. Published online 2020. doi:10.1039/d0cs00304b
119. Stout PJ, Racchini JR, Hilgers ME, Noujaim SE. Continuous glucose monitoring: key challenges to replacing episodic SMBG. Diabetes Res Clin Pract. Published online 2006. doi:10.1016/S0168-8227(06)70007-9

120. Scarritt ME, Londono R, Badylak SF. Host response to implanted materials and devices: An overview. In: The Immune Response to Implanted Materials and Devices: The Impact of the Immune System on the Success of an Implant. Springer International Publishing; 2016:1-14. doi:10.1007/978-3-319-45433-7_1
121. Corradetti B. The Immune Response to Implanted Materials and Devices: The Impact of the Immune System on the Success of an Implant. Springer International Publishing; 2016. doi:10.1007/978-3-319-45433-7
122. Williams DF. On the mechanisms of biocompatibility. Biomaterials. 2008;29(20):2941-2953. doi:10.1016/j.biomaterials.2008.04.023
123. Anderson JM, Jiang S. Implications of the acute and chronic inflammatory response and the foreign body reaction to the immune response of implanted biomaterials. In: The Immune Response to Implanted Materials and Devices: The Impact of the Immune System on the Success of an Implant. Springer International Publishing; 2016:15-36. doi:10.1007/978-3-319-45433-7_2
124. Santambrogio L. Biomaterials in Regenerative Medicine and the Immune System. Springer International Publishing; 2015. doi:10.1007/978-3-319-18045-8
125. Yu T, Tutwiler VJ, Spiller K. The role of macrophages in the foreign body response to implanted biomaterials. In: Biomaterials in Regenerative Medicine and the Immune System. Springer International Publishing; 2015:17-34. doi:10.1007/978-3-319-18045-8_2
126. McKiel LA, Woodhouse KA, Fitzpatrick LE. The role of Toll-like receptor signaling in the macrophage response to implanted materials. MRS Commun. 2020;10(1):55-68. doi:10.1557/mrc.2019.154

127. Franz S, Rammelt S, Scharnweber D, Simon JC. Immune responses to implants - A review of the implications for the design of immunomodulatory biomaterials. Biomaterials. Published online 2011. doi:10.1016/j.biomaterials.2011.05.078
128. Christo SN, Diener KR, Bachhuka A, Vasilev K, Hayball JD. Innate Immunity and Biomaterials at the Nexus: Friends or Foes. BioMed Res Int. 2015;2015:1-23. doi:10.1155/2015/342304
129. Davenport Huyer L, Pascual-Gil S, Wang Y, Mandla S, Yee B, Radisic M. Advanced Strategies for Modulation of the Material–Macrophage Interface. Adv Funct Mater. Published online 2020. doi:10.1002/adfm.201909331
130. Anderson J, Cramer S. Perspectives on the Inflammatory, Healing, and Foreign Body Responses to Biomaterials and Medical Devices. Elsevier Inc.; 2015. doi:10.1016/B978-0-12-800196-7.00002-5
131. Chandorkar Y, Ravikumar K, Basu B. The Foreign Body Response Demystified. ACS Biomater Sci Eng. 2019;5(1):19-44. doi:10.1021/acsbiomaterials.8b00252
132. Geerlings SE, Hoepelman AIM. Immune dysfunction in patients with diabetes mellitus (DM). FEMS Immunol Med Microbiol. Published online 1999. doi:10.1016/S0928-8244(99)00142-X
133. Shoelson SE, Lee J, Goldfine AB. Inflammation and insulin resistance. J Clin Invest. Published online 2006. doi:10.1172/JCI29069
134. Lackey DE, Olefsky JM. Regulation of metabolism by the innate immune system. Nat Rev Endocrinol. Published online 2016. doi:10.1038/nrendo.2015.189

135. Espinoza-Jiménez A, Peón AN, Terrazas LI. Alternatively activated macrophages in types 1 and 2 diabetes. Mediators Inflamm. Published online 2012. doi:10.1155/2012/815953
136. Kopan C, Tucker T, Alexander M, Mohammadi MR, Pone E, Lakey JRT. Approaches in immunotherapy, regenerative medicine, and bioengineering for type 1 diabetes. Front Immunol. 2018;9(JUN). doi:10.3389/fimmu.2018.01354
137. De Candia P, Prattichizzo F, Garavelli S, et al. Type 2 diabetes: How much of an autoimmune disease? Front Endocrinol. Published online 2019. doi:10.3389/fendo.2019.00451
138. Nikolajczyk BS, Jagannathan-Bogdan M, Shin H, Gyurko R. State of the union between metabolism and the immune system in type 2 diabetes. Genes Immun. Published online 2011. doi:10.1038/gene.2011.14
139. Donath MY, Shoelson SE. Type 2 diabetes as an inflammatory disease. Nat Rev Immunol. Published online 2011. doi:10.1038/nri2925
140. Wolf G, Aumann N, Michalska M, et al. Peroxiredoxin III protects pancreatic β cells from apoptosis. J Endocrinol. Published online 2010. doi:10.1677/JOE-09-0455
141. Daryabor G, Atashzar MR, Kabelitz D, Meri S, Kalantar K. The Effects of Type 2 Diabetes Mellitus on Organ Metabolism and the Immune System. Front Immunol. Published online 2020. doi:10.3389/fimmu.2020.01582
142. Zaccardi F, Webb DR, Yates T, Davies MJ. Pathophysiology of type 1 and type 2 diabetes mellitus: A 90-year perspective. Postgrad Med J. Published online 2016. doi:10.1136/postgradmedj-2015-133281

143. Bosi E, Braghi S, Maffi P, et al. Autoantibody Response to Islet Transplantation in Type 1 Diabetes. Diabetes. 2001;50(7-12):2464-2471. doi:10.2337/diabetes.50.11.2464
144. Zorec B, Jelenc J, Miklavčič D, Pavšelj N. Ultrasound and electric pulses for transdermal drug delivery enhancement: Ex vivo assessment of methods with in vivo oriented experimental protocols. Int J Pharm. 2015;490(1-2):65-73. doi:10.1016/j.ijpharm.2015.05.035
145. Monti P, Scirpoli M, Maffi P, et al. Islet transplantation in patients with autoimmune diabetes induces homeostatic cytokines that expand autoreactive memory T cells. J Clin Invest. 2008;118(5):1806-1814. doi:10.1172/JCI35197
146. Pugliese A, Reijonen HK, Nepom J, Burke GW. Recurrence of autoimmunity in pancreas transplant patients: research update. Diabetes Manag. 2011;1(2):229-238. doi:10.2217/dmt.10.21
147. Roep BO, Thomaidou S, van Tienhoven R, Zaldumbide A. Type 1 diabetes mellitus as a disease of the β-cell (do not blame the immune system?). Nat Rev Endocrinol. Published online 2020. doi:10.1038/s41574-020-00443-4
148. Tsalamandris S, Antonopoulos AS, Oikonomou E, et al. The role of inflammation in diabetes: Current concepts and future perspectives. Eur Cardiol Rev. 2019;14(1):50-59. doi:10.15420/ecr.2018.33.1
149. Ferlita S, Yegiazaryan A, Noori N, et al. Type 2 Diabetes Mellitus and Altered Immune System Leading to Susceptibility to Pathogens, Especially Mycobacterium tuberculosis. J Clin Med. Published online 2019. doi:10.3390/jcm8122219

150. Kumar Nathella P, Babu S. Influence of diabetes mellitus on immunity to human tuberculosis. Immunology. Published online 2017. doi:10.1111/imm.12762
151. Li C, Guo C, Fitzpatrick V, et al. Design of biodegradable, implantable devices towards clinical translation. Nat Rev Mater. Published online 2020. doi:10.1038/s41578-019-0150-z
152. Kyriakides TR. Molecular Events at Tissue-Biomaterial Interface. In: Host Response to Biomaterials: The Impact of Host Response on Biomaterial Selection. ; 2015. doi:10.1016/B978-0-12-800196-7.00005-0
153. Stieglitz T, Schuettler M. Material-tissue interfaces in implantable systems. In: Implantable Sensor Systems for Medical Applications. ; 2013. doi:10.1533/9780857096289.1.39
154. Horbett TA. Adsorbed Proteins on Biomaterials. In: Biomaterials Science: An Introduction to Materials: Third Edition. ; 2013. doi:10.1016/B978-0-08-087780-8.00036-X
155. Vogler EA. Protein adsorption in three dimensions. Biomaterials. Published online 2012. doi:10.1016/j.biomaterials.2011.10.059
156. Wei Q, Becherer T, Angioletti-Uberti S, et al. Protein interactions with polymer coatings and biomaterials. Angew Chem - Int Ed. Published online 2014. doi:10.1002/anie.201400546
157. Camilloni C, Bonetti D, Morrone A, et al. Towards a structural biology of the hydrophobic effect in protein folding. Sci Rep. Published online 2016. doi:10.1038/srep28285

158. Dyson HJ, Wright PE, Scheraga HA. The role of hydrophobic interactions in initiation and propagation of protein folding. Proc Natl Acad Sci U S A. Published online 2006. doi:10.1073/pnas.0605504103
159. Schmidt DR, Waldeck H, Kao WJ. Protein Adsorption to Biomaterials. In: Biological Interactions on Materials Surfaces. Springer US; 2009:1-18. doi:10.1007/978-0-387-98161-1_1
160. Dahal YR, Olvera de la Cruz M. Controlling protein adsorption modes electrostatically. Soft Matter. Published online 2020. doi:10.1039/d0sm00632g
161. Hühn D, Kantner K, Geidel C, et al. Polymer-coated nanoparticles interacting with proteins and cells: Focusing on the sign of the net charge. ACS Nano. Published online 2013. doi:10.1021/nn3059295
162. Zhou HX, Pang X. Electrostatic Interactions in Protein Structure, Folding, Binding, and Condensation. Chem Rev. Published online 2018. doi:10.1021/acs.chemrev.7b00305
163. Guseman AJ, Speer SL, Perez Goncalves GM, Pielak GJ. Surface Charge Modulates Protein-Protein Interactions in Physiologically Relevant Environments. Biochemistry. Published online 2018. doi:10.1021/acs.biochem.8b00061
164. Ross AM, Jiang Z, Bastmeyer M, Lahann J. Physical aspects of cell culture substrates: Topography, roughness, and elasticity. Small. 2012;8(3):336-355. doi:10.1002/smll.201100934
165. Ruprecht V, Monzo P, Ravasio A, et al. How cells respond to environmental cues – insights from bio-functionalized substrates. J Cell Sci. 2016;130(1):51-61. doi:10.1242/jcs.196162

166. Damodaran VB, Murthy SN. Bio-inspired strategies for designing antifouling biomaterials. Biomater Res. Published online 2016. doi:10.1186/s40824-016-0064-4

167. Li J, Liang JY, Laken SJ, Langer R, Traverso G. Clinical Opportunities for Continuous Biosensing and Closed-Loop Therapies. Trends Chem. 2020;2(4):319-340. doi:10.1016/j.trechm.2020.02.009

168. Le L V., Mkrtschjan MA, Russell B, Desai TA. Hang on tight: reprogramming the cell with microstructural cues. Biomed Microdevices. 2019;21(2):1-17. doi:10.1007/s10544-019-0394-9

169. Smith Q, Gerecht S. Stem Cell Fate Is a Touchy Subject. Cell Stem Cell. 2016;19(3):289-290. doi:10.1016/j.stem.2016.08.015

170. Jokinen V, Kankuri E, Hoshian S, Franssila S, Ras RHA. Superhydrophobic Blood-Repellent Surfaces. Adv Mater. 2018;30(24). doi:10.1002/adma.201705104

171. Anderson H, Llopis-Hernandez V, Sweeten P, et al. 4.11 Nanoscale Surface Cues and Cell Behavior. Elsevier; 2017:163-179. doi:10.1016/B978-0-12-803581-8.10226-7

172. McNamara LE, McMurray RJ, Dalby MJ, Tsimbouri PM. Surfaces and Cell Behavior. Elsevier; 2011:115-126. doi:10.1016/B978-0-08-055294-1.00010-6

173. Di Cio S, Gautrot JE. Cell sensing of physical properties at the nanoscale: Mechanisms and control of cell adhesion and phenotype. Acta Biomater. 2016;30:26-48. doi:10.1016/j.actbio.2015.11.027

174. Robotti F, Bottan S, Fraschetti F, et al. A micron-scale surface topography design reducing cell adhesion to implanted materials. Sci Rep. 2018;8(1):10887. doi:10.1038/s41598-018-29167-2
175. Mahon OR, Browe DC, Gonzalez-Fernandez T, et al. Nano-particle mediated M2 macrophage polarization enhances bone formation and MSC osteogenesis in an IL-10 dependent manner. Biomaterials. Published online 2020. doi:10.1016/j.biomaterials.2020.119833
176. Karazisis D, Petronis S, Agheli H, et al. The influence of controlled surface nanotopography on the early biological events of osseointegration. Acta Biomater. 2017;53:559-571. doi:10.1016/j.actbio.2017.02.026
177. Abagnale G, Sechi A, Steger M, et al. Surface Topography Guides Morphology and Spatial Patterning of Induced Pluripotent Stem Cell Colonies. Stem Cell Rep. 2017;9(2):654-666. doi:10.1016/j.stemcr.2017.06.016
178. Ermis M, Antmen E, Hasirci V. Micro and Nanofabrication methods to control cell-substrate interactions and cell behavior: A review from the tissue engineering perspective. Bioact Mater. 2018;3(3):355-369. doi:10.1016/j.bioactmat.2018.05.005
179. Galdiero MR, Mantovani A. Macrophage Plasticity and Polarization: Relevance to Biomaterials. Elsevier Inc.; 2015. doi:10.1016/B978-0-12-800196-7.00006-2
180. Sheikh Z, Brooks PJ, Barzilay O, Fine N, Glogauer M. Macrophages, foreign body giant cells and their response to implantable biomaterials. Materials. 2015;8(9):5671-5701. doi:10.3390/ma8095269

181. Lee JK, Choi IS, Oh TI, Lee E. Cell-Surface Engineering for Advanced Cell Therapy. Chem - Eur J. Published online July 30, 2018. doi:10.1002/chem.201801710
182. Londono R, Badylak SF. Factors Which Affect the Host Response to Biomaterials. Elsevier Inc.; 2015. doi:10.1016/B978-0-12-800196-7.00001-3
183. Anderson HJ, Sahoo JK, Ulijn R V., Dalby MJ. Mesenchymal Stem Cell Fate: Applying Biomaterials for Control of Stem Cell Behavior. Front Bioeng Biotechnol. 2016;4:38. doi:10.3389/fbioe.2016.00038
184. Burugapalli K, Wijesuriya S, Wang N, Song W. Biomimetic electrospun coatings increase the in vivo sensitivity of implantable glucose biosensors. J Biomed Mater Res - Part A. 2018;106(4):1072-1081. doi:10.1002/jbm.a.36308
185. Rigla M, Pons B, Rebasa P, et al. Human Subcutaneous Tissue Response to Glucose Sensors: Macrophages Accumulation Impact on Sensor Accuracy. Diabetes Technol Ther. 2018;20(4):296-302. doi:10.1089/dia.2017.0321
186. Carnicer-Lombarte A, Barone DG, Dimov IB, et al. Mechanical matching of implant to host minimises foreign body reaction. Bioarxiv. Published online 2019:1-41.
187. Prasadh S, Ratheesh V, Wong R. Impact of biomaterial mechanics on cellular and molecular responses. In: Handbook of Biomaterials Biocompatibility. Elsevier; 2020:85-109. doi:10.1016/b978-0-08-102967-1.00006-2
188. Lenzini S, Devine D, Shin JW. Leveraging Biomaterial Mechanics to Improve Pluripotent Stem Cell Applications for Tissue Engineering. Front Bioeng Biotechnol. 2019;7:260. doi:10.3389/fbioe.2019.00260

189. Gilbert PM, Weaver VM. Cellular adaptation to biomechanical stress across length scales in tissue homeostasis and disease. Semin Cell Dev Biol. Published online 2017. doi:10.1016/j.semcdb.2016.09.004
190. Vishwakarma A, Bhise NS, Evangelista MB, et al. Engineering Immunomodulatory Biomaterials To Tune the Inflammatory Response. Trends Biotechnol. Published online 2016. doi:10.1016/j.tibtech.2016.03.009
191. Wang L, Wang C, Wu S, Fan Y, Li X. Influence of the mechanical properties of biomaterials on degradability, cell behaviors and signaling pathways: Current progress and challenges. Biomater Sci. 2020;8(10):2714-2733. doi:10.1039/d0bm00269k
192. Carver W, Goldsmith EC. Regulation of tissue fibrosis by the biomechanical environment. BioMed Res Int. Published online 2013. doi:10.1155/2013/101979
193. Bergeron JJM, Di Guglielmo GM, Dahan S, Dominguez M, Posner BI. Spatial and Temporal Regulation of Receptor Tyrosine Kinase Activation and Intracellular Signal Transduction. Annu Rev Biochem. 2016;85(1):573-597. doi:10.1146/annurev-biochem-060815-014659
194. Dharmarajan A, Floren M, Cox L, Ding Y, Johnson R, Tan W. Mechanochemical Effects on Extracellular Signal-Regulated Kinase Dynamics in Stem Cell Differentiation. Tissue Eng - Part A. 2018;24(15-16):1179-1189. doi:10.1089/ten.tea.2017.0365
195. Carver W, Esch AM, Fowlkes V, Goldsmith EC. The biomechanical environment and impact on tissue fibrosis. In: The Immune Response to Implanted Materials and Devices: The Impact of the Immune System on the Success of an Implant.

Springer International Publishing; 2016:169-188. doi:10.1007/978-3-319-45433-7_9

196. Corradetti B. The Immune Response to Implanted Materials and Devices: The Impact of the Immune System on the Success of an Implant. Springer International Publishing; 2016. doi:10.1007/978-3-319-45433-7
197. Farge E. Mechanotransduction in Development. Vol 95.; 2011. doi:10.1016/B978-0-12-385065-2.00008-6
198. Chen W, Kim DH, Lim CT. Special Issue: Biomaterials for Cell Mechanobiology. ACS Biomater Sci Eng. 2019;5(8):3685-3687. doi:10.1021/acsbiomaterials.9b01123
199. Zadpoor AA. Biomaterials and tissue biomechanics: A match made in heaven? Materials. 2017;10(5). doi:10.3390/ma10050528
200. Burdick JA, García AJ. Special Issue: Biomaterials in Mechanobiology. Adv Healthc Mater. 2020;9(8):2000412. doi:10.1002/adhm.202000412
201. Waldeck HM, Guerra AD, Kao WJ. Extracellular Matrix: Inspired Biomaterials. Compr Biomater II. Published online January 1, 2017:132-146. doi:10.1016/B978-0-12-803581-8.10147-X
202. Jansen KA, Donato DM, Balcioglu HE, Schmidt T, Danen EHJ, Koenderink GH. A guide to mechanobiology: Where biology and physics meet. Biochim Biophys Acta - Mol Cell Res. 2015;1853(11):3043-3052. doi:10.1016/j.bbamcr.2015.05.007
203. Janson IA, Putnam AJ. Extracellular matrix elasticity and topography: Material-based cues that affect cell function via conserved mechanisms. J Biomed Mater Res - Part A. 2015;103(3):1246-1258. doi:10.1002/jbm.a.35254

204. Paul CD, Hruska A, Staunton JR, et al. Decoupling cellular response to topography and stiffness in three dimensions. Food Pharm Bioeng Div 2018 - Core Program Area 2018 AIChE Annu Meet. 2018;2:617-618.
205. Jansen KA, Atherton P, Ballestrem C. Mechanotransduction at the cell-matrix interface. Semin Cell Dev Biol. 2017;71:75-83. doi:10.1016/j.semcdb.2017.07.027
206. Helton KL, Ratner BD, Wisniewski NA. Biomechanics of the sensor-tissue interface - Effects of motion, pressure, and design on sensor performance and the foreign body response - Part I: Theoretical framework. In: Journal of Diabetes Science and Technology. ; 2011. doi:10.1177/193229681100500317
207. Ekdahl KN, Lambris JD, Elwing H, et al. Innate immunity activation on biomaterial surfaces: A mechanistic model and coping strategies. Adv Drug Deliv Rev. 2011;63(12):1042-1050. doi:10.1016/j.addr.2011.06.012
208. Brennan T V, Lunsford KE, Kuo PC. Innate pathways of immune activation in transplantation. J Transplant. 2010;2010. doi:10.1155/2010/826240
209. Christo SN, Diener KR, Bachhuka A, Vasilev K, Hayball JD. Innate Immunity and Biomaterials at the Nexus: Friends or Foes. BioMed Res Int. Published online 2015. doi:10.1155/2015/342304
210. Andorko JI, Jewell CM. Designing biomaterials with immunomodulatory properties for tissue engineering and regenerative medicine. Bioeng Transl Med. Published online 2017. doi:10.1002/btm2.10063
211. Dellacherie MO, Seo BR, Mooney DJ. Macroscale biomaterials strategies for local immunomodulation. Nat Rev Mater. 2019;4(6):379-397. doi:10.1038/s41578-019-0106-3

212. Anderson JM, Rodriguez A, Chang DT. Foreign body reaction to biomaterials. Semin Immunol. 2008;20(2):86-100. doi:10.1016/j.smim.2007.11.004
213. Higgins DM, Basaraba RJ, Hohnbaum AC, Lee EJ, Grainger DW, Gonzalez-Juarrero M. Localized immunosuppressive environment in the foreign body response to implanted biomaterials. Am J Pathol. 2009;175(1):161-170. doi:10.2353/ajpath.2009.080962
214. Kelly SH, Shores LS, Votaw NL, Collier JH. Biomaterial strategies for generating therapeutic immune responses. Adv Drug Deliv Rev. Published online 2017. doi:10.1016/j.addr.2017.04.009
215. Swartzlander MD, Blakney AK, Amer LD, Hankenson KD, Kyriakides TR, Bryant SJ. Immunomodulation by mesenchymal stem cells combats the foreign body response to cell-laden synthetic hydrogels. Biomaterials. Published online 2015. doi:10.1016/j.biomaterials.2014.11.020
216. Gattazzo F, Urciuolo A, Bonaldo P. Extracellular matrix: A dynamic microenvironment for stem cell niche. Biochim Biophys Acta - Gen Subj. 2014;1840(8):2506-2519. doi:10.1016/j.bbagen.2014.01.010
217. Galvan, R. F, Barranco V, Galvan JC, Batlle, Sebastian FeliuFajardo S, García. Biomaterials for Tissue Engineering Applications in Diabetes Mellitus. Intech. 2016;i(tourism):13. doi:http://dx.doi.org/10.5772/57353
218. Walters NJ, Gentleman E. Evolving insights in cell-matrix interactions: Elucidating how non-soluble properties of the extracellular niche direct stem cell fate. Acta Biomater. 2015;11(1):3-16. doi:10.1016/j.actbio.2014.09.038

219. Mariani E, Lisignoli G, Borzì RM, Pulsatelli L. Biomaterials: Foreign bodies or tuners for the immune response? Int J Mol Sci. Published online 2019. doi:10.3390/ijms20030636
220. Lewis JS, Roy K, Keselowsky BG. Materials that harness and modulate the immune system. MRS Bull. Published online 2014. doi:10.1557/mrs.2013.310
221. The Immune Response to Implanted Materials and Devices.; 2017. doi:10.1007/978-3-319-45433-7
222. Lopresti ST, Brown BN. Host Response to Naturally Derived Biomaterials. Elsevier Inc.; 2015. doi:10.1016/B978-0-12-800196-7.00004-9
223. Sarkar K, Xue Y, Sant S. Host response to synthetic versus natural biomaterials. In: The Immune Response to Implanted Materials and Devices: The Impact of the Immune System on the Success of an Implant. ; 2016. doi:10.1007/978-3-319-45433-7_5
224. Slaughter G. Improving the Biocompatibility of Implantable Bioelectronics Devices. Implant Bioelectron. 2014;9783527335:265-283. doi:10.1002/9783527673148.ch13
225. Gasperini L, Mano JF, Reis RL. Natural polymers for the microencapsulation of cells. J R Soc Interface. 2014;11(100):20140817-20140817. doi:10.1098/rsif.2014.0817
226. Marchioli G, Van Gurp L, Van Krieken PP, et al. Fabrication of three-dimensional bioplotted hydrogel scaffolds for islets of Langerhans transplantation. Biofabrication. 2015;7(2). doi:10.1088/1758-5090/7/2/025009

227. De Vos P, Lazarjani HA, Poncelet D, Faas MM. Polymers in cell encapsulation from an enveloped cell perspective. Adv Drug Deliv Rev. 2014;67-68:15-34. doi:10.1016/j.addr.2013.11.005
228. Stabler CL, Li Y, Stewart JM, Keselowsky BG. Engineering immunomodulatory biomaterials for type 1 diabetes. Nat Rev Mater. 2019;4(6):429-450. doi:10.1038/s41578-019-0112-5
229. De Vries R, Stell A, Mohammed S, et al. Bioengineering, biomaterials, and β-cell replacement therapy. In: Transplantation, Bioengineering, and Regeneration of the Endocrine Pancreas. ; 2020. doi:10.1016/b978-0-12-814831-0.00033-6
230. Ernst AU, Wang LH, Ma M. Islet encapsulation. J Mater Chem B. 2018;6(42):6705-6722. doi:10.1039/c8tb02020e
231. Adly N, Weidlich S, Seyock S, et al. Printed microelectrode arrays on soft materials: from PDMS to hydrogels. Npj Flex Electron. 2018;2(1):1-9. doi:10.1038/s41528-018-0027-z
232. Kumar M, Nandi SK, Kaplan DL, Mandal BB. Localized Immunomodulatory Silk Macrocapsules for Islet-like Spheroid Formation and Sustained Insulin Production. ACS Biomater Sci Eng. Published online 2017. doi:10.1021/acsbiomaterials.7b00218
233. Song S, Roy S. Progress and challenges in macroencapsulation approaches for type 1 diabetes (T1D) treatment: Cells, biomaterials, and devices. Biotechnol Bioeng. 2016;113(7):1381-1402. doi:10.1002/bit.25895

234. Bochenek MA, Veiseh O, Vegas AJ, et al. Alginate encapsulation as long-term immune protection of allogeneic pancreatic islet cells transplanted into the omental bursa of macaques. Nat Biomed Eng. 2018;2(11). doi:10.1038/s41551-018-0275-1
235. Marchioli G, Luca A Di, de Koning E, et al. Hybrid Polycaprolactone/Alginate Scaffolds Functionalized with VEGF to Promote de Novo Vessel Formation for the Transplantation of Islets of Langerhans. Adv Healthc Mater. 2016;5(13):1606-1616. doi:10.1002/adhm.201600058
236. Strand BL, Coron AE, Skjak-Braek G. Current and future perspectives on alginate encapsulated pancreatic islet. Stem Cells Transl Med. 2017;6(4):1053-1058. doi:10.1002/sctm.16-0116
237. Llacua LA, Hoek A, de Haan BJ, de Vos P. Collagen type VI interaction improves human islet survival in immunoisolating microcapsules for treatment of diabetes. Islets. 2018;10(2). doi:10.1080/19382014.2017.1420449
238. Taraballi F, Corradetti B, Minardi S, et al. Biomimetic collagenous scaffold to tune inflammation by targeting macrophages. J Tissue Eng. Published online 2016. doi:10.1177/2041731415624667
239. Llacua LA, Faas MM, de Vos P. Extracellular matrix molecules and their potential contribution to the function of transplanted pancreatic islets. Diabetologia. 2018;61(6). doi:10.1007/s00125-017-4524-8
240. Llacua LA, de Haan BJ, de Vos P. Laminin and collagen IV inclusion in immunoisolating microcapsules reduces cytokine-mediated cell death in human pancreatic islets. J Tissue Eng Regen Med. Published online 2018. doi:10.1002/term.2472

241. Zakeri Siavashani A, Mohammadi J, Maniura-Weber K, et al. Silk based scaffolds with immunomodulatory capacity: Anti-inflammatory effects of nicotinic acid. Biomater Sci. Published online 2020. doi:10.1039/c9bm00814d
242. Partlow BP, Hanna CW, Rnjak-Kovacina J, et al. Highly Tunable Elastomeric Silk Biomaterials. Adv Funct Mater. 2014;24(29):4615-4624. doi:10.1002/adfm.201400526
243. Fishman JM, Wiles K, Wood KJ. The Acquired Immune System Response to Biomaterials, Including Both Naturally Occurring and Synthetic Biomaterials. Elsevier Inc.; 2015. doi:10.1016/B978-0-12-800196-7.00008-6
244. Nyitray CE, Chang R, Faleo G, et al. Polycaprolactone Thin-Film Micro- and Nanoporous Cell-Encapsulation Devices. ACS Nano. 2015;9(6):5675-5682. doi:10.1021/acsnano.5b00679
245. Rios PD, Skoumal M, Liu J, et al. Evaluation of encapsulating and microporous nondegradable hydrogel scaffold designs on islet engraftment in rodent models of diabetes. Biotechnol Bioeng. Published online June 25, 2018. doi:10.1002/bit.26741
246. Manzoli V, Villa C, Bayer AL, et al. Immunoisolation of murine islet allografts in vascularized sites through conformal coating with polyethylene glycol. Am J Transplant. 2018;18(3). doi:10.1111/ajt.14547
247. Bobrowski T, Schuhmann W. Long-term implantable glucose biosensors. Curr Opin Electrochem. 2018;10:112-119. doi:10.1016/j.coelec.2018.05.004

248. Qi M. Transplantation of Encapsulated Pancreatic Islets as a Treatment for Patients with Type 1 Diabetes Mellitus. Adv Med. 2014;2014:1-15. doi:10.1155/2014/429710
249. Wang Y, Papadimitrakopoulos F, Burgess DJ. Polymeric “smart” coatings to prevent foreign body response to implantable biosensors. J Controlled Release. 2013;169(3):341-347. doi:10.1016/j.jconrel.2012.12.028
250. Kette F, Rojas-Canales D, Drogemuller C, McInnes S, Toby Coates P. Modification of Polyurethane Scaffolds for Localised Immunosuppression of Subcutaneous Islet Transplantation. Transplantation. 2018;102:S77. doi:10.1097/01.tp.0000542659.73899.92
251. Soto RJ, Privett BJ, Schoenfisch MH. In vivo analytical performance of nitric oxide-releasing glucose biosensors. Anal Chem. 2014;86(14):7141-7149. doi:10.1021/ac5017425
252. Hwang PTJ, Shah DK, Garcia JA, et al. Progress and challenges of the bioartificial pancreas. Nano Converg. 2016;3(1):1-11. doi:10.1186/s40580-016-0088-4
253. Skrzypek K, Groot Nibbelink M, Van Lente J, et al. Pancreatic islet macroencapsulation using microwell porous membranes. Sci Rep. 2017;7(1):9186. doi:10.1038/s41598-017-09647-7
254. Song J, Millman JR. Economic 3D-printing approach for transplantation of human stem cell-derived β-like cells. Biofabrication. 2017;9(1). doi:10.1088/1758-5090/9/1/015002

255. Farina M, Ballerini A, Fraga DW, et al. 3D Printed Vascularized Device for Subcutaneous Transplantation of Human Islets. Biotechnol J. Published online 2017. doi:10.1002/biot.201700169
256. Lecomte A, Descamps E, Bergaud C. A review on mechanical considerations for chronically-implanted neural probes. J Neural Eng. 2018;15(3). doi:10.1088/1741-2552/aa8b4f
257. Richbourg NR, Peppas NA, Sikavitsas VI. Tuning the biomimetic behavior of scaffolds for regenerative medicine through surface modifications. J Tissue Eng Regen Med. 2019;(405):0-2. doi:10.1002/term.2859
258. Ward WK. A review of the foreign-body response to subcutaneously-implanted devices: The role of Macrophages and cytokines in biofouling and fibrosis. J Diabetes Sci Technol. 2008;2(5):768-777. doi:10.1177/193229680800200504
259. Peloso A, Citro A, Zoro T, et al. Regenerative medicine and diabetes: Targeting the extracellular matrix beyond the stem cell approach and encapsulation technology. Front Endocrinol. 2018;9(AUG):1-9. doi:10.3389/fendo.2018.00445
260. Badylak SF. Host Response to Biomaterials: The Impact of Host Response on Biomaterial Selection.; 2015.
261. Baker DW, Zhou J, Tang L. Methods Used to Evaluate the Host Responses to Medical Implants In Vivo. Elsevier Inc.; 2015. doi:10.1016/B978-0-12-800196-7.00014-1
262. Hattori K, Sugiura S, Kanamori T. Scaffold fabrication in a perfusion culture microchamber array chip by O2 plasma bonding of poly(dimethylsiloxane)

protected by a physical mask. Biomicrofluidics. 2011;5(2):022204. doi:10.1063/1.3576933

263. Caldeira J, Sousa A, Sousa DM, Barros D. Extracellular matrix constitution and function for tissue regeneration and repair. Pept Proteins Biomater Tissue Regen Repair. Published online January 1, 2018:29-72. doi:10.1016/B978-0-08-100803-4.00002-4

264. Frantz C, Stewart KM, Weaver VM. No Title. 2010;123. doi:10.1242/jcs.023820

265. Nichols SP, Koh A, Brown NL, et al. The effect of nitric oxide surface flux on the foreign body response to subcutaneous implants. Biomaterials. 2012;33(27):6305-6312. doi:10.1016/j.biomaterials.2012.05.053

266. Laschke MW, Augustin V, Kleer S, Tschernig T, Menger MD. Locally applied macrophage-activating lipopeptide-2 (MALP-2) promotes early vascularization of implanted porous polyethylene (Medpor®). Acta Biomater. 2014;10(11):4661-4669. doi:10.1016/j.actbio.2014.07.004

267. Minardi S, Corradetti B, Taraballi F, et al. IL-4 Release from a Biomimetic Scaffold for the Temporally Controlled Modulation of Macrophage Response. Ann Biomed Eng. Published online 2016. doi:10.1007/s10439-016-1580-z

268. Kumar M, Gupta P, Bhattacharjee S, Nandi SK, Mandal BB. Immunomodulatory injectable silk hydrogels maintaining functional islets and promoting anti-inflammatory M2 macrophage polarization. Biomaterials. Published online 2018. doi:10.1016/j.biomaterials.2018.09.037

269. Lee H, Song C, Baik S, Kim D, Hyeon T, Kim DH. Device-assisted transdermal drug delivery. Adv Drug Deliv Rev. 2018;127:35-45. doi:10.1016/j.addr.2017.08.009
270. Lund T, Mangsbo SM, Scholz H, et al. Resolvin E1 reduces proinflammatory markers in human pancreatic islets in vitro. Exp Clin Endocrinol Diabetes. Published online 2010. doi:10.1055/s-0029-1241825
271. Vériter S, Gianello P, Igarashi Y, et al. Improvement of subcutaneous bioartificial pancreas vascularization and function by coencapsulation of pig islets and mesenchymal stem cells in primates. Cell Transplant. 2014;23(11):1349-1364. doi:10.3727/096368913X663550
272. Yu Q, Zhang Y, Wang H, Brash J, Chen H. Anti-fouling bioactive surfaces. Acta Biomater. 2011;7(4):1550-1557. doi:10.1016/j.actbio.2010.12.021
273. Kasoju N, Pátíková A, Wawrzynska E, et al. Bioengineering a pre-vascularized pouch for subsequent islet transplantation using VEGF-loaded polylactide capsules. Biomater Sci. 2020;8(2). doi:10.1039/c9bm01280j
274. Smink AM, Li S, Swart DH, et al. Stimulation of vascularization of a subcutaneous scaffold applicable for pancreatic islet-transplantation enhances immediate post-transplant islet graft function but not long-term normoglycemia. J Biomed Mater Res - Part A. 2017;105(9). doi:10.1002/jbm.a.36101
275. Tom B. Foreign body giant cells in the foreign body reaction to implanted biomaterials , a systematic review. :1-24.

276. Le NN, Rose MB, Levinson H, Klitzman B. Implant healing in experimental animal models of diabetes. J Diabetes Sci Technol. 2011;5(3):605-618. doi:10.1177/193229681100500315
277. Atala A, Kasper FK, Mikos AG. Engineering Complex Tissues. 2012;4(160):1-11.
278. Jiang K, Chaimov D, Patel SN, et al. 3-D physiomimetic extracellular matrix hydrogels provide a supportive microenvironment for rodent and human islet culture. Biomaterials. 2019;198. doi:10.1016/j.biomaterials.2018.08.057
279. Heo YJ, Shibata H, Okitsu T, Kawanishi T, Takeuchi S. Long-term in vivo glucose monitoring using fluorescent hydrogel fibers. Proc Natl Acad Sci U S A. 2011;108(33):13399-13403. doi:10.1073/pnas.1104954108
280. McMurray RJ, Wann AKT, Thompson CL, Connelly JT, Knight MM. Surface topography regulates wnt signaling through control of primary cilia structure in mesenchymal stem cells. Sci Rep. 2013;3:25-28. doi:10.1038/srep03545
281. Orive G, Emerich D, Khademhosseini A, et al. Engineering a Clinically Translatable Bioartificial Pancreas to Treat Type I Diabetes. Trends Biotechnol. 2018;36(4):445-456. doi:10.1016/j.tibtech.2018.01.007
282. Lotti F, Ranieri F, Vadalà G, Zollo L, Di Pino G. Invasive intraneural interfaces: Foreign body reaction issues. Front Neurosci. 2017;11(SEP):1-14. doi:10.3389/fnins.2017.00497
283. Zhao X, Irvine SA, Agrawal A, et al. 3D patterned substrates for bioartificial blood vessels – The effect of hydrogels on aligned cells on a biomaterial surface. Acta Biomater. 2015;26:159-168. doi:10.1016/J.ACTBIO.2015.08.024

284. Lee Y, Matsushima N, Yada S, et al. Revealing How Topography of Surface Microstructures Alters Capillary Spreading. Sci Rep. 2019;9(1):1-11. doi:10.1038/s41598-019-44243-x
285. Kondyurina I, Kondyurin A. Foreign body reaction (immune respond) for artificial implants can be avoided. (Figure 1).
286. Hanson TL, Diaz-Botia CA, Kharazia V, Maharbiz MM, Sabes PN. The “sewing machine” for minimally invasive neural recording. bioRxiv. 2019;(1):578542. doi:10.1101/578542
287. del Campo A, Arzt E. Fabrication approaches for generating complex micro- and nanopatterns on polymeric surfaces. Chem Rev. 2008;108(3):911-945. doi:10.1021/cr050018y
288. Hoffman-Kim D, Mitchel JA, Bellamkonda R V. Topography, Cell Response, and Nerve Regeneration. Annu Rev Biomed Eng. 2010;12(1):203-231. doi:10.1146/annurev-bioeng-070909-105351
289. Yoshinari M, Matsuzaka K, Inoue T. Surface modification by cold-plasma technique for dental implants—Bio-functionalization with binding pharmaceuticals. Jpn Dent Sci Rev. 2011;47(2):89-101. doi:10.1016/J.JDSR.2011.03.001
290. Wang K, Leong KW, Yang Y. Expanding nanopatterned substrates using stitch technique for nanotopographical modulation of cell behavior. J Vis Exp. 2016;2016(118):6-11. doi:10.3791/54840
291. Qin D, Xia Y, Whitesides GM. Soft lithography for micro- and nanoscale patterning. Nat Protoc. 2010;5(3):491-502. doi:10.1038/nprot.2009.234

292. Azemi E, Stauffer WR, Gostock MS, Lagenaur CF, Cui XT. Surface immobilization of neural adhesion molecule L1 for improving the biocompatibility of chronic neural probes: In vitro characterization. Acta Biomater. Published online 2008. doi:10.1016/j.actbio.2008.02.028
293. Weaver JD, Headen DM, Hunckler MD, Coronel MM, Stabler CL, García AJ. Design of a vascularized synthetic poly(ethylene glycol) macroencapsulation device for islet transplantation. Biomaterials. 2018;172:54-65. doi:10.1016/j.biomaterials.2018.04.047
294. Editor S, Iby T. Biomaterials as Stem Cell Niche. Vol 1.; 2010. doi:10.1007/978 3 642 13893 5
295. Giraldo JA, Molano RD, Rengifo HR, et al. The impact of cell surface PEGylation and short-course immunotherapy on islet graft survival in an allogeneic murine model. Acta Biomater. 2017;49. doi:10.1016/j.actbio.2016.11.060
296. Sun C, Miao J, Yan J, et al. Applications of antibiofouling PEG-coating in electrochemical biosensors for determination of glucose in whole blood. Electrochimica Acta. 2013;89:549-554. doi:10.1016/j.electacta.2012.11.005
297. Nugent WH, Sheppard FR, Dubick MA, et al. Microvascular and Systemic Impact of Resuscitation with PEGylated Carboxyhemoglobin-Based Oxygen Carrier or Hetastarch in a Rat Model of Transient Hemorrhagic Shock. Shock Augusta Ga. Published online 2020. doi:10.1097/SHK.0000000000001370
298. Headen DM, Woodward KB, Coronel MM, et al. Local immunomodulation with Fas ligand-engineered biomaterials achieves allogeneic islet graft acceptance. Nat Mater. 2018;17(8):732-739. doi:10.1038/s41563-018-0099-0

299. Skoumal M, Woodward KB, Zhao H, et al. Localized immune tolerance from FasL-functionalized PLG scaffolds. Biomaterials. 2019;192:271-281. doi:10.1016/j.biomaterials.2018.11.015
300. Lou S, Zhang X, Zhang J, Deng J, Kong D, Li C. Pancreatic islet surface bioengineering with a heparin-incorporated starPEG nanofilm. Mater Sci Eng C. 2017;78. doi:10.1016/j.msec.2017.03.295
301. Wallace A, Albadawi H, Patel N, et al. Anti-fouling strategies for central venous catheters. Cardiovasc Diagn Ther. 2017;7(S3):S246-S257. doi:10.21037/cdt.2017.09.18
302. Weis GCC, Assmann CE, Cadoná FC, et al. Immunomodulatory effect of mancozeb, chlorothalonil, and thiophanate methyl pesticides on macrophage cells. Ecotoxicol Environ Saf. 2019;182. doi:10.1016/j.ecoenv.2019.109420
303. Xu Y, Takai M, Ishihara K. Protein adsorption and cell adhesion on cationic, neutral, and anionic 2-methacryloyloxyethyl phosphorylcholine copolymer surfaces. Biomaterials. Published online 2009. doi:10.1016/j.biomaterials.2009.06.005
304. Goda T, Konno T, Takai M, Moro T, Ishihara K. Biomimetic phosphorylcholine polymer grafting from polydimethylsiloxane surface using photo-induced polymerization. Biomaterials. Published online 2006. doi:10.1016/j.biomaterials.2006.05.046
305. Ishihara K, Ando B, Takai M. Phosphorylcholine group-immobilized surface prepared on polydimethylsiloxane membrane by in situ reaction for its reduced biofouling. Nanobiotechnology. Published online 2007. doi:10.1007/s12030-008-9006-0

306. Komatsu H, Gonzalez N, Salgado M, et al. A subcutaneous pancreatic islet transplantation platform using a clinically applicable, biodegradable Vicryl mesh scaffold - an experimental study. Transpl Int. 2020;33(7):806-818. doi:10.1111/tri.13607
307. Veiseh O, Doloff JC, Ma M, et al. Size- and shape-dependent foreign body immune response to materials implanted in rodents and non-human primates. Nat Mater. 2015;14(6):643-651. doi:10.1038/nmat4290
308. Bhushan B. Nanotribology and Materials Characterization of MEMS/NEMS and BioMEMS/BioNEMS Materials and Devices. In: Springer Handbook of Nanotechnology. Springer Berlin Heidelberg; 2007:1575-1638. doi:10.1007/978-3-540-29857-1_50
309. Wang GJ, Chen CL, Hsu SH, Chiang YL. Bio-MEMS fabricated artificial capillaries for tissue engineering. In: Microsystem Technologies. Vol 12. Springer; 2005:120-127. doi:10.1007/s00542-005-0017-7
310. Subramani K, Ahmed W. Fabrication of PEG Hydrogel Micropatterns by Soft-Photolithography and PEG Hydrogel as Guided Bone Regeneration Membrane in Dental Implantology. In: Emerging Nanotechnologies in Dentistry. Elsevier Inc.; 2012:171-187. doi:10.1016/B978-1-4557-7862-1.00011-0
311. Cao Y, Zeng X, Cai Z, Duan J. Laser micro/nano-fabrication techniques and their applications in electronics11. In: Advances in Laser Materials Processing: Technology, Research and Application. Elsevier Inc.; 2010:629-670. doi:10.1533/9781845699819.7.629

312. Caldorera-Moore M, Peppas NA. Micro- and nanotechnologies for intelligent and responsive biomaterial-based medical systems. Adv Drug Deliv Rev. 2009;61(15):1391-1401. doi:10.1016/j.addr.2009.09.002
313. Engstrom DS, Porter B, Pacios M, Bhaskaran H. Additive nanomanufacturing - A review. J Mater Res. 2014;29(17):1792-1816. doi:10.1557/jmr.2014.159
314. Steele JAM, Hallé JP, Poncelet D, Neufeld RJ. Therapeutic cell encapsulation techniques and applications in diabetes. Adv Drug Deliv Rev. 2014;67-68. doi:10.1016/j.addr.2013.09.015
315. Liu R, Qin Y, Wang H, Zhao Y, Hu Z, Wang S. The in vivo blood compatibility of bio-inspired small diameter vascular graft: Effect of submicron longitudinally aligned topography. BMC Cardiovasc Disord. 2013;13. doi:10.1186/1471-2261-13-79
316. Lee SJ, Nowicki M, Harris B, Zhang LG. Fabrication of a Highly Aligned Neural Scaffold via a Table Top Stereolithography 3D Printing and Electrospinning . Tissue Eng Part A. 2017;23(11-12):491-502. doi:10.1089/ten.tea.2016.0353
317. Semnani D, Naghashzargar E, Hadjianfar M, et al. Evaluation of PCL/chitosan electrospun nanofibers for liver tissue engineering. http://dx.doi.org/101080/009140372016119093l. Published online 2016. doi:10.1080/00914037.2016.1190931
318. Peres C, Matos AI, Conniot J, et al. Poly(lactic acid)-based particulate systems are promising tools for immune modulation. Acta Biomater. Published online 2017. doi:10.1016/j.actbio.2016.11.012

319. McCrea Z, Arnanthigo Y, Cryan SA, O'Dea S. A Novel Methodology for Bio-electrospraying Mesenchymal Stem Cells that Maintains Differentiation, Immunomodulatory and Pro-reparative Functions. J Med Biol Eng. 2018;38(3):497-513. doi:10.1007/s40846-017-0331-4
320. Joddar B, Sarang-Sieminski AL, Hogrebe NJ, Tennant CJ, Gooch KJ. 5.4 Biomaterials and the Microvasculature ☆. In: Comprehensive Biomaterials II. Elsevier; 2017:67-87. doi:10.1016/B978-0-12-803581-8.09820-9
321. Hughes RA, Menumerov E, Neretina S. When lithography meets self-Assembly: A review of recent advances in the directed assembly of complex metal nanostructures on planar and textured surfaces. Nanotechnology. 2017;28(28):282002. doi:10.1088/1361-6528/aa77ce
322. Kharbikar BN, Kumar S. H, Kr. S, Srivastava R. Hollow silicon microneedle array based trans-epidermal antiemetic patch for efficient management of chemotherapy induced nausea and vomiting. In: Eggleton BJ, Palomba S, eds. Micro+Nano Materials, Devices, and Systems. Vol 9668. SPIE; 2015:96682W. doi:10.1117/12.2207407
323. Jell G, Minelli C, Stevens MM. Biomaterial-related approaches: Surface structuring. In: Fundamentals of Tissue Engineering and Regenerative Medicine. Springer Berlin Heidelberg; 2009:469-484. doi:10.1007/978-3-540-77755-7_35
324. Helton KL, Ratner BD, Wisniewski NA. Biomechanics of the sensor-tissue interface - Effects of motion, pressure, and design on sensor performance and foreign body response - Part II: Examples and application. In: Journal of Diabetes Science and Technology. ; 2011. doi:10.1177/193229681100500318

325. Scharp DW, Marchetti P. Encapsulated islets for diabetes therapy: History, current progress, and critical issues requiring solution. Adv Drug Deliv Rev. 2014;67-68:35-73. doi:10.1016/j.addr.2013.07.018
326. Toda S, Fattah A, Asawa K, et al. Optimization of islet microencapsulation with thin polymer membranes for long-term stability. Micromachines. 2019;10(11). doi:10.3390/mi10110755
327. Onuki Y, Bhardwaj U, Papadimitrakopoulos F, Burgess DJ. A review of the biocompatibility of implantable devices: Current challenges to overcome foreign body response. J Diabetes Sci Technol. 2008;2(6):1003-1015. doi:10.1177/193229680800200610
328. Cobelli C, Renard E, Kovatchev B. Artificial pancreas: Past, present, future. Diabetes. 2011;60(11):2672-2682. doi:10.2337/db11-0654
329. Rege NK, Phillips NFB, Weiss MA. Development of glucose-responsive “smart” insulin systems. Curr Opin Endocrinol Diabetes Obes. Published online 2017. doi:10.1097/MED.0000000000000345
330. Pareta R, Mcquilling JP, Farney AC, Opara EC. 4 Bioartificial Pancreas: Evaluation of Crucial Barriers to Clinical Application.
331. Mason McClatchey P, McClain ES, Williams IM, et al. Fibrotic encapsulation is the dominant source of continuous glucose monitor delays. Diabetes. 2019;68(10):1892-1901. doi:10.2337/db19-0229
332. Yuan J, Wang K, Xia X. Highly ordered platinum-nanotubule arrays for amperometric glucose sensing. Adv Funct Mater. 2005;15(5):803-809. doi:10.1002/adfm.200400321

333. Holt-Hindle P, Nigro S, Asmussen M, Chen A. Amperometric glucose sensor based on platinum-iridium nanomaterials. Electrochem Commun. 2008;10(10):1438-1441. doi:10.1016/j.elecom.2008.07.042
334. Lucisano JY, Routh TL, Lin JT, Gough DA. Glucose Monitoring in Individuals with Diabetes Using a Long-Term Implanted Sensor/Telemetry System and Model. IEEE Trans Biomed Eng. 2017;64(9):1982-1993. doi:10.1109/TBME.2016.2619333
335. Lee H, Hong YJ, Baik S, Hyeon T, Kim DH. Enzyme-Based Glucose Sensor: From Invasive to Wearable Device. Adv Healthc Mater. 2018;7(8). doi:10.1002/adhm.201701150
336. Ahmad R, Tripathy N, Ahn MS, et al. Highly Efficient Non-Enzymatic Glucose Sensor Based on CuO Modified Vertically-Grown ZnO Nanorods on Electrode. Sci Rep. 2017;7(1):1-10. doi:10.1038/s41598-017-06064-8
337. Moser O, Münzker J, Korsatko S, et al. A prolonged run-in period of standard subcutaneous microdialysis ameliorates quality of interstitial glucose signal in patients after major cardiac surgery. Sci Rep. 2018;8(1):1-8. doi:10.1038/s41598-018-19768-2
338. Zhu Z, Garcia-Gancedo L, Flewitt AJ, Xie H, Moussy F, Milne WI. A critical review of Glucose biosensors based on Carbon nanomaterials: Carbon nanotubes and graphene. Sens Switz. 2012;12(5):5996-6022. doi:10.3390/s120505996
339. Chen C, Zhao XL, Li ZH, Zhu ZG, Qian SH, Flewitt AJ. Current and emerging technology for continuous glucose monitoring. Sens Switz. 2017;17(1). doi:10.3390/s17010182

340. Elsherif M, Hassan MU, Yetisen AK, Butt H. Glucose Sensing with Phenylboronic Acid Functionalized Hydrogel-Based Optical Diffusers. ACS Nano. 2018;12(3):2283-2291. doi:10.1021/acsnano.7b07082
341. Dong Y, Wang W, Veiseh O, et al. Injectable and Glucose-Responsive Hydrogels Based on Boronic Acid-Glucose Complexation. Langmuir. 2016;32(34):8743-8747. doi:10.1021/acs.langmuir.5b04755
342. Kajisa T, Sakata T. Glucose-responsive hydrogel electrode for biocompatible glucose transistor. Sci Technol Adv Mater. 2017;18(1):26-33. doi:10.1080/14686996.2016.1257344
343. Tanne J, Schäfer D, Khalid W, Parak WJ, Lisdat F. Light-controlled bioelectrochemical sensor based on CdSe/ZnS quantum dots. Anal Chem. 2011;83(20):7778-7785. doi:10.1021/ac201329u
344. Li Z, Dong C, Tang L, Zhu X, Chen H, Ren J. Aqueous synthesis of CdTe/CdS/ZnS quantum dots and their optical and chemical properties. Luminescence. 2011;26(6):439-448. doi:10.1002/bio.1250
345. Zhang C, Zhang Z, Yang Q, Chen W. Graphene-based Electrochemical Glucose Sensors: Fabrication and Sensing Properties. Electroanalysis. 2018;30(11):2504-2524. doi:10.1002/elan.201800522
346. Al-Sagur H, Komathi S, Khan MA, Gurek AG, Hassan A. A novel glucose sensor using lutetium phthalocyanine as redox mediator in reduced graphene oxide conducting polymer multifunctional hydrogel. Biosens Bioelectron. 2017;92:638-645. doi:10.1016/j.bios.2016.10.038

347. Olejnik A, Siuzdak K, Karczewski J, Grochowska K. A Flexible Nafion Coated Enzyme-free Glucose Sensor Based on Au-dimpled Ti Structures. Electroanalysis. 2020;32(2):323-332. doi:10.1002/elan.201900455
348. Chen D, Wang C, Chen W, Chen Y, Zhang JXJ. PVDF-Nafion nanomembranes coated microneedles for in vivo transcutaneous implantable glucose sensing. Biosens Bioelectron. 2015;74:1047-1052. doi:10.1016/j.bios.2015.07.036
349. Vaidya R, Atanasov P, Wilkins E. Effect of interference on the performance of glucose enzyme electrodes using Nafion® coatings. Med Eng Phys. 1995;17(6):416-424. doi:10.1016/1350-4533(94)00006-U
350. Nery EW, Kundys M, Jeleń PS, Jönsson-Niedziólka M. Electrochemical glucose sensing: Is there still room for improvement? Anal Chem. 2016;88(23):11271-11282. doi:10.1021/acs.analchem.6b03151
351. Xie X, Doloff JC, Yesilyurt V, et al. Reduction of measurement noise in a continuous glucose monitor by coating the sensor with a zwitterionic polymer. Nat Biomed Eng. 2018;2(12):894-906. doi:10.1038/s41551-018-0273-3
352. Nichols SP, Koh A, Storm WL, Shin JH, Schoenfisch MH. Biocompatible materials for continuous glucose monitoring devices. Chem Rev. 2013;113(4):2528-2549. doi:10.1021/cr300387j
353. Unruh RM, Roberts JR, Nichols SP, Gamsey S, Wisniewski NA, McShane MJ. Preclinical evaluation of Poly(HEMA-co-acrylamide) hydrogels encapsulating glucose oxidase and palladium benzoporphyrin as fully implantable glucose sensors. J Diabetes Sci Technol. 2015;9(5):985-992. doi:10.1177/1932296815590439

354. Wang C, Yu B, Knudsen B, Harmon J, Moussy F, Moussy Y. Synthesis and performance of novel hydrogels coatings for implantable glucose sensors. Biomacromolecules. 2008;9(2):561-567. doi:10.1021/bm701102y
355. Keum DH, Kim SK, Koo J, et al. Wireless smart contact lens for diabetic diagnosis and therapy. Sci Adv. 2020;6(17):eaba3252. doi:10.1126/sciadv.aba3252
356. Mugweru A, Clark BL, Pishko M V. Electrochemical sensor array for glucose monitoring fabricated by rapid immobilization of active glucose oxidase within photochemically polymerized hydrogels. J Diabetes Sci Technol. 2007;1(3):366-371. doi:10.1177/193229680700100308
357. Quinn CAP, Connor RE, Heller A. Biocompatible, glucose-permeable hydrogel for in situ coating of implantable biosensors. Biomaterials. 1997;18(24):1665-1670. doi:10.1016/S0142-9612(97)00125-7
358. Lin P, Lin CW, Mansour R, Gu F. Improving biocompatibility by surface modification techniques on implantable bioelectronics. Biosens Bioelectron. Published online 2013. doi:10.1016/j.bios.2013.01.071
359. Song B, Zhang E, Han X, Zhu H, Shi Y, Cao Z. Engineering and Application Perspectives on Designing an Antimicrobial Surface. ACS Appl Mater Interfaces. 2020;12(19):21330-21341. doi:10.1021/acsami.9b19992
360. Wang Z, Li J, Jiang L, Xiao S, Liu Y, Luo J. Zwitterionic Hydrogel Incorporated Graphene Oxide Nanosheets with Improved Strength and Lubricity. Langmuir. 2019;35(35):11452-11462. doi:10.1021/acs.langmuir.9b01640

361. Chou YN, Chang Y, Wen TC. Applying thermosettable zwitterionic copolymers as general fouling-resistant and thermal-tolerant biomaterial interfaces. ACS Appl Mater Interfaces. 2015;7(19):10096-100107. doi:10.1021/acsami.5b01756
362. Yang W, Xue H, Carr LR, Wang J, Jiang S. Zwitterionic poly(carboxybetaine) hydrogels for glucose biosensors in complex media. Biosens Bioelectron. 2011;26(5):2454-2459. doi:10.1016/j.bios.2010.10.031
363. Sun M, Qiu H, Su C, et al. Solvent-Free Graft-From Polymerization of Polyvinylpyrrolidone Imparting Ultralow Bacterial Fouling and Improved Biocompatibility. ACS Appl Bio Mater. 2019;2(9):3983-3991. doi:10.1021/acsabm.9b00529
364. Koschwanez HE, Yap FY, Klitzman B, Reichert WM. In vitro and in vivo characterization of porous poly-L-lactic acid coatings for subcutaneously implanted glucose sensors. J Biomed Mater Res - Part A. 2008;87(3):792-807. doi:10.1002/jbm.a.31824
365. Klueh U, Qiao Y, Czajkowski C, Ludzinska I, Antar O, Kreutzer DL. Basement membrane-based glucose sensor coatings enhance continuous glucose monitoring in vivo. J Diabetes Sci Technol. 2015;9(5):957-965. doi:10.1177/1932296815598776
366. Klueh U, Ludzinska I, Czajkowski C, Qiao Y, Kreutzer DL. Crosslinked basement membrane-based coatings enhance glucose sensor function and continuous glucose monitoring in vivo. J Biomed Mater Res - Part A. 2018;106(1):7-16. doi:10.1002/jbm.a.36206

367. Wang N, Burugapalli K, Wijesuriya S, et al. Electrospun polyurethane-core and gelatin-shell coaxial fibre coatings for miniature implantable biosensors. Biofabrication. Published online 2014. doi:10.1088/1758-5082/6/1/015002
368. Wang N, Burugapalli K, Song W, et al. Electrospun fibro-porous polyurethane coatings for implantable glucose biosensors. Biomaterials. Published online 2013. doi:10.1016/j.biomaterials.2012.10.049
369. Lanzalaco S, Molina BG. Polymers and plastics modified electrodes for biosensors: A review. Molecules. 2020;25(10). doi:10.3390/MOLECULES25102446
370. Bridges AW, García AJ. Anti-inflammatory polymeric coatings for implantable biomaterials and devices. In: Journal of Diabetes Science and Technology. Vol 2. SAGE Publications Inc.; 2008:984-994. doi:10.1177/193229680800200628
371. Locke AK, Means AK, Dong P, Nichols TJ, Coté GL, Grunlan MA. A Layer-by-Layer Approach to Retain a Fluorescent Glucose Sensing Assay within the Cavity of a Hydrogel Membrane. ACS Appl Bio Mater. 2018;1(5):1319-1327. doi:10.1021/acsabm.8b00267
372. Fei R, Means AK, Abraham AA, Locke AK, Coté GL, Grunlan MA. Self-Cleaning, Thermoresponsive P(NIPAAm-co-AMPS) Double Network Membranes for Implanted Glucose Biosensors. Macromol Mater Eng. 2016;301(8):935-943. doi:10.1002/mame.201600044
373. Means AK, Dong P, Clubb FJ, et al. A self-cleaning, mechanically robust membrane for minimizing the foreign body reaction: towards extending the lifetime of sub-Q glucose biosensors. J Mater Sci Mater Med. 2019;30(7):79. doi:10.1007/s10856-019-6282-2

374. Xu J, Lee H. Anti-Biofouling Strategies for Long-Term Continuous Use of Implantable Biosensors. Chemosensors. 2020;8(3):66. doi:10.3390/chemosensors8030066
375. Bridges AW, García AJ. Anti-inflammatory polymeric coatings for implantable biomaterials and devices. In: Journal of Diabetes Science and Technology. Vol 2. SAGE Publications Inc.; 2008:984-994. doi:10.1177/193229680800200628
376. Vallejo-Heligon SG, Klitzman B, Reichert WM. Characterization of porous, dexamethasone-releasing polyurethane coatings for glucose sensors. Acta Biomater. 2014;10(11):4629-4638. doi:10.1016/j.actbio.2014.07.019
377. Klueh U, Kaur M, Montrose DC, Kreutzer DL. Infammation and glucose sensors: Use of dexamethasone to extend glucose sensor function and life span in vivo. J Diabetes Sci Technol. 2007;1(4):496-504. doi:10.1177/193229680700100407
378. Welch NG, Winkler DA, Thissen H. Antifibrotic strategies for medical devices. Adv Drug Deliv Rev. Published online June 15, 2020. doi:10.1016/j.addr.2020.06.008
379. Avula M, Jones D, Rao AN, et al. Local release of masitinib alters in vivo implantable continuous glucose sensor performance. Biosens Bioelectron. 2016;77:149-156. doi:10.1016/j.bios.2015.08.059
380. Avula MN, Rao AN, McGill LD, Grainger DW, Solzbacher F. Modulation of the foreign body response to implanted sensor models through device-based delivery of the tyrosine kinase inhibitor, masitinib. Biomaterials. 2013;34(38):9737-9746. doi:10.1016/j.biomaterials.2013.08.090

381. Avula M, Jones D, Rao AN, et al. Local release of masitinib alters in vivo implantable continuous glucose sensor performance. Biosens Bioelectron. 2016;77:149-156. doi:10.1016/j.bios.2015.08.059
382. Soto RJ, Privett BJ, Schoenfisch MH. In vivo analytical performance of nitric oxide-releasing glucose biosensors. Anal Chem. 2014;86(14):7141-7149. doi:10.1021/ac5017425
383. Cha KH, Meyerhoff ME. Compatibility of Nitric Oxide Release with Implantable Enzymatic Glucose Sensors Based on Osmium (III/II) Mediated Electrochemistry. ACS Sens. 2017;2(9):1262-1266. doi:10.1021/acssensors.7b00430
384. Cha KH, Wang X, Meyerhoff ME. Nitric oxide release for improving performance of implantable chemical sensors – A review. Appl Mater Today. 2017;9:589-597. doi:10.1016/j.apmt.2017.10.002
385. Zhang WJ, Laue C, Hyder A, Schrezenmeir J. Purity of alginate affects the viability and fibrotic overgrowth of encapsulated porcine islet xenografts. Transplant Proc. Published online 2001. doi:10.1016/S0041-1345(01)02419-8
386. Mallett AG, Korbutt GS. Alginate modification improves long-term survival and function of transplanted encapsulated islets. Tissue Eng Part A. 2009;15(6):1301-1309. doi:10.1089/ten.tea.2008.0118
387. Kulseng B, Skjåk-Braek G, Ryan L, et al. Transplantation of alginate microcapsules: generation of antibodies against alginates and encapsulated porcine islet-like cell clusters. Transplantation. 1999;67(7):978-984. doi:10.1097/00007890-199904150-00008

388. Villa C, Manzoli V, Abreu MM, et al. Effects of Composition of Alginate-Polyethylene Glycol Microcapsules and Transplant Site on Encapsulated Islet Graft Outcomes in Mice. Transplantation. 2017;101(5):1025-1035. doi:10.1097/TP.0000000000001454
389. S S, Pj F, O K, et al. Biocompatibility of Alginates for Grafting: Impact of Alginate Molecular Weight. Artif Cells Blood Substit Immobil Biotechnol. 2003;31(4). doi:10.1081/bio-120025409
390. Lum ZP, Krestow M, Tai IT, Vacek I, Sun AM. Xenografts of rat islets into diabetic mice. An evaluation of new smaller capsules. Transplantation. 1992;53(6):1180-1183. doi:10.1097/00007890-199206000-00002
391. Schneider S, Feilen PJ, Slotty V, et al. Multilayer capsules: A promising microencapsulation system for transplantation of pancreatic islets. Biomaterials. 2001;22(14):1961-1970. doi:10.1016/S0142-9612(00)00380-X
392. Park HS, Kim JW, Lee SH, et al. Antifibrotic effect of rapamycin containing polyethylene glycol-coated alginate microcapsule in islet xenotransplantation. J Tissue Eng Regen Med. 2017;11(4):1274-1284. doi:10.1002/term.2029
393. Farah S, Doloff JC, Müller P, et al. Long-term implant fibrosis prevention in rodents and non-human primates using crystallized drug formulations. Nat Mater. 2019;18(August). doi:10.1038/s41563-019-0377-5
394. Vegas AJ, Veiseh O, Doloff JC, et al. Combinatorial hydrogel library enables identification of materials that mitigate the foreign body response in primates. Nat Biotechnol. 2016;34(3):345-352. doi:10.1038/nbt.3462

395. Anselmo AC, Gokarn Y, Mitragotri S. Non-invasive delivery strategies for biologics. Nat Rev Drug Discov. 2018;18(1):19-40. doi:10.1038/nrd.2018.183
396. An D, Chiu A, Flanders JA, et al. Designing a retrievable and scalable cell encapsulation device for potential treatment of type 1 diabetes. Proc Natl Acad Sci U S A. 2017;115(2):E263-E272. doi:10.1073/pnas.1708806115
397. Vegas AJ, Veiseh O, Gürtler M, et al. Long-term glycemic control using polymer-encapsulated human stem cell-derived beta cells in immune-competent mice. Nat Med. 2016;22(3):306-311. doi:10.1038/nm.4030
398. Alagpulinsa DA, Cao JJL, Driscoll RK, et al. Alginate-microencapsulation of human stem cell–derived β cells with CXCL12 prolongs their survival and function in immunocompetent mice without systemic immunosuppression. Am J Transplant. 2019;19(7):1930-1940. doi:10.1111/ajt.15308
399. Citro A, Moser PT, Dugnani E, et al. Biofabrication of a vascularized islet organ for type 1 diabetes. Biomaterials. 2019;199:40-51. doi:10.1016/j.biomaterials.2019.01.035
400. Vaithilingam V, Kollarikova G, Qi M, et al. Beneficial effects of coating alginate microcapsules with macromolecular heparin conjugates-in vitro and in vivo study. Tissue Eng Part A. 2014;20(1-2):324-334. doi:10.1089/ten.TEA.2013.0254
401. Safley SA, Kenyon NS, Berman DM, et al. Microencapsulated adult porcine islets transplanted intraperitoneally in streptozotocin-diabetic non-human primates. Xenotransplantation. 2018;25(6). doi:10.1111/xen.12450
402. Yang HK, Ham DS, Park HS, et al. Long-term Efficacy and Biocompatibility of Encapsulated Islet Transplantation With Chitosan-Coated Alginate Capsules in

Mice and Canine Models of Diabetes. Transplantation. 2016;100(2):334-343. doi:10.1097/TP.0000000000000927

403. Vegas AJ, Veiseh O, Doloff JC, et al. Combinatorial hydrogel library enables identification of materials that mitigate the foreign body response in primates. Nat Biotechnol. 2016;34(3):345-352. doi:10.1038/nbt.3462
404. Bochenek MA, Veiseh O, Vegas AJ, et al. Alginate encapsulation as long-term immune protection of allogeneic pancreatic islet cells transplanted into the omental bursa of macaques. Nat Biomed Eng. 2018;2(11):810-821. doi:10.1038/s41551-018-0275-1
405. Liu Q, Chiu A, Wang LH, et al. Zwitterionically modified alginates mitigate cellular overgrowth for cell encapsulation. Nat Commun. 2019;10(1):1-14. doi:10.1038/s41467-019-13238-7
406. Liu Q, Chiu A, Wang L, et al. Developing mechanically robust, triazole-zwitterionic hydrogels to mitigate foreign body response (FBR) for islet encapsulation. Biomaterials. 2020;230:119640. doi:10.1016/j.biomaterials.2019.119640
407. Dang TT, Thai A V., Cohen J, et al. Enhanced function of immuno-isolated islets in diabetes therapy by co-encapsulation with an anti-inflammatory drug. Biomaterials. 2013;34(23):5792-5801. doi:10.1016/j.biomaterials.2013.04.016
408. Vaithilingam V, Evans MDM, Lewy DM, Bean PA, Bal S, Tuch BE. Co-encapsulation and co-transplantation of mesenchymal stem cells reduces pericapsular fibrosis and improves encapsulated islet survival and function when allografted. Sci Rep. 2017;7(1). doi:10.1038/s41598-017-10359-1

409. Luca G, Calafiore R, Basta G, et al. Improved function of rat islets upon co-microencapsulation with Sertoli's cells in alginate/poly-L-ornithine. AAPS PharmSciTech. 2001;2(3):E15. doi:10.1208/pt020315
410. Kobayashi T, Aomatsu Y, Iwata H, et al. Indefinite islet protection from autoimmune destruction in nonobese diabetic mice by agarose microencapsulation without immunosuppression. Transplantation. 2003;75(5):619-625. doi:10.1097/01.TP.0000053749.36365.7E
411. Kobayashi T, Aomatsu Y, Iwata H, et al. Survival of microencapsulated islets at 400 days posttransplantation in the omental pouch of NOD mice. Cell Transplant. 2006;15(4):359-365. doi:10.3727/000000006783981954
412. Bratlie KM, York RL, Invernale MA, Langer RL, Anderson DG. Materials for diabetes therapeutics. Adv Healthc Mater. Published online 2012. doi:10.1002/adhm.201200037
413. Yin C, Chia SM, Quek CH, et al. Microcapsules with improved mechanical stability for hepatocyte culture. Biomaterials. 2003;24(10):1771-1780. doi:10.1016/S0142-9612(02)00580-X
414. Peterson KP, Peterson CM, Pope EJA. Silica Sol-Gel Encapsulation of Pancreatic Islets. Exp Biol Med. 1998;218(4):365-369. doi:10.3181/00379727-218-44305
415. Harrington S, Williams J, Rawal S, Ramachandran K, Stehno-Bittel L. Hyaluronic Acid/Collagen Hydrogel as an Alternative to Alginate for Long-Term Immunoprotected Islet Transplantation. Tissue Eng - Part A. 2017;23(19-20):1088-1099. doi:10.1089/ten.tea.2016.0477

416. Wang T, Lacík I, Brissová M, et al. An Encapsulation System for the Immunoisolation of Pancreatic Islets. Nat Biotechnol. 1997;15(4):358-362. doi:10.1038/nbt0497-358
417. Lee DY, Park SJ, Nam JH, Byun Y. A combination therapy of PEGylation and immunosuppressive agent for successful islet transplantation. J Controlled Release. 2006;110(2):290-295. doi:10.1016/j.jconrel.2005.10.023
418. Giraldo JA, Molano RD, Rengifo HR, et al. The impact of cell surface PEGylation and short-course immunotherapy on islet graft survival in an allogeneic murine model. Acta Biomater. 2017;49:272-283. doi:10.1016/j.actbio.2016.11.060
419. Stabler CL, Giraldo JA, Berman DM, et al. Transplantation of PEGylated islets enhances therapeutic efficacy in a diabetic nonhuman primate model. Am J Transplant. 2020;20(3):689-700. doi:10.1111/ajt.15643
420. Panza JL, Wagner WR, Rilo HLR, Harsha Rao R, Beckman EJ, Russell AJ. Treatment of rat pancreatic islets with reactive PEG. Biomaterials. 2000;21(11):1155-1164. doi:10.1016/S0142-9612(99)00283-5
421. Tomei AA, Manzoli V, Fraker CA, et al. Device design and materials optimization of conformal coating for islets of Langerhans. Proc Natl Acad Sci U S A. 2014;111(29):10514-10519. doi:10.1073/pnas.1402216111
422. Korsgren O. Islet encapsulation: Physiological possibilities and limitations. Diabetes. 2017;66(7):1748-1754. doi:10.2337/db17-0065
423. Wee YM, Lim DG, Kim YH, et al. Cell surface modification by activated polyethylene glycol prevents allosensitization after islet transplantation. Cell Transplant. 2008;17(10-11):1257-1269. doi:10.3727/096368908787236657

424. Jeong JH, Yook S, Hwang JW, et al. Synergistic effect of surface modification with poly(ethylene glycol) and immunosuppressants on repetitive pancreatic islet transplantation into antecedently sensitized rat. Transplant Proc. 2013;45(2):585-590. doi:10.1016/j.transproceed.2012.02.028
425. Dong YL, Sang JP, Lee S, Jong HN, Byun Y. Highly poly(ethylene) glycolylated islets improve long-term islet allograft survival without immunosuppressive medication. Tissue Eng. 2007;13(8):2133-2141. doi:10.1089/ten.2006.0009
426. Dong H, Fahmy TM, Metcalfe SM, et al. Immuno-Isolation of Pancreatic Islet Allografts Using Pegylated Nanotherapy Leads to Long-Term Normoglycemia in Full MHC Mismatch Recipient Mice. Fiorina P, ed. PLoS ONE. 2012;7(12):e50265. doi:10.1371/journal.pone.0050265
427. Vaithilingam V, Bal S, Tuch BE. Encapsulated islet transplantation: Where do we stand? Rev Diabet Stud. 2017;14(1). doi:10.1900/RDS.2017.14.51
428. King A. Microencapsulation of islets of Langerhans: impact of cellular overgrowth. Ups J Med Sci. Published online 2001. doi:10.3109/2000-1967-140
429. Kumagai-Braesch M, Jacobson S, Mori H, et al. The theracyteTM device protects against islet allograft rejection in immunized hosts. Cell Transplant. 2013;22(7):1137-1146. doi:10.3727/096368912X657486
430. Chendke GS, Faleo G, Juang C, et al. Supporting Survival of Transplanted Stem-Cell-Derived Insulin-Producing Cells in an Encapsulation Device Augmented with Controlled Release of Amino Acids. Adv Biosyst. 2019;3(9). doi:10.1002/adbi.201900086

431. Chang R, Faleo G, Russ HA, et al. Nanoporous Immunoprotective Device for Stem-Cell-Derived β-Cell Replacement Therapy. ACS Nano. 2017;11(8):7747-7757. doi:10.1021/acsnano.7b01239
432. Nyitray CE, Chang R, Faleo G, et al. Polycaprolactone Thin-Film Micro- and Nanoporous Cell-Encapsulation Devices. ACS Nano. 2015;9(6):5675-5682. doi:10.1021/acsnano.5b00679
433. Jalili RB, Moeen Rezakhanlou A, Hosseini-Tabatabaei A, Ao Z, Warnock GL, Ghahary A. Fibroblast populated collagen matrix promotes islet survival and reduces the number of islets required for diabetes reversal. J Cell Physiol. 2011;226(7):1813-1819. doi:10.1002/jcp.22515
434. Bose S, Volpatti LR, Thiono D, et al. A retrievable implant for the long-term encapsulation and survival of therapeutic xenogeneic cells. Nat Biomed Eng. 2020;4(8):814-826. doi:10.1038/s41551-020-0538-5
435. An D, Ji Y, Chiu A, et al. Developing robust, hydrogel-based, nanofiber-enabled encapsulation devices (NEEDs) for cell therapies. Biomaterials. 2015;37:40-48. doi:10.1016/j.biomaterials.2014.10.032
436. Daoud J, Rosenberg L, Tabrizian M. Pancreatic islet culture and preservation strategies: Advances, challenges, and future outlook. Cell Transplant. 2010;19(12):1523-1535. doi:10.3727/096368910X515872
437. Saleem S, Li J, Yee SP, Fellows GF, Goodyer CG, Wang R. β1 integrin/FAK/ERK signalling pathway is essential for human fetal islet cell differentiation and survival. J Pathol. 2009;219(2):182-192. doi:10.1002/path.2577

438. Montesano R, Mouron P, Amherdt M, Orci L. Collagen matrix promotes reorganization of pancreatic endocrine cell monolayers into islet-like organoids. J Cell Biol. 1983;97(3):935-939. doi:10.1083/jcb.97.3.935
439. Weber LM, Hayda KN, Anseth KS. Cell–Matrix Interactions Improve β-Cell Survival and Insulin Secretion in Three-Dimensional Culture. Tissue Eng Part A. 2008;14(12):1959-1968. doi:10.1089/ten.tea.2007.0238
440. Stephens CH, Orr KS, Acton AJ, et al. In situ type I oligomeric collagen macroencapsulation promotes islet longevity and function in vitro and in vivo. Am J Physiol - Endocrinol Metab. 2018;315(4):E650-E661. doi:10.1152/ajpendo.00073.2018
441. Rios PD, Zhang X, Luo X, Shea LD. Mold-casted non-degradable, islet macro-encapsulating hydrogel devices for restoration of normoglycemia in diabetic mice. Biotechnol Bioeng. Published online 2016. doi:10.1002/bit.26005
442. Song S, Blaha C, Moses W, et al. An intravascular bioartificial pancreas device (iBAP) with silicon nanopore membranes (SNM) for islet encapsulation under convective mass transport. Lab Chip. 2017;17(10):1778-1792. doi:10.1039/c7lc00096k
443. Nilsson B, Ekdahl KN, Korsgren O. Control of instant blood-mediated inflammatory reaction to improve islets of Langerhans engraftment. Curr Opin Organ Transplant. 2011;16(6):620-626. doi:10.1097/MOT.0b013e32834c2393
444. Schweicher J, Nyitray C, Desai TA. Membranes to achieve immunoprotection of transplanted islets. Front Biosci - Landmark. 2014;19(1):49-76. doi:10.2741/4195

445. La Flamme KE, Popat KC, Leoni L, et al. Biocompatibility of nanoporous alumina membranes for immunoisolation. Biomaterials. 2007;28(16):2638-2645. doi:10.1016/j.biomaterials.2007.02.010
446. Mendelsohn A, Desai T. Inorganic nanoporous membranes for immunoisolated cell-based drug delivery. Adv Exp Med Biol. 2010;670:104-125. doi:10.1007/978-1-4419-5786-3_10
447. Kwon J, Trivedi K, Krishnamurthy N V., Hu W, Lee JB, Gimi B. SU-8-based immunoisolative microcontainer with nanoslots defined by nanoimprint lithography. J Vac Sci Technol B Microelectron Nanometer Struct. 2009;27(6):2795. doi:10.1116/1.3258146
448. Iqbal Z, Moses W, Kim S, Kim EJ, Fissell WH, Roy S. Sterilization effects on ultrathin film polymer coatings for silicon-based implantable medical devices. J Biomed Mater Res B Appl Biomater. 2018;106(6):2327-2336. doi:10.1002/jbm.b.34039
449. Francolini I, Piozzi A. Antimicrobial Polyurethanes for Intravascular Medical Devices. In: Advances in Polyurethane Biomaterials. Elsevier Inc.; 2016:349-385. doi:10.1016/B978-0-08-100614-6.00012-3
450. Rickels MR, Schutta MH, Markmann JF, Barker CF, Naji A, Teff KL. β-Cell function following human islet transplantation for type 1 diabetes. Diabetes. 2005;54(1):100-106. doi:10.2337/diabetes.54.1.100
451. Bogdan C, Röllinghoff M, Diefenbach A. The role of nitric oxide in innate immunity. Immunol Rev. Published online 2000. doi:10.1034/j.1600-065X.2000.917307.x

452. Hashimoto H, Olson EN, Bassel-Duby R. Therapeutic approaches for cardiac regeneration and repair. Nat Rev Cardiol. 2018;15(10):585-600. doi:10.1038/s41569-018-0036-6
453. Carter CS, Giovaninni S, Seo DO, et al. Differential effects of enalapril and losartan on body composition and indices of muscle quality in aged male Fischer 344 x Brown Norway rats. Age. 2011;33(2):167-183. doi:10.1007/s11357-010-9196-y
454. Johansson U, Ria M, Åvall K, et al. Pancreatic Islet Survival and Engraftment Is Promoted by Culture on Functionalized Spider Silk Matrices. Wagner B, ed. PLOS ONE. 2015;10(6):e0130169. doi:10.1371/journal.pone.0130169
455. Skrzypek K, Groot Nibbelink M, Van Lente J, et al. Pancreatic islet macroencapsulation using microwell porous membranes. Sci Rep. 2017;7(1):1-12. doi:10.1038/s41598-017-09647-7
456. Moberg L, Olsson A, Berne C, et al. Nicotinamide inhibits tissue factor expression in isolated human pancreatic islets: implications for clinical islet transplantation1. Transplantation. 2003;76(9):1285-1288. doi:10.1097/01.TP.0000098905.86445.0F
457. Johansson U, Olsson A, Gabrielsson S, Nilsson B, Korsgren O. Inflammatory mediators expressed in human islets of Langerhans: Implications for islet transplantation. Biochem Biophys Res Commun. Published online 2003. doi:10.1016/S0006-291X(03)01392-5
458. Contreras JL, Eckstein C, Smyth CA, et al. Activated protein C preserves functional islet mass after intraportal transplantation: A novel link between endothelial cell activation, thrombosis, inflammation, and islet cell death. Diabetes. 2004;53(11):2804-2814. doi:10.2337/diabetes.53.11.2804

459. Elizondo DM, Brandy NZD, da Silva RLL, et al. Pancreatic islets seeded in a novel bioscaffold forms an organoid to rescue insulin production and reverse hyperglycemia in models of type 1 diabetes. Sci Rep. 2020;10(1):1-11. doi:10.1038/s41598-020-60947-x
460. Narang AS, Mahato RI. Biological and biomaterial approaches for improved islet transplantation. Pharmacol Rev. 2006;58(2):194-243. doi:10.1124/pr.58.2.6
461. Webb MA, Dennison AR, James RF. The potential benefit of non-purified islets preparations for islet transplantation. Biotechnol Genet Eng Rev. 2012;28:101-114. doi:10.5661/bger-28-101
462. Jacobson EF, Tzanakakis ES. Human pluripotent stem cell differentiation to functional pancreatic cells for diabetes therapies: Innovations, challenges and future directions. J Biol Eng. 2017;11(1):21. doi:10.1186/s13036-017-0066-3
463. Bogdani M, Suenens K, Bock T, Pipeleers-Marichal M, In't Veld P, Pipeleers D. Growth and functional maturation of β-cells in implants of endocrine cells purified from prenatal porcine pancreas. Diabetes. 2005;54(12):3387-3394. doi:10.2337/diabetes.54.12.3387
464. Beuneu C, Vosters O, Ling Z, et al. N-Acetylcysteine derivative inhibits procoagulant activity of human islet cells. Diabetologia. 2007;50(2):343-347. doi:10.1007/s00125-006-0529-4
465. Khosravi-Maharlooei M, Hajizadeh-Saffar E, Tahamtani Y, et al. Therapy of endocrine disease: Islet transplantation for type 1 diabetes: So close and yet so far away. Eur J Endocrinol. 2015;173(5):R165-R183. doi:10.1530/EJE-15-0094

466. Berman DM, Molano RD, Fotino C, et al. Bioengineering the endocrine pancreas: Intraomental islet transplantation within a biologic resorbable scaffold. Diabetes. 2016;65(5):1350-1361. doi:10.2337/db15-1525
467. Lee S, Sathialingam M, Alexander M, Lakey J. Physical Protection of Pancreatic Islets for Transplantation. In: Biomaterials - Physics and Chemistry - New Edition. InTech; 2018. doi:10.5772/intechopen.71285
468. Cui W, Angsana J, Wen J, Chaikof EL. Liposomal formulations of thrombomodulin increase engraftment after intraportal islet transplantation. Cell Transplant. 2010;19(11):1359-1367. doi:10.3727/096368910X513964
469. Gmyr V, Bonner C, Moerman E, et al. Human recombinant antithrombin (ATryn®) administration improves survival and prevents intravascular coagulation after intraportal islet transplantation in a piglet model. Cell Transplant. 2017;26(2):309-317. doi:10.3727/096368916X693554
470. Hu S, de Vos P. Polymeric approaches to reduce tissue responses against devices applied for islet-cell encapsulation. Front Bioeng Biotechnol. Published online 2019. doi:10.3389/fbioe.2019.00134
471. Quintana J, Stinchcomb A, Kostyo J, Robichaud B, Plunk M, Kane R. Chemical Strategies for Improving Islet Transplant Outcomes. OBM Transplant. 2018;2(4):1-1. doi:10.21926/obm.transplant.1804036
472. Phelps EA, Templeman KL, Thulé PM, García AJ. Engineered VEGF-releasing PEG–MAL hydrogel for pancreatic islet vascularization. Drug Deliv Transl Res. 2015;5(2):125-136. doi:10.1007/s13346-013-0142-2

473. Wang D, Ding X, Xue W, et al. A new scaffold containing small intestinal submucosa and mesenchymal stem cells improves pancreatic islet function and survival in vitro and in vivo. Int J Mol Med. 2017;39(1):167-173. doi:10.3892/ijmm.2016.2814
474. Sorelle JA, Itoh T, Peng H, et al. Withaferin A inhibits pro-inflammatory cytokine-induced damage to islets in culture and following transplantation. Diabetologia. 2013;56(4):814-824. doi:10.1007/s00125-012-2813-9
475. Barra JM, Tse HM. Redox-dependent inflammation in islet transplantation rejection. Front Endocrinol. 2018;9(APR):175. doi:10.3389/fendo.2018.00175
476. Kumano K, Vasu S, Shabbir R, Darden C, Lawrence M, Naziruddin B. Characterizing and overcoming innate immunity in beta-cell replacement therapy. J Immunol Regen Med. Published online October 24, 2020:100034. doi:10.1016/j.regen.2020.100034
477. Mastellos DC, Yancopoulou D, Kokkinos P, et al. Compstatin: A C3-targeted complement inhibitor reaching its prime for bedside intervention. Eur J Clin Invest. 2015;45(4):423-440. doi:10.1111/eci.12419
478. Johansson H, Goto M, Siegbahn A, Elgue G, Korsgren O, Nilsson B. Low molecular weight dextran sulfate: A strong candidate drug to block IBMIR in clinical islet transplantation. Am J Transplant. 2006;6(2):305-312. doi:10.1111/j.1600-6143.2005.01186.x
479. Gamble A, Pepper AR, Bruni A, Shapiro AMJ. The journey of islet cell transplantation and future development. Islets. 2018;10(2):80-94. doi:10.1080/19382014.2018.1428511

480. Song S, Faleo G, Yeung R, et al. Silicon nanopore membrane (SNM) for islet encapsulation and immunoisolation under convective transport. Sci Rep. 2016;6. doi:10.1038/srep23679
481. Pathak V, Pathak NM, O'Neill CL, Guduric-Fuchs J, Medina RJ. Therapies for Type 1 Diabetes: Current Scenario and Future Perspectives. Clin Med Insights Endocrinol Diabetes. 2019;12:117955141984452. doi:10.1177/1179551419844521
482. Salg GA, Giese NA, Schenk M, et al. The emerging field of pancreatic tissue engineering: A systematic review and evidence map of scaffold materials and scaffolding techniques for insulin-secreting cells. J Tissue Eng. 2019;10:2041731419884708. doi:10.1177/2041731419884708
483. Skrzypek K, Nibbelink MG, Karbaat LP, Karperien M, van Apeldoorn A, Stamatialis D. An important step towards a prevascularized islet macroencapsulation device—effect of micropatterned membranes on development of endothelial cell network. J Mater Sci Mater Med. 2018;29(7):91. doi:10.1007/s10856-018-6102-0
484. Dolan EB, Varela CE, Mendez K, et al. An actuatable soft reservoir modulates host foreign body response. Sci Robot. 2019;4(33):eaax7043. doi:10.1126/scirobotics.aax7043
485. Pepakayala V, Stein J, Gianchandani Y. Resonant magnetoelastic microstructures for wireless actuation of liquid flow on 3D surfaces and use in glaucoma drainage implants. Microsyst Nanoeng. Published online 2015. doi:10.1038/micronano.2015.32

486. Robotti F, Sterner I, Bottan S, et al. Microengineered biosynthesized cellulose as anti-fibrotic in vivo protection for cardiac implantable electronic devices. Biomaterials. 2020;229:119583. doi:10.1016/j.biomaterials.2019.119583

Chapter 2. Supporting Survival of Transplanted Stem-Cell-Derived Insulin-Producing Cells in an Encapsulation Device Augmented with Controlled Release of Amino Acids

2.1 Introduction

Type 1 diabetes (T1D) can potentially be cured through islet transplantation, but limited beta cell availability and the need for immunosuppressive therapies pose challenges. [1–12] Encapsulation devices have been developed to protect transplanted cells from the immune system without requiring immunosuppressive drugs, but cell survival within these devices remains a significant obstacle due to limited nutrient and gas diffusion (**Figure 2.1**).[9–13]

Previously, a nanoporous polycaprolactone (PCL) macroencapsulation device developed in our laboratory has shown to be conducive to cell survival if implanted on the surface of the liver.[13,14] However, this transplantation site is invasive and difficult to monitor.[15] A preferred site for transplantation of experimental cell source such as stem-cell derived beta cells would be the subcutaneous space, which is a minimally invasive, accessible, and retrievable site. A drawback to this implantation site is that it is poorly vascularized and does not maintain viability and function of islets as well as the richly vascularized liver capsule.[16–18] We have shown previously that hypoxia and nutrient deprivation, consequences of ischemia, synergistically kill stem cell-derived insulin-producing cells. Moreover, supplementation of single amino acid, particularly alanine and glutamine, effectively rescued beta cells from nutrient deprivation.[19] Therefore, in this study, we present an improvement in the encapsulation device by fabricating a

compartment that releases amino acids within the encapsulation device to sustain graft viability after transplant.

2.2 Materials and Methods

All chemicals were purchased from Sigma-Aldrich, unless stated otherwise.

2.2.1. Nonporous and microporous film fabrication

Using polycaprolactone (PCL, 80 kDa Mn) and 2,2,2-trifluoroethanol (TFE), 150 mg/mL PCL solution was spun cast onto silicon wafers for 90 s at 1000 RPM, and heated at 110 °C for 30 s, which resulted in nonporous membranes. The microporous films were fabricated by spin casting 150 mg/mL polyethylene glycol (PEG, 2 kDa Mn) and 150 mg/mL PCL solution onto silicon wafers for 90 s at 1000 RPM, after which the films were placed in DI water overnight to allow the PEG to leach out.

2.2.2. Assembly of devices

To make the amino acid devices, two nonporous films were placed onto PDMS (Sylgard 184) with an embedded U-shaped nichrome wire, which was 0.7 cm in width. When current was applied to the nichrome wire, resistive heating occurred and fused the two films together. With a 10 second current of 1.2 amps the films were sealed, and the wire shape was designed to provide an opening for amino acid loading. Approximately 10 mg of amino acid was loaded into the device, after which the opening of the device was heat sealed. Devices containing both alanine and glutamine were created by creating an equal mixture of the amino acids, after which the mixture was loaded into the device. To attach

the amino acid devices inside the microencapsulation device, the amino acid device was carefully placed on the perimeter of the two microporous films. Together, the film was placed on a PDMS with an embedded U-shaped nichrome wire, which was 2 cm in diameter. With a 10 second current of 1.2 amps the films were sealed with an opening on one side. After loading a maximum volume of 200 μL cell medium, the open side of the device was heat sealed with a straight nichrome wire embedded in PDMS.

2.2.3. Scanning electron microscopy

Microporous PCL thin films were mounted on a flat SEM mount with colloidal graphite (Ted Pella). The cross sections were mounted after flash-dipping in isopropyl alcohol and liquid nitrogen freeze fracturing. Using the Carl Zeis Ultra 55 field emission electron microscope at San Francisco State University, the samples were imaged.

2.2.4. Release study assay

Nonporous films in thickness (10 μm thickness) were used to fabricate amino acid devices containing 5-7 mg of either alanine or glutamine. These devices were submerged in 1 mL of phosphate buffer solution (PBS) at 37 °C and sampled every 2-3 days. Alanine and glutamine quantification assays (Kit #s MAK001-1KT and GLN1-1KT, respectively) from Sigma-Aldrich were performed to determine the diffusion rates of the amino acids.

2.2.5. Cells

Stem cell-derived insulin-producing cells (SCIPC) were differentiated from human embryonic stem cells using a previously established protocol (SCIPC corresponds to the immature beta-like stage).[1]

2.2.6. *In vitro* viability assessment

Amino devices were submerged in non-treated suspension cell plates containing SCIPC. In order to simulate the extreme nutrient-lacking conditions the of encapsulated cells in vivo, 200 SCIPC clusters and devices were placed in 3 mL of depleted media (1:100 dilution of replete media in Hank's solution) that contained no supplemental amino acids or nutrient. Cells were also placed in depleted media that contained 10 mM of free/dissolved alanine and glutamine. After 24 and 48 hours, propidium iodide staining was performed to determine the cell viability. Similar experiment was repeated to check cell viability after 2 weeks. However, to ensure survival of some cells, a 1:10 dilution was used for deplete media.

2.2.7. Mice

NOD.Cg-Prkdcscid Il2rgtm1Wjl/SzJ mice (NSG) and C57BL/6J mice were purchased from Jackson Laboratories. Mice use in this study were housed and handled according to ethical guidelines approved by the Institutional Animal Care and Use Committee (IACUC) at the University of California, San Francisco, Committee on Laboratory Animal Resource Center.

2.2.8. Transplantation

For transplants into the subcutaneous space, approximately 2.0 × 10^6 SCIPC clusters were transplanted as previously described.[2,3] The PCL encapsulation devices were implanted in the subcutaneous space via a small incision made under the mouse shoulder. The space between the skin and the muscle layer was dissected using a blunt instrument to create a pocket. The encapsulation device was implanted in this newly formed space, and the skin wound was closed using surgical staples.

2.2.9. Bioluminescent imaging

Graft-bearing animals were injected IP with D-luciferin solution (Goldbio, St. Louis, MO) at the dose of 150 mg/kg 8 min before imaging to capture the peak in bioluminescent intensity. The mice were anesthetized with an isoflurane mixture (2% in 98% O2) and the bioluminescent signal is quantified using a Xenogen IVIS 200 imaging system (PerkinElmer). Images were acquired for 1 min and then analyzed using the Living Image analysis software (Xenogen, Alameda, CA). Regions of interest (ROI) were centered over where the devices were located. Photons collected over the acquisition time were counted within the ROI. The same imaging protocol was repeated for every imaging session on different days to ensure consistency for longitudinal studies.

2.2.10. Histology

At the end of the experiment, PCL devices were collected together with the surrounding tissue and fixed in paraformaldehyde (Sigma), incubated overnight in 30% sucrose

(Sigma), and embedded in tissue-Tek® OCT (Sakura Finetek, Torrance,CA). Frozen OCT blocks were sliced to obtain thin cross-sections incorporating the tissue around the devices. The slides were stained with hematoxylin- and eosin-staining and/or DAPI (0.2 mg/mL) for 15 minutes and then mounted in Crystal Mount (Biomeda, Foster City, CA). Images were taken using Leica SP5 upright confocal microscope (Leica Microsystem, Buffalo Grove, IL) and analyzed with LAS X Life Science Microscope Software (Leica).

2.3 Results

2.3.1 Device fabrication

Using the fabrication technique described in previous literature, thin-film nanoporous and nonporous films were fabricated.[13] Nanoporous films, with pores ranging from 200 nm – 1 μm, were used for the encapsulation device. The pores in these outer membranes are large enough to allow transport of small molecules and peptides and yet small enough to prevent immune cells from penetrating and attacking the encapsulated cells.[13,14] These pores were generated by leaching PEG from PEG:PCL films, which is advantageous as it allows for tunable pore size and distribution.[20–24] To provide better control over the release rate, nonporous PCL films were used to create the small nutrient reservoir.[25] To build this reservoir, approximately 10 mg of dry amino acid powder was encapsulated between two nonporous films, and the films were sealed using resistive heating (**Figure 2.2a**). The amino acid reservoir was then sandwiched between two nanoporous films, and the assembly was sealed, leaving a small opening available for a cell loading port (**Figure 2.2b**).

Once the encapsulation device with the nutrient-supplying internal compartment was assembled, cells were loaded in fresh medium, and the cell loading port was sealed to create the final, implantable device (**Figure 2.2c**). The resulting encapsulation device was reinforced by the addition of a thicker, nonporous backing layer which was heat sealed to the rim of the device so that the device would maintain its shape after implantation. Overall, the encapsulation device is 1.8 cm in diameter while the amino acid device is 0.7 cm in diameter (**Figure 2.2d**). The cross-section scanning electron microscopy (SEM) images of the nanoporous (**Figure 2.2e**) and nonporous films (**Figure 2.2f**) further confirm the porosity and successful fabrication of the desired films.

2.3.2 In vitro characterization and functionality of amino acid reservoirs

To support beta cell survival after transplant, steady release of amino acid is needed for at least 2 weeks since that is the time it takes for device vascularization to reach its plateau.[13] Diffusion rate of the amino acids from the reservoir was controlled by manipulating film thickness.[22,26] Films were fabricated with thicknesses of 10.7±0.8 μm, 24.3±3.7 μm, and 37.8±1.7 μm, and the release of alanine and glutamine from devices was monitored *in vitro* for 18 days. ~10 μm films released alanine at a rate of 203.1±56.4 μg/day, whereas ~25 μm and ~37 μm films released alanine at 116.9±32.6 μg/day and 54.6±20.6 μg/day, respectively (**Figure 2.3a**). Similarly, glutamine was released at a rate of 162.7±73.6 μg/day for the ~10 μm films, 73.2±34.3 μg/day for the ~25 μm films, and 43.7±14.4 μg/day for the ~37 μm films (**Figure 2.3b**). The linear regression of the cummulative release across all devices showed R^2 values of approximately 0.99, thus confirming the linear zero order release of amino acids from these devices (**Table 2.1**).

As expected, the release rates of the devices increased proportionally with membrane thickness regardless of the amino acid used (**Figure 2.4**). Also, across all devices, the release profile shows zero order kinetics for over 2 weeks, which attests to the ability of the devices in providing consistent amount of sustained release (**Figure 2.5**). Approximately 10 mg of each amino acid was encapsulated in the devices, and by 18 days, 36.1% of alanine and 29.2% of glutamine was released from the thinnest 10 μm films, confirming that the device will provide a sustained released for at least two weeks (**Figure 2.6**).

Although the average loading amount of alanine and glutamine was similar in all the reservoirs, the release rates of these amino acids were different. The higher release rate of alanine was expected since alanine is more lipophilic and has a lower molecular weight (89.09 g/mol) than glutamine (146.01 g/mol). This further shows that with the knowledge of critical parameters such as properties of the membrane and the encapsulated drug, one can roughly predict the release rate from the reservoirs and easily manipulate the reservoirs to achieve the desired rate of release.[25,26] Alternatively, other groups have looked at changing porosity to control the release rate; however it is not applicable to this study since amino acids are small molecules that diffuse rapidly through porous thin-film membranes.[22]

After demonstrating sustained release for more than 2 weeks, *in vitro* tests were performed to determine the effectiveness of the amino acid devices in increasing viability of stem cell-derived beta cells when placed under nutrient deprivation. To ensure the best survival conditions for the cells, reservoirs made with 10 μm films were used as they provide the highest rate of release. Cells were placed in wells containing either nutrient

rich, regular media (RM) or nutrient lacking, deplete media (DM). Cells were also incubated in deplete media containing either 10 mM of free, dissolved amino acid or amino acid devices. After both, 24 hours and 48 hours, the results show that in the presence of amino acid devices, there is a significant decrease in beta cell death when compared to cells cultured in nutrient-depleted media alone (**Figure 2.3c, d**). Moreover, at 24 hours, this viability benefit is equivalent to using nutrient replete media and at 48 hours, the viability benefit is significantly higher than using nutrient replete media. This not only indicates that alanine and glutamine are important in enhancing cell viability but also that the release rate from the 10 μm thick reservoirs is sufficient in providing a survival benefit. Cell viability was also tested at 2 weeks, and the results again demonstrated that there was increase in cell viability in the presence of amino acid reservoirs compared to both nutrient replete and deplete media (**Figure 2.3e**). Although the data is not statistically significant, it is still promising since it is not expected for cells to last for more than 3-4 days in nutrient deprived conditions in culture. The lower percent cell death at the 2-week time point is due to the fact that 10X diluted media was used instead of the 100X dilution used for the short-term experiments. Also, since all the experiments were performed with cells from different batches, the batch-to-batch variability of stem cell-derived beta cell differentiations might have led to further fluctuations of cell death absolute numbers across all the *in vitro* assays.

2.3.3 *In vivo* cell survival

To assess the ability of the amino acid releasing reservoirs in sustaining beta cell survival after transplant, luciferase-expressing stem cell-derived insulin-producing cells

were encapsulated into various PCL devices and transplanted in the dorsal subcutaneous space of NOD.Cg-Prkdcscid Il2rgtm1Wjl/SxJ (NSG) mice (**Figure 2.7a**). Survival of the encapsulated beta cells after transplant was assessed in longitudinal studies by monitoring luciferase activity via bioluminescence imaging (**Figure 2.7b**). We measured the bioluminescence signal intensity associated with the graft starting immediately after transplant on day 0 and throughout a 21-day period. When stem cell-derived beta cells were encapsulated alone, the graft rapidly lost its bioluminescent signal within the first few days, and ~0% of cell survived at day 21. With the addition of the amino acid reservoir, graft survival significantly improved. When alanine reservoir were present, graft survival showed improvement up to 17.5%. Glutamine reservoirs showed similar graft protection with cell survival persisting at 19.8%. When both alanine and glutamine were added to the reservoir, graft survival at day 21 increased to 33.3% (**Figure 2.7c**). Moreover, after 1 month, the thin film devices and those containing amino acid reservoir were explanted along with the surrounding tissue, and H&E staining and immunostaining was performed (**Figure 2.7d**). The cross-sectioned H&E tissue staining shows no deposition of fibrotic tissue along the graft, showing the *in vivo* biocompatibility of the thin-film devices. The immunostaining shows that in the presence of amino acid reservoir, the GFP expressing insulin producing cells were encapsulated within the thin-film device. This further shows that encapsulation devices containing amino acid reservoirs help increase survival of encapsulated cells when tranplanted subcutaneously.

2.4 Discussion

Together, these results show that the fabricated encapsulation device with a nutrient-releasing internal compartment substantially increases cell viability *in vitro* and *in vivo*. Engraftment of beta cells in the subcutaneous space has been a challenge due to the inherently low vascularization present in this area, which results in prolonged ischemia of the graft and high percent of cell death post transplantation.[16–18] To prevent ischemia, encapsulated cells can be supplied with nutrients, alanine and glutamine in particular, until the blood supply at the transplant site is restored.[19] The challenge is to design a device which will contain an internal compartment that can provide a steady and sustained supply of nutrients directly to the encapsulated cells while vascularization occurs. The conducted studies show that amino acid devices fabricated from 10 μm thick nonporous PCL membranes provide sustained release of both alanine and glutamine for more than 2 weeks, at constant rates of 203.1 μg/day and 162.7 μg/day, respectively. The amino acid reservoirs provided greater than 80% viability of cells, during, both, short term (24 hours, 48 hours) and long term (2 weeks) *in vitro* nutrient deprivation challenge. The *in vivo* results also showed that the amino acid devices increased survival of grafts to 17.5% and 19.8% when single amino acid reservoirs were added alone, and cell survival was up to 33.3% in the presence of a reservoir containing, both, alanine and glutamine. The lower rate of survival with amino acid supplementation observed *in vivo* when compared to the *in vitro* results is likely due to the additional hypoxic stress experienced by the cells in the *in vivo* condition that is not addressed. Previously, we have shown that optimal beta cell survival *in vivo* required prior adaptation of the beta cells to lower oxygen tension and amino acid provision.[19] Therefore, in the future, we can

potentially increase graft survival in these devices by preconditiong cells to survive at low oxygen levels.

The device design approach utilized here allows for flexible design, tunable scaling, and manipulation of membrane properties. Characterization of these devices also demonstrated the predictability of the model through knowledge of drug properties, membrane thickness, porosity, and drug payload. To further enhance the device and increase the viability of encapsulated cells, multiple internal and/or external compartments can be fabricated to release various molecules, such as immunosuppressive drugs, hormones, molecules that promote stem cell differentiation, or a more refined cocktail of nutrients to sustain cell viability for a longer period. Other approaches include expediting the vascularization of the devices by releasing angiogenic molecules, such as VEGF and/or releasing anti-inflammatory molecules such as IL1RA from an external compartment to protect the graft from immune response post transplantation.[2,8] The concept developed herein is applicable to many cell encapsulation technologies, and further enhancement of these devices can be scaled for clinical applications to treat T1D

Table 2.1. Linear regression of cumulative release across all ALA and GLN devices

Film Thickness	R^2 Value of Internal Reservoir Containing Alanine	R^2 Value of Internal Reservoir Containing Glutamine
10 μm	0.9889	0.9871
25 μm	0.9892	0.9936
40 μm	0.9873	0.9912

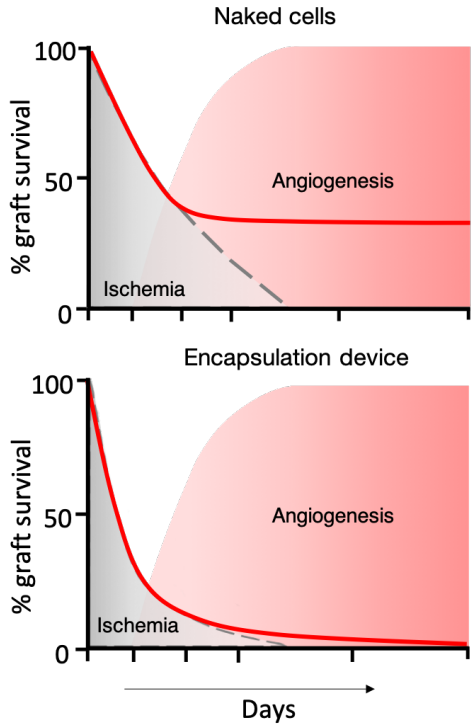

Figure 2.1. Simulated schematic showing percent graft survival post transplantation. Post transplantation, cells undergo a period of ischemia, which causes a significant drop in graft survival. This is exacerbated when cells are encapsulated due to the lack of vascularization, unless cells are provided with supplemental nutrients that can prolong cell survival until angiogenesis begins.

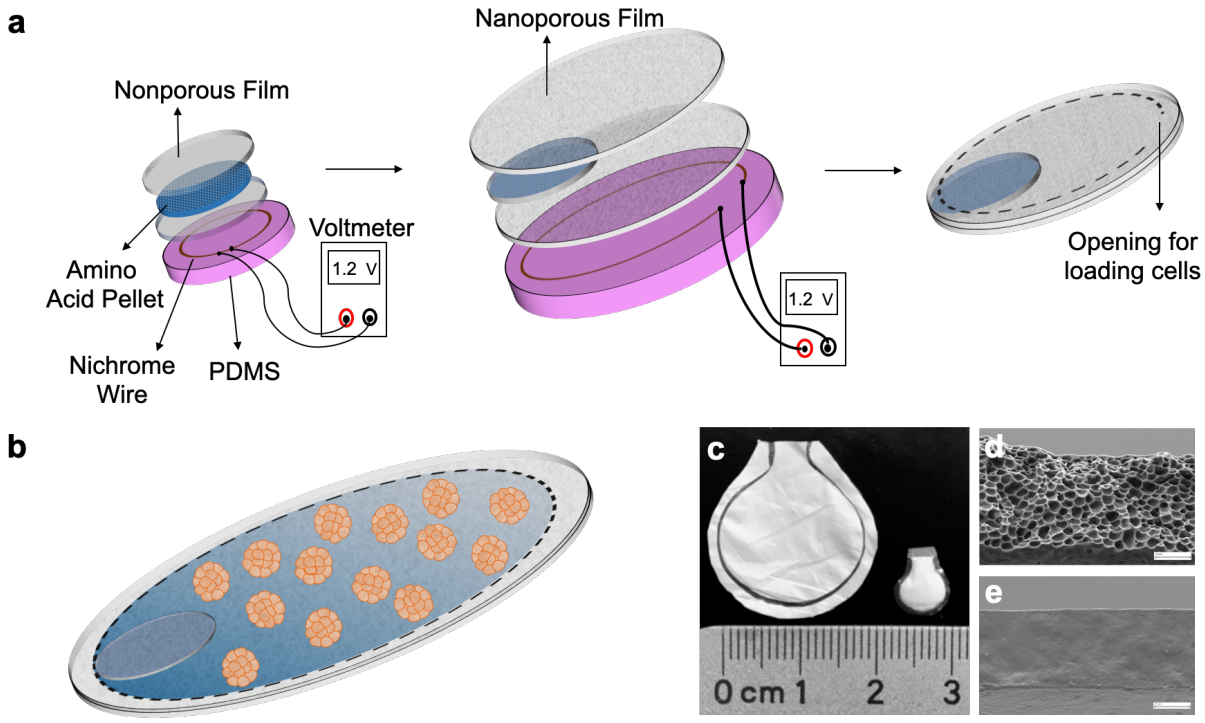

Figure 2.2. Schematic showing the fabrication of encapsulation device with internal compartment. **(a)** Amino acid devices were created by encapsulating a formulation of dry amino acid powder inside nonporous films and was sealed by the current flowing through the nichrome wire. The amino acid device was sealed within the interior of the encapsulation device by sandwiching the device along the edge of the encapsulation device membranes. The encapsulation device was sealed in a U shape (indicated by the dotted line) between two nanoporous films. Using a 200 μL pipet tip, cells and medium were added, after which the opening was heat sealed. **(b)** Cartoon illustration of sealed encapsulation device containing the internal amino acid reservoir. **(c)** Image of assembled amino acid device (left; 0.7 cm) and encapsulation device (right; 1.8 cm). Cross-section SEM of **(d)** nanoporous and **(e)** nonporous thin-films of ~10 μm in thickness (scale bar = 10 μm).

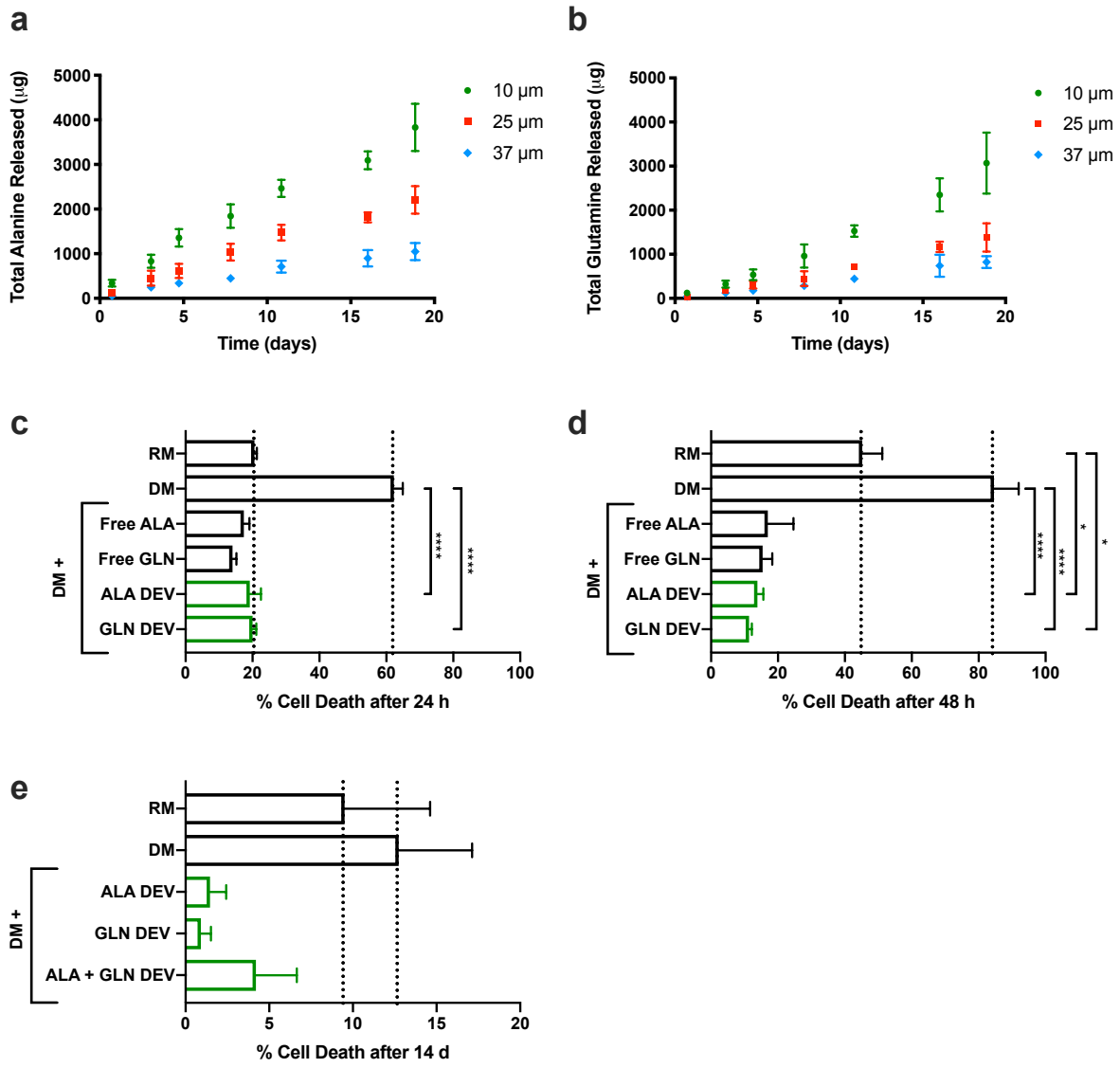

Figure 2.3. *In vitro* evaluation of amino acid reservoirs in providing release and increase in cell viability. Sustained release of **(a)** alanine (ALA) and **(b)** glutamine (GLN) from thin film devices made with membranes of thicknesses varying from 10 μm, 25 μm, and 37 μm. Cumulative release of amino acids (μg) measured over the course of 18 days in PBS at 37 °C (N = 4 for each thickness; error bars represent ± SE relative to the mean). Cell survival benefit with ALA and GLN devices in depleted media (DM) compared to replete media (RM), DM (1:100 dilution of RM in PBS), and dissolved ALA and GLN in DM (Free ALA, Free GLN, respectively), over the course of **(c)** 18 hours, **(d)** 48 hours, and **(e)** 2 weeks. Propidium iodide staining used to measure the decreased cell death shown in the presence of amino acid devices compared to DM (N = 3 per condition). Significance of differences of graft survival vs device control groups was determined using multiple unpaired t test, corrected for multiple comparison using Holm-Sidak method (error bars represent ± SE relative to the mean; *p < 0.05; ****p < 0.0001). Additionally,

for the 2 week follow up experiment, DM was changed to 1:10 dilution of RM in PBS in order to ensure long term cell survival.

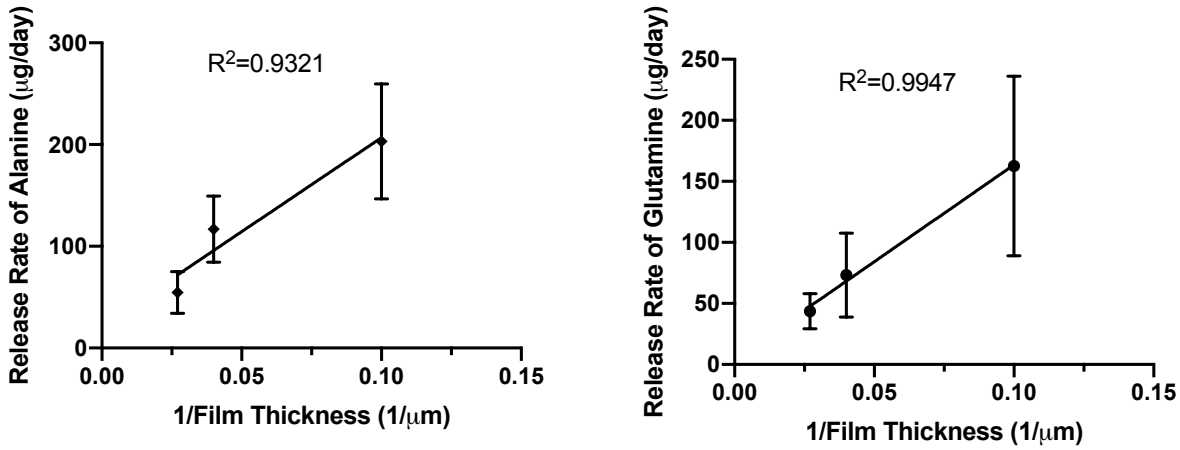

Figure 2.4. Correlation between film thickness and release rates of amino acids from devices. The linear regression performed on the release rate of amino acids and inverse thickness shows that there is a correlation between film thickness and release rates, which was expected.

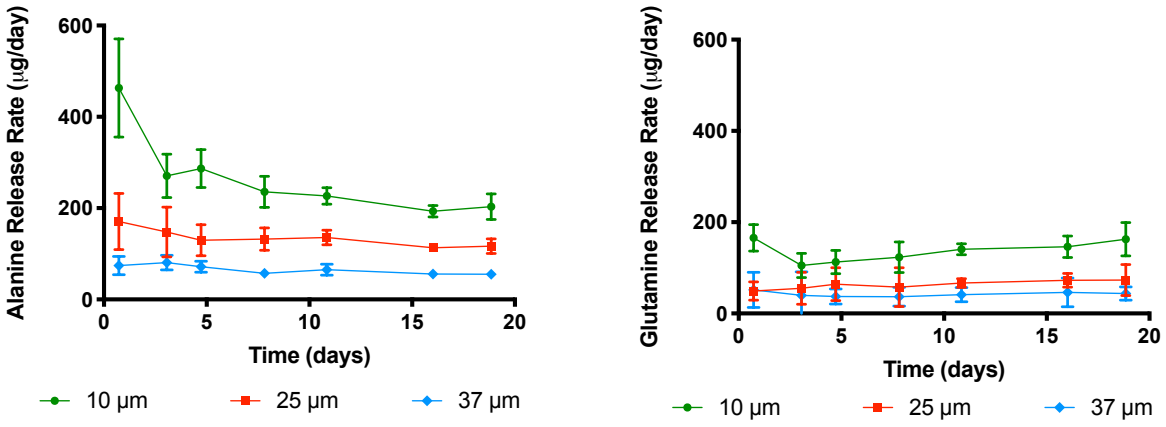

Figure 2.5. Release rates of amino acid from devices. The release rates of both the amino acids from devices is relatively constant, despite of the change in membrane thickness. The release rate is proportional to the thickness of the films.

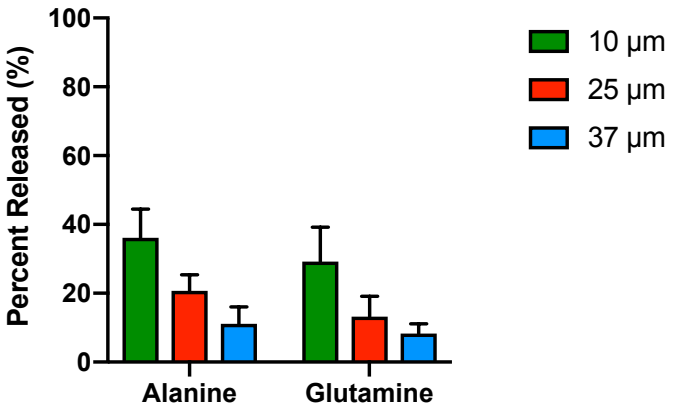

Figure 2.6. Percent payload of ALA and GLN devices. After 18 days, approximately 36.1%, 20.7%, and 11.1% of alanine and 29.2%, 13.1%, 8.3% of glutamine was released from 10 µm, 25 µm, and 37 µm thick membranes, respectively. Assuming the release rate stays constant, the devices can potentially provide amino acids for approximately a month.

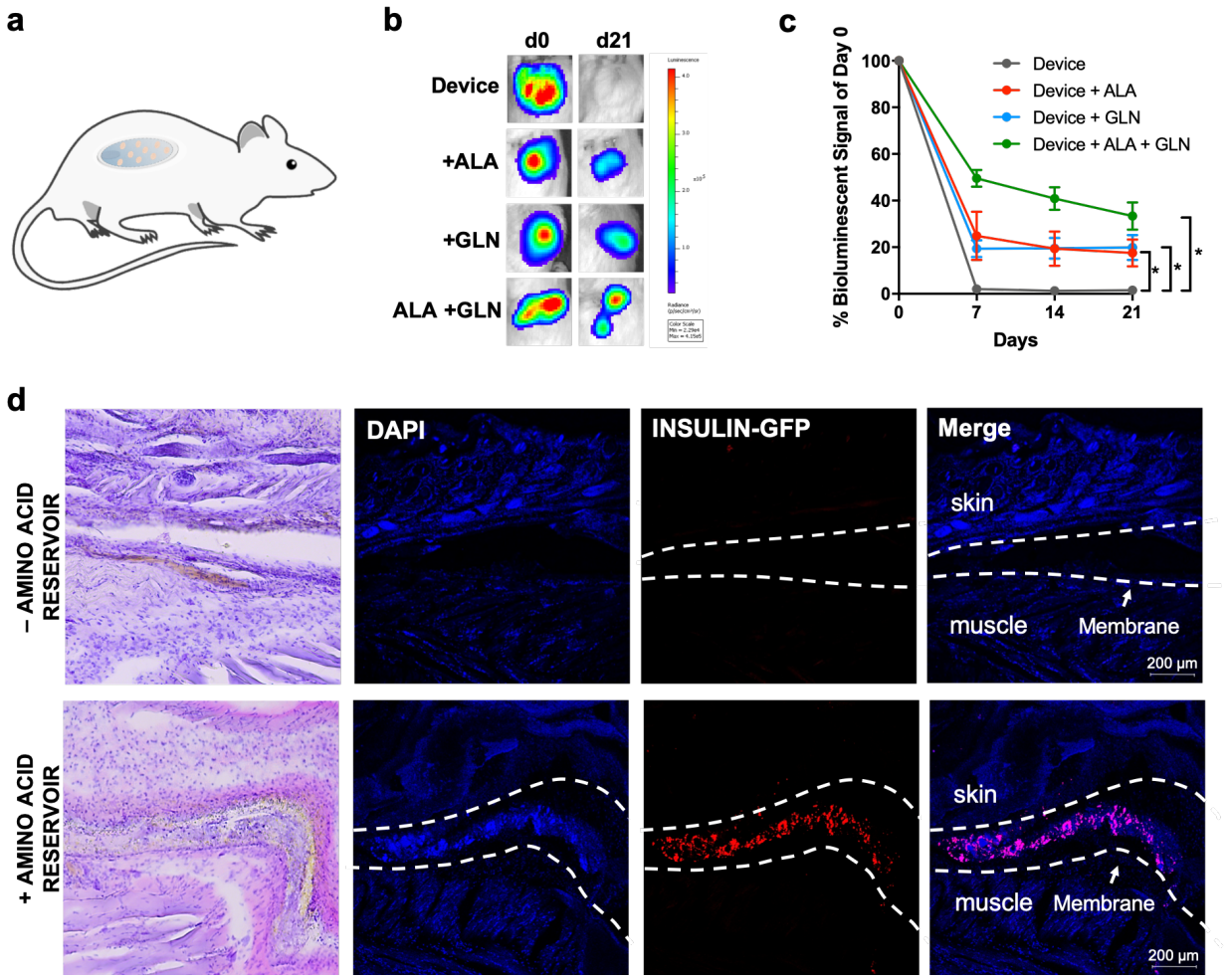

Figure 2.7. *In vivo* viability of encapsulated cells in the presence of amino acid devices. (a) PCL device transplanted in the subcutaneous space of NSG mice. **(b)** Representative images of encapsulated SCIPC.LUC in PCL devices alone (N = 7), device + ALA reservoir (N = 6), device + GLN reservoir (N = 6), and device + ALA + GLN reservoir (N = 6). **(c)** Quantification of bioluminescent signal of cells transplanted into encapsulation devices with or without amino acid reservoirs. Significance of differences of graft survival vs device control groups was determined using multiple unpaired t test, corrected for multiple comparison using Holm-Sidak method (error bars represent ± SE relative to the mean; *p < 0.05). **(d)** H&E staining and immunofluorescent staining of tissue sections of encapsulation devices with and without amino acid reservoir,obtained from NSG mice 21 days post-transplantation. Nuclei are visualized by DAPI staining and insulin-producing cells are genetically modified to express GFP. The dotted white lines delineate the perimeter of the thin-film encapsulation devices. Magnification 10X.

2.5 References

1. Shapiro AMJ, Pokrywczynska M, Ricordi C. Clinical pancreatic islet transplantation. Nature Reviews Endocrinology. 2017;13(5):268-277. doi:10.1038/nrendo.2016.178
2. Sneddon JB, Tang Q, Stock P, et al. Stem Cell Therapies for Treating Diabetes: Progress and Remaining Challenges. Cell Stem Cell. 2018;22(6):810-823. doi:10.1016/j.stem.2018.05.016
3. Ryan EA, Paty BW, Senior PA, et al. Five-year follow-up after clinical islet transplantation. Diabetes. 2005;54(12):2060-2069. doi:10.2337/diabetes.54.7.2060
4. Tharavanij T, Betancourt, ArthurCure P, Messinger S, et al. Improved Long-Term Health-Related Quality of Life After Islet Transplantation. Transplantation. 2008;86(9):1161-1167. doi:10.1097/tp.0b013e31818a7f45
5. Buder B, Alexander M, Krishnan R, Chapman DW, Lakey JR. Encapsulated Islet Transplantation: Strategies and Clinical Trials. Immune Network. 2013;13(6):235-239.
6. Shapiro AMJ, Lakey JRT, Ryan EA, et al. Islet Transplantation in Sevent Patients with Type 1 Diabetes Mellitus Using a Glucocorticoid-Free Immunosuppressive Regimen. The New England Journal of Medicine. 2000;343(4):230-238. doi:10.1056/NEJM200007273430401
7. Ludwig B, Reichel A, Steffen A, et al. Transplantation of human islets without immunosuppression. Proceedings of the National Academy of Sciences. 2013;110(47):19054-19058. doi:10.1073/pnas.1317561110
8. Desai T, Shea LD. Advances in islet encapsulation technologies. Nature Reviews Drug Discovery. 2017;16(5):338-350. doi:10.1038/nrd.2016.232

9. Calafiore R, Basta G. Clinical application of microencapsulated islets: Actual prospectives on progress and challenges. Advanced Drug Delivery Reviews. 2014;67-68:84-92. doi:10.1016/j.addr.2013.09.020
10. Desai TA. Microfabrication technology for pancreatic cell encapsulation. Expert Opinion on Biological Therapy. 2005;2(6):633-646. doi:10.1517/14712598.2.6.633
11. Kieffer TJ, Woltjen K, Osafune K, Yabe D, Inagaki N. Beta-cell replacement strategies for diabetes. Journal of Diabetes Investigation. 2018;9(3):457-463. doi:10.1111/jdi.12758
12. Ludwig B, Ludwig S. Transplantable bioartificial pancreas devices: Current status and future prospects. Langenbeck's Archives of Surgery. 2015;400(5):531-540. doi:10.1007/s00423-015-1314-y
13. Nyitray CE, Chang R, Faleo G, et al. Polycaprolactone Thin-Film Micro- and Nanoporous Cell-Encapsulation Devices. ACS Nano. 2015;9(6):5675-5682. doi:10.1021/acsnano.5b00679
14. Chang R, Faleo G, Russ HA, et al. Nanoporous Immunoprotective Device for Stem-Cell-Derived β-Cell Replacement Therapy. ACS Nano. 2017;11(8):7747-7757. doi:10.1021/acsnano.7b01239
15. Fowler M, Virostko J, Chen Z, et al. Assessment of pancreatic islet mass after islet transplantation using in vivo bioluminescence imaging. Transplantation. 2005;79(7):768-776. doi:10.1097/01.TP.0000152798.03204.5C
16. Komatsu H, Rawson J, Barriga A, et al. Posttransplant oxygen inhalation improves the outcome of subcutaneous islet transplantation: A promising clinical alternative to

the conventional intrahepatic site. American Journal of Transplantation. 2018;18:832-842. doi:10.1111/ajt.14497

17. Farina M, Ballerini A, Fraga DW, et al. 3D Printed Vascularized Device for Subcutaneous Transplantation of Human Islets. Biotechnology Journal. 2017;12:1700169. doi:10.1002/biot.201700169
18. Conkling N, Tang Q, Faleo G, Stock P, WIsel S, Desai T. Prevascularization of the Subcutaneous Space Improves Survival of Transplanted Mouse Islets. Transplantation. 2018;10(7S):372. doi:10.1097/01.tp.0000543124.81125.ef
19. Faleo G, Russ HA, Wisel S, et al. Mitigating Ischemic Injury of Stem Cell-Derived Insulin-Producing Cells after Transplant. Stem Cell Reports. 2017;9(3):807-819. doi:10.1016/j.stemcr.2017.07.012
20. Bernards DA, Desai TA. Nanoscale porosity in polymer films: Fabrication and therapeutic applications. Soft Matter. 2010;6:1621-1631. doi:10.1039/b922303g
21. Bernards DA, Lance KD, Ciaccio NA, Desai TA. Nanostructured thin film polymer devices for constant-rate protein delivery. Nano Letters. 2012;12:5355-5361. doi:10.1021/nl302747y
22. Desai TA, Bhisitkul RB, Wynn P, et al. Ocular Biocompatibility and Structural Integrity of Micro- and Nanostructured Poly(caprolactone) Films. Journal of Ocular Pharmacology and Therapeutics. 2013;29(2):249-257. doi:10.1089/jop.2012.0152
23. Dash TK, Konkimalla VB. Poly-ε-caprolactone based formulations for drug delivery and tissue engineering: A review. Journal of Controlled Release. 2012;158:15-33. doi:10.1016/j.jconrel.2011.09.064

24. Abedalwafa M, Wang F, Wang L, Li C. Biodegradable poly-epsilon-caprolactone (PCL) for tissue engineering applications: A review. Reviews on Advanced Materials Science. 2013;34:123-140.
25. Desai TA, Bhisitkul RB, Schlesinger EB, et al. Device design methodology and formulation of a protein therapeutic for sustained release intraocular delivery. Bioengineering & Translational Medicine. 2018;4(1):152-163. doi:10.1002/btm2.10121
26. Lance KD, Good SD, Mendes TS, et al. In vitro and in vivo sustained zero-order delivery of Rapamycin (sirolimus) from a biodegradable intraocular device. Investigative Ophthalmology and Visual Science. 2015;56(12):7331-7337. doi:10.1167/iovs.15-17757

Chapter 3. Replenishable Prevascularized Cell Encapsulation Devices Increase Graft Survival and Function in the Subcutaneous Space

3.1 Introduction

Cell encapsulation using macroencapsulation devices has shown to be a promising approach to address the requirement for patients to remain on immunosuppressive drugs after receiving beta cell transplants.[1,2,7–13] Encapsulation devices offer a physical barrier to protect transplanted beta cells from immune attack; however, this barrier can limit the diffusion of oxygen and nutrients, causing ischemic stress detrimental to graft survival. This ischemic stress varies based on the transplantation site of the device. [1,2,4,7–10,14,15]

An ideal transplantation site for cell encapsulation devices includes 1) a dense vascular network that allows for insulin and glucose exchange, along with high oxygen and nutrient supply to the graft; 2) a hospitable microenvironment that prevents initial loss of cells post-transplant; and 3) a minimally invasive procedure for implanting, monitoring, and retrieving the graft. Transplantation in the subcutaneous space allows for minimally invasive implantation and retrieval.[5,11,12,16–23] However, a significant challenge that remains unaddressed in subcutaneous cell transplantation is the loss of beta cell viability that occurs shortly after transplantation. During surgical implantation, the inherently low vasculature in the subcutaneous space is further destroyed, leading to an even lower supply of oxygen and nutrients at the transplantation site. This is particularly detrimental to highly metabolic beta cells.[1,2,7,16,17,22,24,25]

Several studies have shown that subcutaneous transplantation sites can be modified to promote neovascularization post-transplantation. These methods involve use

of biologics such as growth factors (beta-fibroblast growth factor, VEGF)[26–28], chemical modifications of the encapsulation material[29], anti-inflammatory drugs[14,30,31], co-delivery of mesenchymal stem cells[32–34], and the use of oxygen generators[10,35–37], among others. While these strategies may improve blood vessel formation, these methods require at least 10 days to create a dense vascular network that is well integrated with the host vasculature after cells have already been implanted in the subcutaneous space. Due to this limitation, these methods cannot rescue most of the graft loss that occurs within the initial days of implantation.[7,11,12,15,21,38]

Another promising strategy to improve islet vascularization is the pre-vascularization of encapsulation devices at the transplantation site. In this approach, a non-vascularized device is implanted before transplanting beta cells in the vascularized site. The advantage of this approach is that the host vasculature is well incorporated at the transplantation site, improving access to oxygen and nutrient supplies.[7,11,20,21,32,39–41] However, a drawback of this strategy is that the vascularized device is typically removed prior to beta cell transplantation. Device removal can rupture some newly formed vascular networks and create a sub-optimal microenvironment for subsequent islet transplantation. Several groups have sought to overcome this drawback; however, these approaches involve *in vitro* pre-vascularized devices or more complex encapsulation devices that require different membranes, drugs, and surface modification to promote *in vivo* vascular growth.[7,42–44] To our knowledge, there are currently no strategies for encapsulation devices that create a pre-vascularized transplantation site that allows for the direct insertion of cells without disrupting the surrounding vasculature.

Here we report a pre-vascularization strategy using a replenishable encapsulation device that prevents the initial loss of cell viability and function of stem cell-derived insulin-producing beta cell clusters in the subcutaneous space. Our method was designed to prepare the transplantation site such that a functional vascular network surrounds the encapsulation device prior to the transplantation of cells. This approach was developed using thin-film polycaprolactone (PCL) cell encapsulation devices that have been previously shown to maintain the viability and function of insulin-producing cells in the liver lobe for at least 6 months.[45] We have also demonstrated that such devices support the viability of insulin-producing cells in the subcutaneous space by incorporating nutrient depots.[24] Devices were implanted subcutaneously for 2 weeks, after which, they were loaded with stem cell-derived insulin-producing beta cell clusters without disrupting the integrity of the surrounding vascular network. After 28 days, more than 80% of pre-vascularized replenishable devices showed signal, leading to a measurable C-peptide secretion in response to a glucose challenge.

3.2 Materials & Methods

3.2.1. Device Fabrication

Chemicals were purchased from Sigma-Aldrich unless otherwise noted. Porous polycaprolactone (PCL) thin films were fabricated by dissolving PCL (80 kDa Mn) and poly (ethylene) glycol (2 kDa Mn) in 2,2,2-trifluoroethanol (TFE). The 150 mg/mL PEG:PCL solution was spun and cast onto silicon wafers for 90 s at 1000 RPM, after which the films were immersed in water to allow for PEG leaching and pore formation. To fabricate the device, two ~10 μm thick, porous, thin films were sandwiched onto a PDMS

(Sylgard 40) mold with a spoon-shaped nichrome wire embedded. The two films fused through resistive heating by passing a 1.2 A current through the nichrome wire, creating a spoon-shaped device with an opening at the neck. The resulting device was 1.5 cm in diameter, with a final 1 cm long neck that resulted in a total volume capacity of 160 µL. A thicker PCL film (spun cast on silicon wafers for 30 s at 300 RPM) was used to create a wider border around the device. For devices that were pre-vascularized, a small cannula was placed inside the device and sealed. For devices that were not pre-vascularized, the opening was sealed using resistive heating after cells in 70 µL of cell medium were pipetted inside the device. Although the total volume capacity was 160 µL, we only added 70 µL to ensure proper sealing and no spillage of cells when cells were inserted in RPVIM devices *in vivo*.

3.2.2 Mice

NOD.Cg-*Prkdc*^{scid} *Il2rg*^{tm1Wjl}/SzJ mice (NSG; Jackson Strain 005557) mice were purchased from Jackson Laboratories. Mice used in this study were housed and handled according to ethical guidelines approved by the Institutional Animal Care and Use Committee (IACUC) at the University of California, San Francisco Laboratory Animal Resource Center (LARC).

3.2.3. Culture of pluripotent cells

A previously published gene-targeting approach of the insulated human AAVS1 locus was used to generate a cell line that expresses a constitutive firefly luciferase gene. Cell culture was performed using a version of the NIH-approved hESC line MEL-1 (NIH

registration number: 0139), in which GFP was knocked into one allele of the endogenous insulin locus ($INS^{GFP/W}$ hESCs). $INS^{GFP/W}$ hESCs was cultured on irradiated mouse embryonic fibroblasts (MEFs) (Thermo Fisher) in hESC maintenance media composed of DMEM/F12, 20% (v/v) KnockOut serum replacement (Thermo Fisher Scientific), nonessential amino acids (Thermo Fisher Scientific), GlutaMAX (Thermo Fisher Scientific), and 2-mercaptoethanol (Millipore). The maintenance media was supplemented with 4 ng/mL recombinant human fibroblast growth factor 2 (FGF-2; R&D Systems). Confluent hESCs were dissociated into single-cell suspension by incubation with TrypLE Select (Gibco) and passaged every 3–4 days. G-banded karyotyping performed by Cell Line Genetics confirmed normal karyotype of $INS^{GFP/W}$ hESCs. Cells have been confirmed to be mycoplasma-free using the MycoProbe Mycoplasma Detection Kit (R&D Systems) or the Venor GeM Mycoplasma Detection Kit (Sigma)

3.2.4. Differentiation into pancreatic cells

To initiate differentiation, we dissociated confluent cultures into single-cell suspensions using TrypLE Select, counted cells, and seeded them in six-well suspension plates at a density of 5.5×10^6 cells per 5.5 mL of hESC maintenance media supplemented with 10 ng/mL activin A (R&D Systems) and 10 ng/mL heregulinB (PeproTech). The plates were incubated at 37°C and 5% CO_2 on an orbital shaker set at 100 rpm to induce 3D sphere formation. After 24 h, the spheres were differentiated as previously described (Nair et al., 2019a, 2019b). Spheres were collected in 50-mL tubes, allowed to settle by gravity, washed once with PBS or RPMI (Gibco), and resuspended in d1 differentiation

media. The resuspended spheres were distributed into fresh six-well suspension plates for a final volume of 5.5 mL of d1 media per well. Until d3, spheres were fed daily by removing media and replenishing with 5.5 mL of fresh media. From d4 to d20, media was removed daily, and 5 mL of fresh media was added. Media compositions for differentiation of $INS^{GFP/W}$ hESCs are as follows: d1, RPMI (Gibco) containing 0.2% FBS, 1:5,000 ITS (Gibco), 100 ng/mL activin A, and 50 ng/mL WNT3a (R&D Systems); d2, RPMI containing 0.2% FBS, 1:2,000 ITS, and 100 ng/mL activin A; d3, RPMI containing 0.2% FBS, 1:1,000 ITS, 2.5 μM TGFbi IV (Calbiochem), and 25 ng/mL keratinocyte growth factor (KGF; R&D Systems); d4–5, RPMI containing 0.4% FBS, 1:1,000 ITS, and 25 ng/mL KGF; d6–7, DMEM (Gibco) with 25 mM glucose containing 1:100 B27 (Gibco) and 3 nM TTNPB (Sigma); d8, DMEM with 25 mM glucose containing 1:100 B27, 3 nM TTNPB, and 50 ng/mL epidermal growth factor (EGF; R&D Systems); d9–11, DMEM with 25 mM glucose containing 1:100 B27, 50 ng/mL EGF, and 50 ng/mL KGF; d12+, DMEM with 25 mM glucose containing 1:100 B27, 1:100 GlutaMAX (Gibco), 1:100 NEAA (Gibco), 10 μm ALKi II (Axxora), 500 nM LDN-193189 (Stemgent), 1 μm Xxi (Millipore), 1 μM T3 (Sigma-Aldrich), 0.5 mM vitamin C, 1 mM *N*-acetylcysteine (Sigma-Aldrich),10 μM zinc sulfate (Sigma-Aldrich), and 10 μg/mL heparin sulfate.

For transplantation experiments for IVIS imaging, MEL1 $INS^{GFP/W}$ hESCs were differentiated up to d19–20, while for *in vivo* glucose measurement experiments the cells were cultured for an additional 7 days in CMRL containing 10% FBS, 1:100 Glutamax (Gibco), 1:100 NEAA (Gibco), 10 μm ALKi II (Axxora), 0.5 mM vitamin C, 1μM

T3 (Sigma-Aldrich), 1 mM N-acetyl Cysteine (Sigma-Aldrich), 10 μM zinc sulfate (Sigma-Aldrich) and 10 μg/mlof heparin sulfate) supplemented with 10 μM of the ROCK inhibitor Y-27632 (Tocris) and Penicillin Streptomycin (Corning) before transplantation

3.2.5. Transplantation

PCL encapsulation devices were implanted in the subcutaneous space via a small incision in the mouse's lower back. The space between the skin and the muscle layer was dissected using blunt forceps, and saline was injected to create an easily accessible pocket. The encapsulation device was implanted in this newly formed space, and the skin wound was closed using surgical staples. For devices containing cells, 2.5×10^3 clusters in 70 μL of media were transplanted. For pre-vascularized devices, a small incision was made near the previous incision site, and a blunt instrument was used to open the space such that the neck of the device was visible. Without disrupting the device's position, scissors were used to cut open the neck, and a 200 uL pipet tip was used to insert cells, after which the cannula inside the device was removed, and a cautery pen was used to seal the device.

3.2.6. Lectin Perfusion to Assess Functional Vasculature

To analyze the vasculature around the grafts, lectin perfusion was performed on mice containing empty (no cell) devices. 0.1 mL of 1 mg/mL Tomato-lectin Dylight 647 (Thermo Fisher) was injected into the atrium of mice after anesthetizing with isoflurane. The right atrium of the mouse was cut, and after the mouse was allowed to bleed out, 10 mL of PBS was injected into the left ventricle using a pump. Finally, 10 mL of 4% PFA was

injected into the left ventricle using the pump, after which the device and surrounding skin were dissected and stored in 4% PFA overnight. Samples were transferred to 30% sucrose, washed with PBS, and imaged using a Nikon 6D/High Throughput microscope and a Leica Widefield microscope. To quantify the vasculature around the entire device, 4x magnification images were used. These acquired images were analyzed using the Fiji software (NIH, version 2.0.0-rc-69/1.53c). Specifically, the Fiji software set a manual threshold for each image, after which the area covered by the stained vessels was manually highlighted and then calculated by the program. This area was divided by the total area of the image to determine the percentage of vasculature over the total area. To determine the fold change in the vasculature, all values were divided by the average percentage of vasculature over the total area on day 7. For each time point, n=5 animals were used, and five images of 4x magnifications per animal were used for the analysis. The number of branches and nodes were manually calculated for each image. A node was defined as a point at which two vessels intersect, and a branch was defined as vessels that were extending from the main blood vessel.

3.2.7. Bioluminescent Imaging

Graft-bearing animals were injected intraperitoneally (IP) with D-luciferin solution (Goldbio) at 150 mg/kg 30 min before imaging to capture the peak in bioluminescent intensity. Mice were anesthetized with an isoflurane mixture (2% in 98% O2), and the bioluminescent signal was quantified using a Xenogen IVIS 200 imaging system (PerkinElmer). Images were acquired for 1 min and then analyzed using the Living Image analysis software (Xenogen). Regions of interest (ROI) were centered over the location

of the devices and background signal was obtained by capturing ROI of a non-bioluminescent signal. Photons collected over the acquisition time were counted within the ROI. The same imaging protocol was applied each time to ensure consistency across longitudinal studies.

3.2.8. Intraperitoneal Glucose Tolerance Test

Mice were subjected to an IP glucose tolerance test (IPGTT) at 28 days post-transplantation to assess function of the grafted cells. The test was split into two parts to prevent undue stress on mice. In the first round, mice were fasted overnight, after which the blood glucose levels and blood samples were obtained via tail vein and cheek bleeds, respectively. After five days of rest, mice were fasted overnight, and blood glucose levels were measured from the tail vein. 3 mg/kg glucose was injected into the intraperitoneal space of mice, and after 45 minutes, blood glucose and blood samples were obtained from the tail vein, and cheek bleeds, respectively. C-peptide-levels were measured using an ultrasensitive insulin ELISA kit (Alpco 80-CPTHU-CH05)

3.2.9. Histology

Explanted grafts were collected and fixed in 4% paraformaldehyde for 24 h and dehydrated in 30% sucrose for 48 h. Tissue samples were embedded in optimal cutting temperature (OCT) and 8 μm sections were placed on TOMO adhesive slides for immunostaining. Slides were stained with hematoxylin and eosin (H&E, StatLab), picrosirius red (Polysciences), and tri-chrome (Sigma) staining kits. Images for H&E and tri-chrome staining were obtained on a brightfield microscope, and picrosirius red staining

was visualized using a circular polarized light microscope. For immunostaining, slides were fixed in 95% methanol and permeabilized in 0.1% Triton X-100. Sections were treated with primary antibodies against CD31 (R&D systems AF3628) diluted 1:50, vWF (Millipore AB7356) diluted 1:10, and C-peptide (DSHB GN-ID4) diluted 1:200, overnight at 4 C. Samples were rinsed with PBS followed by 1 h room temperature incubation with 1:500 dilution of secondary antibody (AF 546, Sigma) and/or Alexa Fluor 647-conjugated glucagon antibody (Novus Biologics IC1249R) diluted 1:2000. Samples were then rinsed with PBS, incubated with Hoechst 3322 for 5 minutes, and mounted using anti-fade mounting medium (ProLong, LifeTechnologies). Images were obtained using a NIKON widefield fluorescence microscope.

3.2.10. Statistical analysis

Data were analyzed using GraphPad Prism software version 9.4. All differences in vasculature between experimental groups were evaluated using One-way ANOVA or Two-way ANOVA, followed by Tukey's post hoc test or Student's t-test. Graft survival was compared using Kaplan-Meier survival curves. $P<0.05$ was considered statistically significant.

3.3. Results

3.3.1. Design of subcutaneous thin film PCL device and implantation technique

To create a refillable device, we modified the fabrication of thin film devices described in previous work.[24,45,46] We fabricated a small device that was 2 cm in length and width to permit the insertion of the device in the subcutaneous space with minimal

stress to the animal. In brief, the new design included a 1 cm long and 0.6 cm wide neck with an enclosed catheter that allows for a facile opening of the device and the insertion of cells (**Figure 3.1**). The long neck was crucial in opening the device and inserting cells without removing the device from the transplant site and disrupting the surrounding vasculature. After inserting the cells, a cauterizer was used to seal the device opening through resistive heating. The circular region, where the cells reside, has a diameter of 1.6 cm and maximum volume capacity of 160 µL. To provide mechanical support, we also incorporated a 100 µm thick PCL border around the device, which keeps it sturdy and prevents it from folding over *in vivo*. Additionally, transplantation in the subcutaneous space allowed for multiple surgeries where no adverse side effects were observed (based on whole animal and gross site observation). This may not be possible with other implantation sites, where repeated administration may lead to greater adverse events.[16,17,19]

Once encapsulation devices were assembled, we next determined the ability of devices to maintain cellular viability and function, with and without pre-vascularization and/or device removal. Devices were either loaded with cells and immediately transplanted into an unmodified subcutaneous space ("Standard Implantation Method", SIM), or were first implanted as an empty device to establish vasculature before loading with cells (Refillable Pre-Vascularized Implantation Method, RPVIM). For the pre-vascularized devices, an empty device was allowed to vascularize for 14 days. After that, stem cell-derived insulin-producing beta cell clusters were inserted, and devices were sealed without disrupting the newly formed vasculature around the device. To demonstrate that maintaining an intact vascular network in RPVIM is critical for graft

survival, we also compared with a previously reported approach where pre-vascularized empty devices were explanted and replaced with a SIM device ("Standard Pre-Vascularization Method", SPVIM). We hypothesized that disruption of the pre-vascularized zone around the device would limit its ability to preserve graft survival in the subcutaneous space.

3.3.2. Vasculature formation after transplantation of encapsulation device in subcutaneous space

Lectin perfusion assay was used to quantify vascular density around implanted empty devices at 1, 2, 4 weeks and compared the vascular density in the native skin of immunodeficient NSG mice (**Figure 3.2A**). At 1 week, no increase of vasculature was seen in the transplantation site. By 2 weeks, the total amount of functional vasculature around the implant doubled from baseline. After 2 weeks, the increase in vascular density diminishes, and only an additional ~10-15% increase in the percent vasculature is observed after 4 weeks of implantation (**Figure 3.2A-C**). The progression of angiogenesis was also evident by the increase in nodes and number of branches from pre-existing blood vessels. After 2 weeks of implantation, nearly 3-fold more nodes and branches were seen around the device compared to 1 week of implantation. Again, although there was an increase in the number of nodes and branches between week 2 and week 4, this increase was less than 1-fold (**Figure 3.2D, E**). These results suggest that a vascularized site for islet engraftment can be created in the subcutaneous space after 2 weeks of implantation.

3.3.3. Survival of stem cell-derived insulin-producing beta cell clusters in pre-vascularized replenishable encapsulation devices

We next asked whether pre-vascularization, with or without removal of the device, affects the survival of stem cell-derived insulin-producing beta cell clusters. These luciferase-labeled cell clusters were generated using a previously established protocol.[47,48] For cell survival studies, two different stages of stem cell-derived insulin-producing beta cell clusters were used. Cells generated after 20 days of differentiation (d20) are immature beta cell-like clusters, while day 28 (d28) cells are mature beta cell-like clusters that display enhanced functional properties (**Figure 3.3**).[47,48] Cells were encapsulated in devices and transplanted into the subcutaneous space of immunodeficient NSG mice, after which bioluminescence imaging was used to monitor the surviving graft mass of encapsulated cells over a period of 28 days. The d20 cells in SIM devices showed less than 15% of the baseline signal within the first 7 days, indicating that the initial transplantation site microenvironment was not hospitable for cells (**Figure 3.4A**). SPVIM devices also showed around 90% decrease in the average fractional change in bioluminescence signal compared to the baseline at day 7. In comparison, the RPVIM devices showed only around 20% decrease in bioluminescence signal after day 7, and these maintained greater than 40% of the baseline bioluminescence signal after 28 days of implantation (**Figure 3.4B**). Additionally, when plotting the percentage of grafts showing greater than 15% of the baseline bioluminescence signal across the different conditions, ~88% of the RPVIM devices showed a signal over 28 days (**Figure 3.4C**). This percentage was significantly greater than the SPVIM and SIM groups, indicating that the pre-vascularization without subsequent device removal improves survivability of

immature stem cell-derived insulin-producing beta cell clusters in the subcutaneous space.

Moreover, this same trend was observed with the d28 cells, which are believed to be more susceptive to ischemia due to higher metabolic activity.[47,48] The change in bioluminescence compared to the baseline for cells in RPVIM was ~60% after 28 days, while the SIM and SPVIM showed only ~10-15% fractional change (**Figure 3.4D, E**). The percent of grafts that survived by day 28 for RPVIM was 75%; other conditions showed little to no survival after day 7 (**Figure 3.4F**). These results support our hypothesis that pre-vascularization without vascular disruption creates a highly suitable post-transplant environment, allowing for increased graft survival.

3.3.4. Function of mature insulin-producing cells within pre-vascularized replenishable encapsulation devices

Given the viability data, we hypothesized that RPVIM devices would show greater glucose-stimulated insulin secretion than SIM or SPVIM devices. Since the d20 cells are immature and do not respond significantly to glucose challenge, we conducted functional tests on d28 cells that more closely resemble mature beta-cell-like clusters and demonstrate glucose-stimulate insulin secretion.[47,48] To assess the function of the encapsulated cells, after 28 days of implantation, we performed an intraperitoneal glucose tolerance test (IPGTT), in which mice were fasted overnight (“fasting”) and then challenged with a bolus intraperitoneal injection of 20 mM glucose (“fed”). d28 cells in the RPVIM device groups produced a significant increase of approximately 2-fold more C-

peptide in in the fed vs. fasted state. In contrast, cells in the SIM and SPVIM groups showed no evidence of glucose-stimulated insulin secretion (**Figure 3.5A**). Additionally, the amount of C-peptide produced by cells in RPVIM devices post-bolus of glucose was 5-fold higher than cells in SIM and SPVIM groups. This post-glucose response in RPVIM group was significantly greater than SIM and SPVIM groups (**Figure 3.5B**).

Explantation and histological analysis of RPVIM devices containing stem cell-derived insulin-producing beta cell clusters showed the presence of viable and insulin secreting beta-like clusters inside the vascularized device. The trichrome staining showed multiple beta cell-like clusters lined between the skin and muscle layers (**Figure 3.6A-B**). These beta cell-like clusters are not found in the SIM and SPVIM device explants (**Figures 3.7, 3.8**, respectively) The hematoxylin and eosin staining show biocompatibility of the devices as there was no visible deposition of fibrotic tissue along the graft and no irregularities in size or shape at the tissue and cellular levels indicating that there are no detrimental effects caused by the implant (**Figure 3.6C**). Immunostaining of cells for glucagon and human C-peptide confirmed the presence of islet-like clusters within the device (**Figure 3.6D**). Additionally, like the H&E staining, picrosirius red staining also confirmed little to no levels of collagen present on the periphery of the device, confirming minimal fibrosis (**Figure 3.6E**). Immunofluorescence staining of von Willebrand Factor and CD31 demonstrate increased angiogenesis and higher levels of platelet endothelial cell adhesion molecule 1, a marker for vascular differentiation (**Figure 3.6F-G**). Collectively, the IPGTT and histological analysis of grafts demonstrate robust glucose stimulated insulin secretion and morphological integrity of stem cell-derived insulin-producing beta cell clusters within the RPVIM devices.

3.4. Discussion

Our results confirm other studies reporting that implantation within the subcutaneous space does not allow for the survival of beta cells, which are typically highly vascularized in their native environment.[5,19,41,49,50] Low oxygen tension and lack of nutrient supply caused by insufficient vasculature often lead to ischemia and necrosis of the highly metabolic beta cells.[2,4,24,25,39,51,52] It has also been shown that beta cell function and insulin secretion are severely impacted by the dense vascular network through blood flow-dependent and independent pathways.[5,38,50] Therefore, it is crucial for encapsulated beta cells to have functional and robust vasculature around the implant.

Here, we demonstrate an easy-to-implement pre-vascularization approach that aims to relieve the ischemic stress experienced by encapsulated cells upon implantation in immunodeficient NSG mice. Our results indicate that in the subcutaneous space, pre-vascularization of replenishable devices increases the survival of encapsulated stem cell-derived insulin-producing beta cell clusters post-transplantation. The nanoporous thin-film encapsulation device was designed such that after pre-vascularization, cells could be loaded easily through the port without the need to remove the device from the transplant site. After the cells were loaded, the device was resealed using resistive heating. This technique maintains the device's shape and structure while also preserving the surrounding vasculature (**Figure 3.1**). Additionally, previously published research suggested that a functional, planar encapsulation device should be no more than 550 μm in thickness with a volume fraction of ~2.5%.[53] In our encapsulation devices, the total volume of transplanted beta cell cluster mass was 4.423 μL, which results in a volume fraction of ~2.7%. Also, we estimated that these loaded encapsulation devices had a

thickness of ~100 μm demonstrating that our device design satisfies the optimized parameters. Analysis of the vasculature around the encapsulation device showed that after 14 days of pre-vascularization in the subcutaneous space, the device is surrounded with twice as many new, functional blood vessels compared to 7 days of implantation (**Figure 3.2**). The presence of these blood vessels plays an important role in cell survival and function inside the encapsulation device as we observed greater than 80% graft survival in RPVIM devices in the subcutaneous space (**Figure 3.4**). The RPVIM devices also show greater performance than SPVIM devices, a technique used previously by several groups to enhance cell engraftment.[7,20,32,39,43] This was also observed in more mature stem cell-derived insulin-producing beta cell clusters, which are highly metabolic and require robust sources of nutrients and oxygen.[47,48] Moreover, the mature cells in pre-vascularized grafts also demonstrate significantly higher levels of glucose-stimulated insulin secretion compared to controls (**Figure 3.5**). The histological analysis demonstrates *in vivo* biocompatibility and the presence of functional stem cell-derived insulin-producing beta cell clusters inside RPVIM devices (**Figure 3.6**). While functional beta cell clusters were observed in the device, some necrotic areas were also present, likely due to insufficient oxygen supply. This is also indicated by the 50% reduction in cluster mass observed in RPVIM devices (**Figure 3.4**). However, overall, the RPVIM approach resulted in a significant increase in vascular coverage and oxygen availability, leading to better preservation of beta cell cluster mass and function compared to controls. Results from this study confirm that the RPVIM devices effectively provide a hospitable microenvironment for encapsulated stem cell-derived insulin-producing beta cell clusters in the subcutaneous space for 28 days. Future studies include longer-term survival and

function studies using the RPVIM devices and testing the ability of these devices to reverse diabetes in a diabetic mouse model. These studies will provide key insights into the clinical benefit of this approach.

Our approach involves modification of the subcutaneous site to create a highly vascularized implantation site without introducing multiple devices, materials, or biologics whose long-term safety and biocompatibility need to be accounted for. This strategy utilized only FDA-approved biomaterials and took advantage of the naturally occurring vascularization process in the body.[24,45,45,46] The lectin perfusion studies demonstrated functional vasculature surrounding the implant at 14 days, which we deemed sufficient time to create a favorable transplantation site. We observed robust vascular response with vessel branching, ingrowth, and outgrowth on and around the encapsulation device in the subcutaneous site. Additionally, since neovascularization is a dynamic process, we expect the vasculature to remodel extensively over time, especially with the addition of encapsulated cells.[5,50] Furthermore, our approach showed that not only is a pre-vascularized site necessary for subcutaneous implants, but it is also crucial to ensure that we preserve the vascular network while transplanting the cells in the pre-vascularized site.

Islet transplantation using cell encapsulation devices can offer a long-term treatment for T1D. A major limitation that remains unaddressed is the loss of cell viability post-transplant. A major cause of this is the ischemic stress experienced by encapsulated cells that are transplanted in the inherently low vascularized subcutaneous space. However, transplantation of cellular grafts in the subcutaneous space is highly attractive as it allows for noninvasive graft monitoring, ease in device retrieval, or re-filling the

implanted device with new islets if required. Previous research has shown that modifying the subcutaneous space to increase vascular network formation prior to the transplantation of encapsulation devices can increase graft survival and function. However, these approaches often involve the use of biologics or techniques that disrupt the vasculature when inserting the encapsulation device.

Our replenishable pre-vascularized device allows the transplantation of insulin-producing cells in encapsulation devices without disrupting the hospitable environment formed around the device during the pre-vascularization period. Thus, we can take advantage of the body's ability to form robust vasculature around PCL devices. Our results show that this method increases the survival and function of cells encapsulated within thin-film PCL devices in the subcutaneous space over 28 days. We anticipate that the results of this work are relevant to a broader range of cell therapy devices in which ischemic stress leads to a loss in graft post-transplantation.

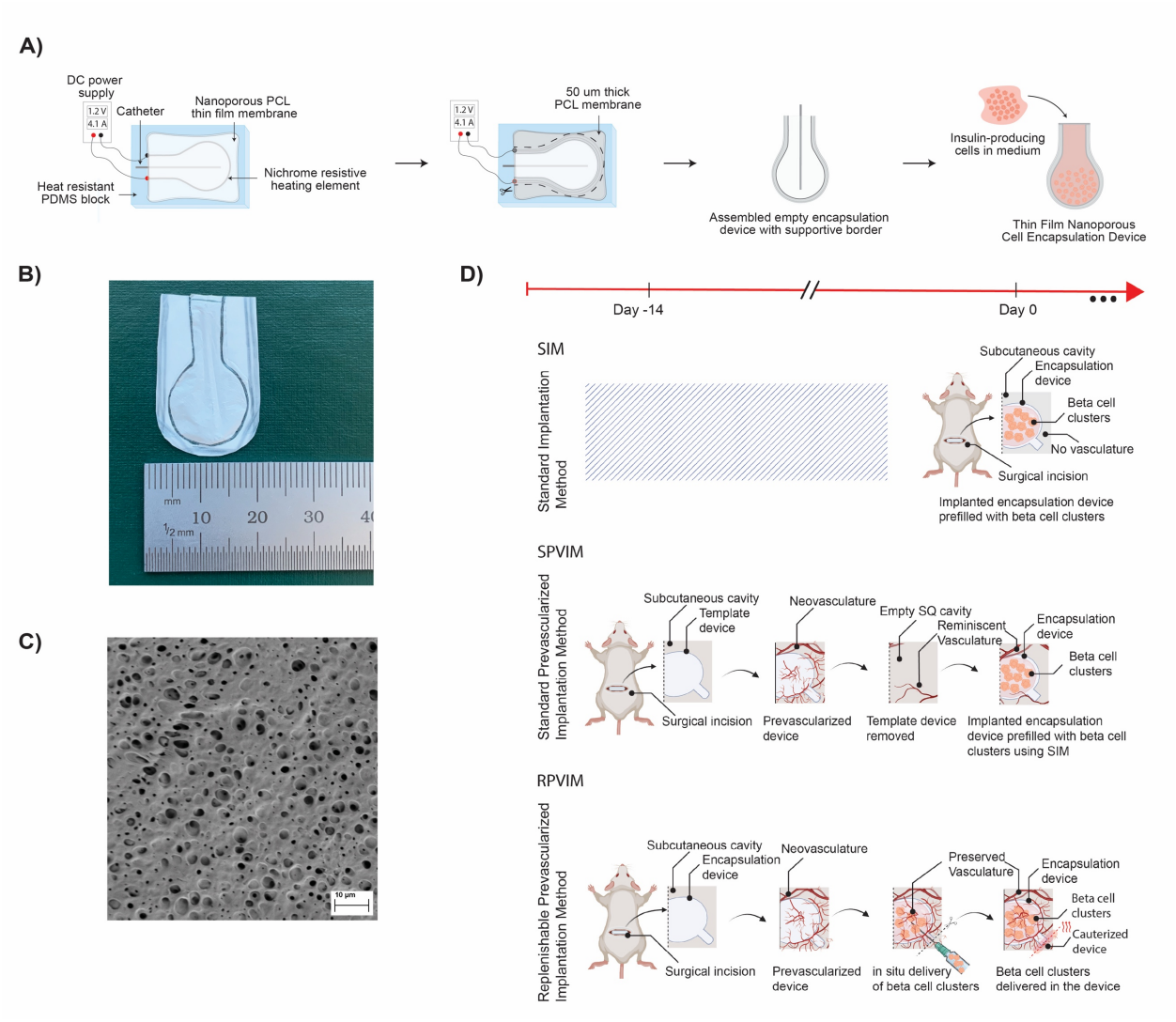

Figure 3.1. Schematic of cell encapsulation device and pre-vascularization methodology. **A)** Illustration of the fabrication of thin film PCL encapsulation devices assembled using a resistive heating method. **B)** Image of the 2 cm wide encapsulation device showing the long neck that allows for easy insertion of cells and thicker surrounding membrane that provides mechanical support. **C)** Cross-sectional SEM image of nanoporous PCL membrane used to fabricate encapsulation devices. The inner pores of the membranes are ~200 nm in size, and the membrane thickness is ~10 μm. **D)** Implantation strategies for comparing standard implantation, standard pre-vascularization implantation, and replenishable pre-vascularization implantation methods.

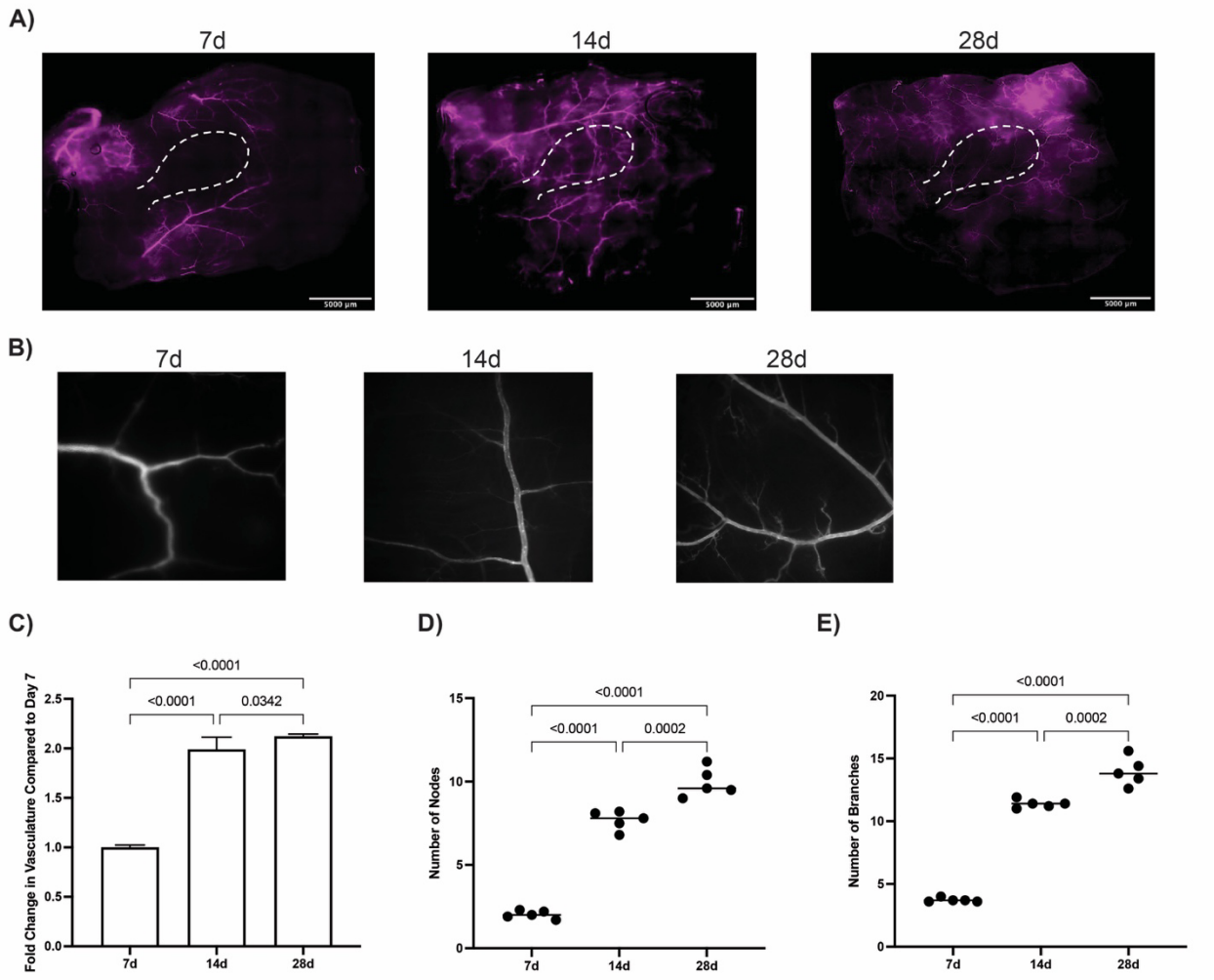

Figure 3.2. Vasculature formation around empty implanted devices. **A)** Lectin-perfusion assay (stained in purple) was performed to visualize functional vasculature after 7 (n=6), 14 (n=6), and 28 days (n=6) of implantation. **B)** Representative images of vascular networks (detected using lectin-perfusion assay) used to quantify changes in C) total vascular area, **D)** number of nodes, and **E)** number of branches around the implant. The significance across all experimental groups was performed using One-way ANOVA, followed by Tukey's post hoc test.

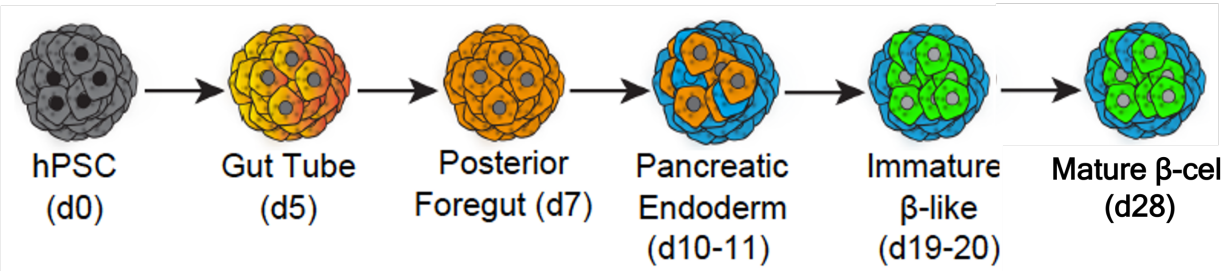

Figure 3.3. Schematic showing differentiation of stem cell-derived insulin-producing beta cell clusters. The beta cell clusters are derived from human embryonic pluripotent stem cells and are differentiated to produce immature beta cell-like clusters (d20) or mature beta cell-like clusters (d28).

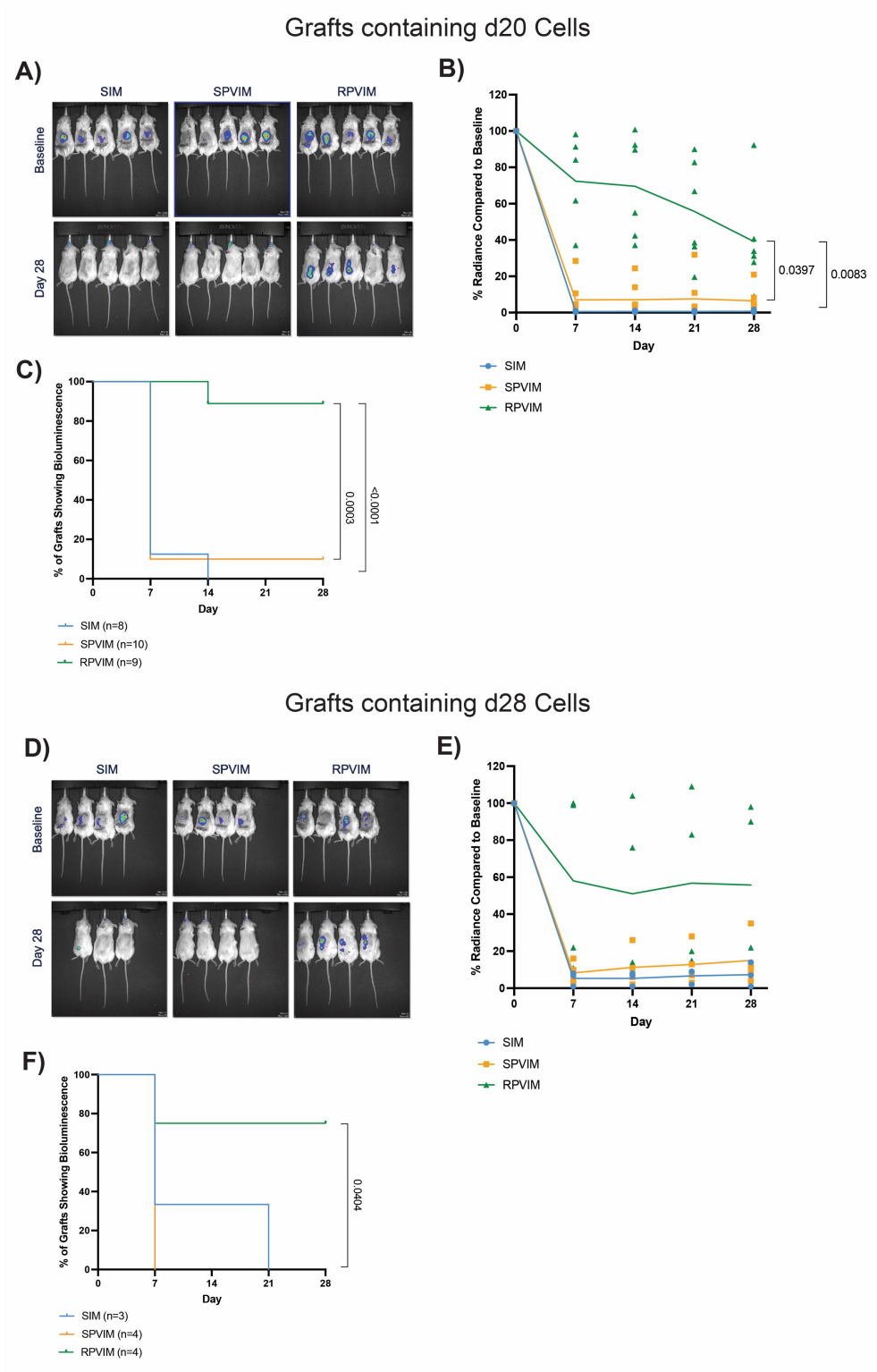

Figure 3.4. *In vivo* viability of stem cell-derived insulin-producing cells encapsulated in RPVIM devices. Representative images of encapsulated **A)** Luciferase positive d20 (d20.LUC) cells in SIM devices (n=8, blue circles), SPVIM devices (n=10, orange squares), and RPVIM devices (n=9, green triangles) and **D)** Luciferase positive d28

(d28.LUC) in SIM devices (n=3, blue circles), SPVIM devices (n=4, orange squares), RPVIM devices (n=4, green triangles). Quantification of bioluminescence signal from cells transplanted in devices compared to baseline for **B)** d20.LUC and **E)** d28.LUC cells. The significance of changes in bioluminescent signal at day 28 vs. baseline was determined using multiple unpaired t-tests, corrected for multiple comparisons using Holm–Sidak method. Quantification of the percent of **C)** d20.LUC and **F)** d28.LUC grafts showing bioluminescence over a period of 28 days. The significance between survival curves was determined using the Kaplan-Meier test, and comparisons were made using a Log-rank (Mantel-Cox) method.

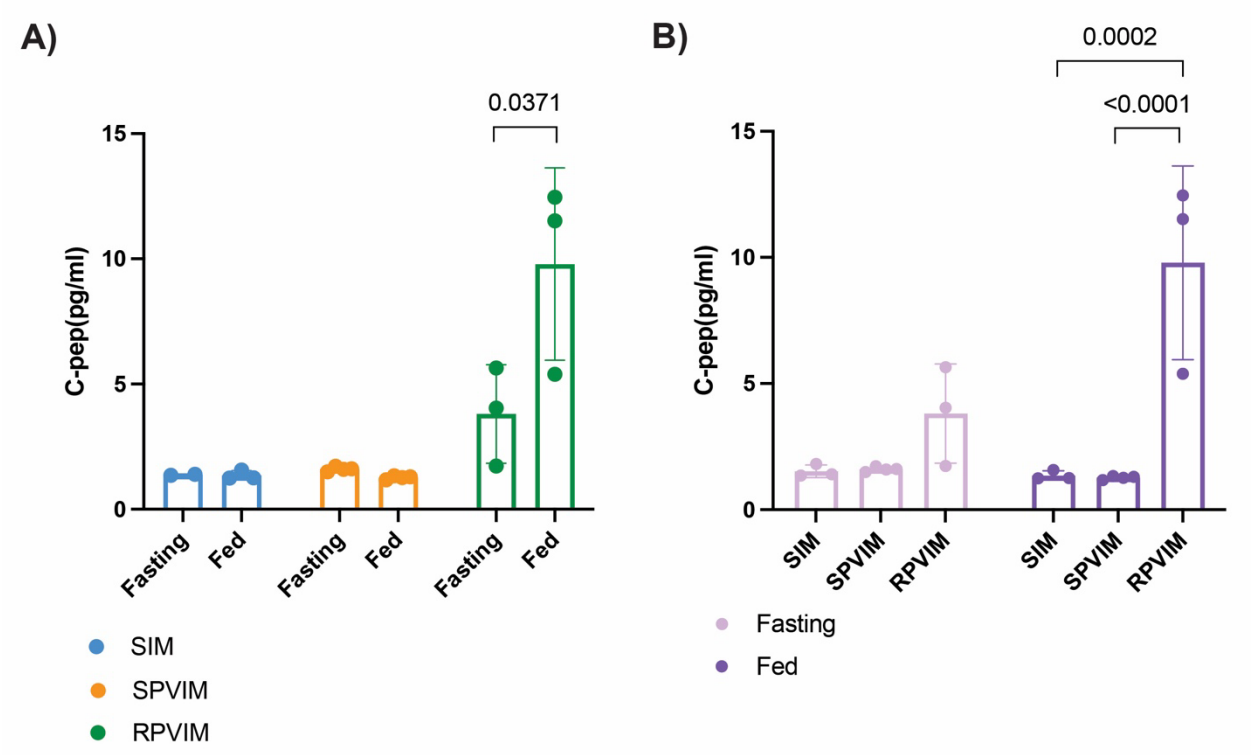

Figure 3.5. Glucose response and insulin secretion from RPVIM devices containing d28 stem cell-derived insulin-producing cells. **A)** Levels of secreted C-peptide from cells in RPVIM devices significantly increase 45 minutes post-intraperitoneal glucose injection. The significance between fasting and glucose groups was determined using a one-tailed unpaired t-test. **B)** Systemic C-peptide levels in RPVIM devices are greater post-IPGTT compared to SIM and SPVIM devices. Statistical significance across the groups was determined using a 2-way ANOVA fitting a mixed-effects model followed by Tukey's post hoc test.

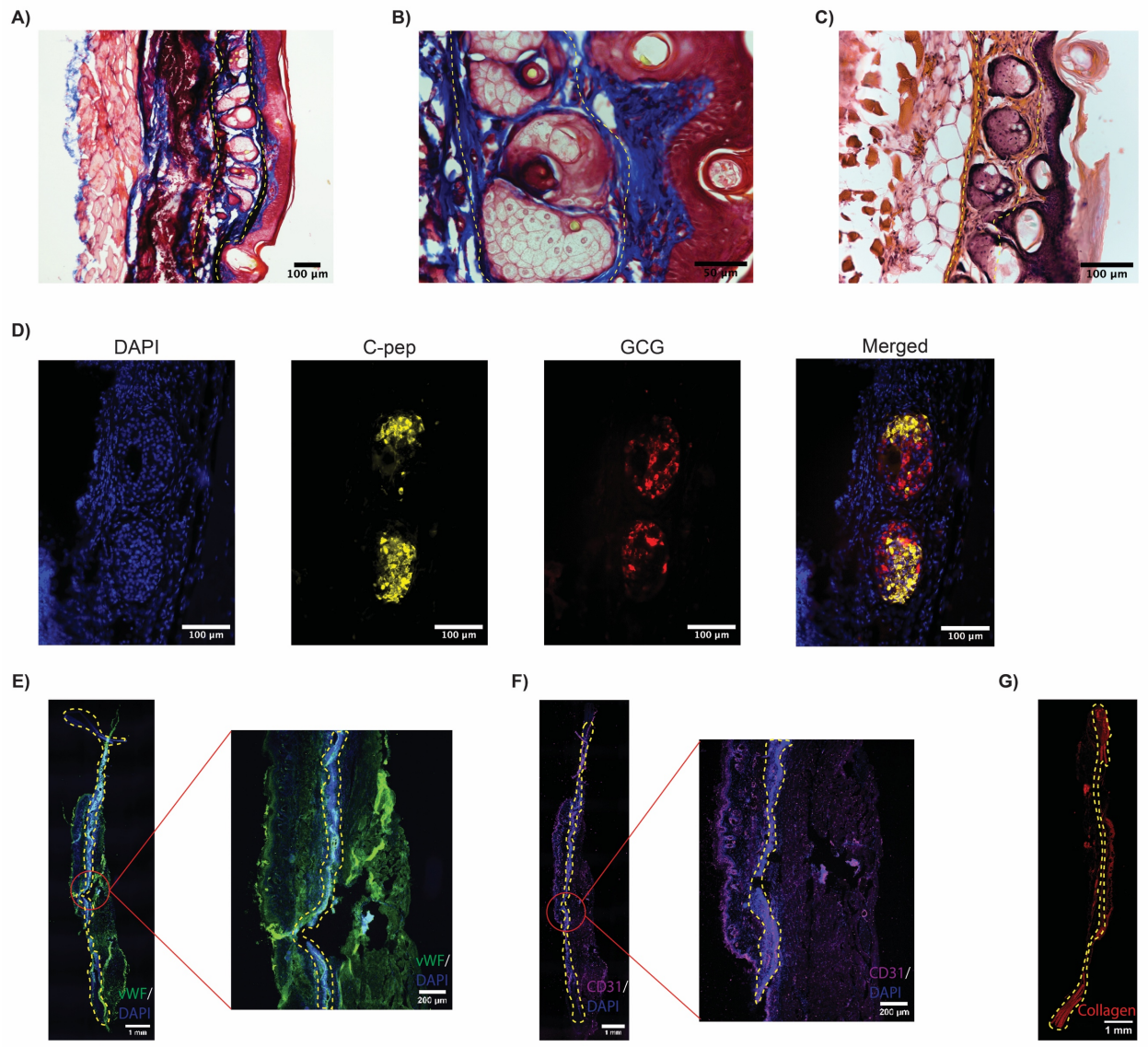

Figure 3.6. Histological analysis of RPVIM devices shows the presence of viable and functional D28 cells. In all the images, the outline of the device is shown using a yellow dashed line. **A)** 20x and **B)** 40x images of trichrome staining shows the presence of stem-cell derived insulin producing cell clusters inside the device. The device resets between the skin and muscle layer, with numerous blood vessels surrounding the implant. **C)** Representative 20X image of H&E staining confirms the presence of islets and *in vivo* biocompatibility. **D)** Representative immunofluorescence staining of stem cell-derived insulin-producing cells inside RPVIM device for human C-peptide (C-PEP, yellow), human glucagon (GCG, red), and nuclei (DAPI, blue). **E)** Host vasculature (detected by staining with mouse-specific anti-vWF, green) is present around the outskirts of RPVIM device showing the presence of neovasculature. Nuclei are stained with DAPI in blue. **F)** Host endothelial cells (detected by mouse specific anti-CD31 staining) are found primarily near the muscle layer in RPVIM devices. **G)** Minimal collagen (detected by picrosirius red staining) is observed around the graft.

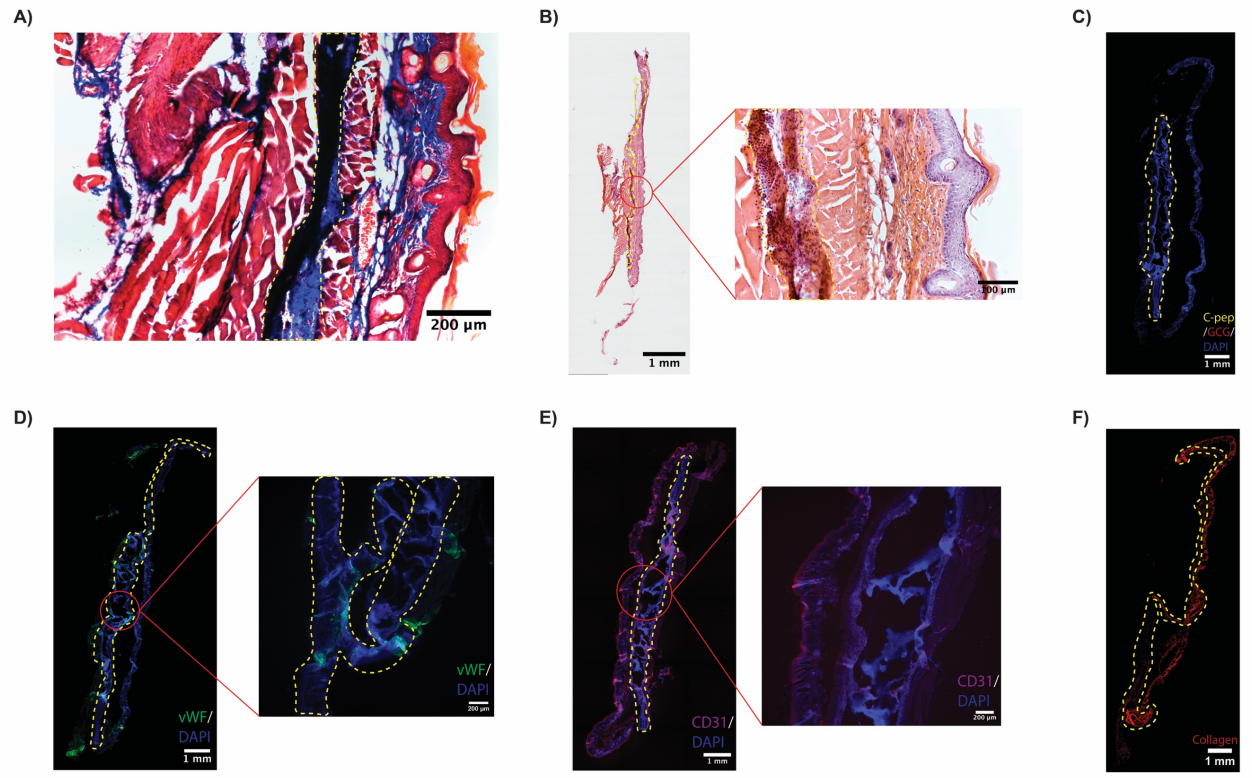

Figure 3.7. Histological analysis of SIM devices shows lack of stem cell-derived insulin-producing beta cell clusters. In all the images, the outline of the device is shown using a yellow dashed line. **A)** 20x images of trichrome staining shows that there are no beta cell clusters as seen in SIM devices. **B)** 4X and representative 2X image of H&E staining confirms the *in vivo* biocompatibility of the SIM devices. **C)** Representative immunofluorescence staining of stem cell-derived insulin-producing cells inside RPVIM device for human C-peptide (C-PEP, yellow), human glucagon (GCG, red), and nuclei (DAPI, blue). No signal for human C-peptide and/or human glucagon was seen. **D)** Negligible host vasculature (detected by staining with mouse-specific anti-vWF, green) is present around the outskirts of SIM devices. Nuclei are stained with DAPI in blue. **E)** Host endothelial cells (detected by mouse specific anti-CD31 staining) are found primarily near the muscle layer in SIM devices.

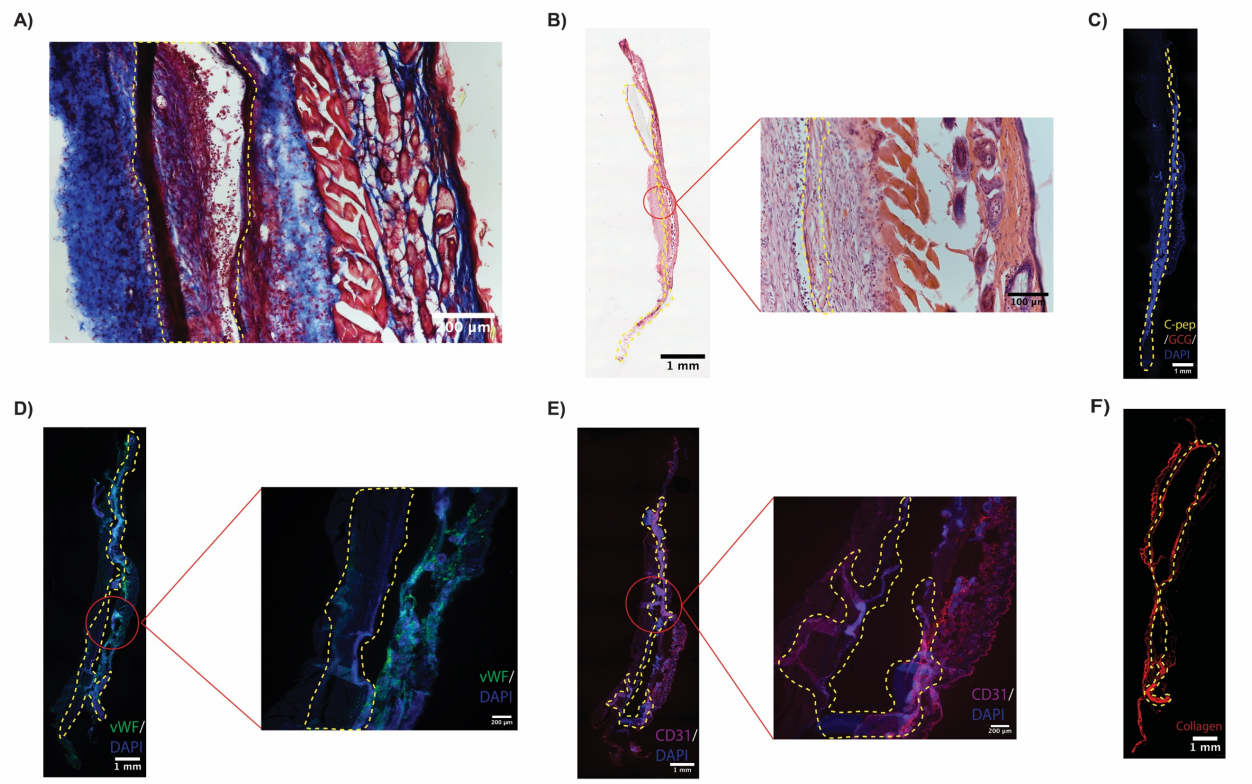

Figure 3.8. Histological analysis of SPVIM devices shows similar results as SIM devices. In all the images, the outline of the device is shown using a yellow dashed line. **A)** 20x image of trichrome staining shows that there are no beta cell clusters as seen in SPVIM devices. **B)** 4X and representative 2X image of H&E staining confirms the *in vivo* biocompatibility of the SPVIM devices. **C)** Representative immunofluorescence staining of stem cell-derived insulin-producing cells inside SPVIM device for human C-peptide (C-PEP, yellow), human glucagon (GCG, red), and nuclei (DAPI, blue). No signal for human C-peptide and/or human glucagon was seen. **D)** Little to no amount of host vasculature (detected by staining with mouse-specific anti-vWF, green) is present around the outskirts of SIM devices. Nuclei are stained with DAPI in blue. **E)** Host endothelial cells (detected by mouse specific anti-CD31 staining) are found primarily near the muscle layer in RPVIM devices.

3.5. References

1. Desai T, Shea LD. Advances in islet encapsulation technologies. Nat Rev Drug Discov. 2017;16(5):338-350. doi:10.1038/nrd.2016.232

2. Desai TA, Tang Q. Islet encapsulation therapy — racing towards the finish line? Nat Rev Endocrinol. 2018;14(11):630-632. doi:10.1038/s41574-018-0100-7

3. Bouwens L, Houbracken I, Mfopou JK. The use of stem cells for pancreatic regeneration in diabetes mellitus. Nat Rev Endocrinol. 2013;9:598-606. doi:10.1038/nrendo.2013.145

4. Kharbikar BN, Chendke GS, Desai TA. Modulating the foreign body response of implants for diabetes treatment. Adv Drug Deliv Rev. 2021;174:87-113. doi:10.1016/j.addr.2021.01.011

5. Bowers DT, Song W, Wang LH, Ma M. Engineering the vasculature for islet transplantation. Acta Biomater. 2019;95:131-151. doi:10.1016/j.actbio.2019.05.051

6. Greenbaum C, VanBuecken D, Lord S. Disease-Modifying Therapies in Type 1 Diabetes: A Look into the Future of Diabetes Practice. Drugs. 2019;(0123456789):1-19. doi:10.1007/s40265-018-1035-y

7. Goswami D, Domingo-Lopez DA, Ward NA, et al. Design Considerations for Macroencapsulation Devices for Stem Cell Derived Islets for the Treatment of Type 1 Diabetes. Adv Sci. 2021;8(16):2100820. doi:10.1002/advs.202100820

8. Correia CR, Reis RL, Mano JF. Design Principles and Multifunctionality in Cell Encapsulation Systems for Tissue Regeneration. Adv Healthc Mater. 2018;7(19):1-20. doi:10.1002/adhm.201701444

9. Tomei AA, Villa C, Ricordi C. Development of an encapsulated stem cell-based therapy for diabetes. Expert Opin Biol Ther. 2015;15(9):1321-1336. doi:10.1517/14712598.2015.1055242

10. Brusko TM, Russ HA, Stabler CL. Strategies for durable β cell replacement in type 1 diabetes. Science. 2021;373(6554):516-522. doi:10.1126/science.abh1657

11. Stabler CL, Li Y, Stewart JM, Keselowsky BG. Engineering immunomodulatory biomaterials for type 1 diabetes. Nat Rev Mater. 2019;4(6):429-450. doi:10.1038/s41578-019-0112-5

12. Krentz NAJ, Shea LD, Huising MO, Shaw JAM. Restoring normal islet mass and function in type 1 diabetes through regenerative medicine and tissue engineering. Lancet Diabetes Endocrinol. 2021;9(10):708-724. doi:10.1016/S2213-8587(21)00170-4

13. Ozawa F, Nagata S, Oda H, Yabe SG, Okochi H, Takeuchi S. Lotus-root-shaped cell-encapsulated construct as a retrieval graft for long-term transplantation of human iPSC-derived β-cells. iScience. 2021;24(4):102309. doi:10.1016/j.isci.2021.102309

14. Teramura Y, Iwata H. Islet encapsulation with living cells for improvement of biocompatibility. Biomaterials. 2009;30(12):2270-2275. doi:10.1016/j.biomaterials.2009.01.036

15. Zhang Q, Gonelle-Gispert C, Li Y, et al. Islet Encapsulation: New Developments for the Treatment of Type 1 Diabetes. Front Immunol. 2022;13. Accessed November 22, 2022. https://www.frontiersin.org/articles/10.3389/fimmu.2022.869984

16. Buder B, Alexander M, Krishnan R, Chapman DW, Lakey JR. Encapsulated Islet Transplantation: Strategies and Clinical Trials. Immune Netw. 2013;13(6):235-239.

17. Cayabyab F, Nih LR, Yoshihara E. Advances in Pancreatic Islet Transplantation Sites for the Treatment of Diabetes. Front Endocrinol. 2021;12:732431. doi:10.3389/fendo.2021.732431

18. Kharbikar BN, Mohindra P, Desai TA. Biomaterials to enhance stem cell transplantation. Cell Stem Cell. 2022;29(5):692-721. doi:10.1016/j.stem.2022.04.002

19. Shapiro AMJ, Pokrywczynska M, Ricordi C. Clinical pancreatic islet transplantation. Nat Rev Endocrinol. 2017;13(5):268-277. doi:10.1038/nrendo.2016.178

20. Pepper AR, Gala-Lopez B, Pawlick R, Merani S, Kin T, Shapiro AMJ. A prevascularized subcutaneous device-less site for islet and cellular transplantation. Nat Biotechnol. 2015;33(5):518-523. doi:10.1038/nbt.3211

21. Tomei AA. Engineering Confined and Prevascularized Sites for Islet Transplantation. Transplantation. 2018;102(11):1793-1794. doi:10.1097/TP.0000000000002290

22. Robert T, De Mesmaeker I, Van Hulle FO, et al. Cell Mass Increase Associated with Formation of Glucose-Controlling β-Cell Mass in Device-Encapsulated Implants of hiPS-Derived Pancreatic Endoderm. Stem Cells Transl Med. 2019;8(12):1296-1305. doi:10.1002/sctm.19-0043

23. Haller C, Piccand J, De Franceschi F, et al. Macroencapsulated Human iPSC-Derived Pancreatic Progenitors Protect against STZ-Induced Hyperglycemia in Mice. Stem Cell Rep. 2019;12(4):787-800. doi:10.1016/j.stemcr.2019.02.002

24. Chendke GS, Faleo G, Juang C, et al. Supporting Survival of Transplanted Stem-Cell-Derived Insulin-Producing Cells in an Encapsulation Device Augmented with Controlled Release of Amino Acids. Adv Biosyst. 2019;3(9):1900086. doi:10.1002/adbi.201900086

25. Faleo G, Russ HA, Wisel S, et al. Mitigating Ischemic Injury of Stem Cell-Derived Insulin-Producing Cells after Transplant. Stem Cell Rep. 2017;9(3):807-819. doi:10.1016/j.stemcr.2017.07.012

26. Lou S, Zhang X, Zhang J, Deng J, Kong D, Li C. Pancreatic islet surface bioengineering with a heparin-incorporated starPEG nanofilm. Mater Sci Eng C. 2017;78:24-31. doi:10.1016/j.msec.2017.03.295

27. Marchioli G, Luca AD, de Koning E, et al. Hybrid Polycaprolactone/Alginate Scaffolds Functionalized with VEGF to Promote de Novo Vessel Formation for the Transplantation of Islets of Langerhans. Adv Healthc Mater. 2016;5(13):1606-1616. doi:10.1002/adhm.201600058

28. Wang W, Gu Y, Tabata Y, et al. Reversal of diabetes in mice by xenotransplantation of a bioartificial pancreas in a prevascularized subcutaneous site. Transplantation. 2002;73(1):122-129. doi:10.1097/00007890-200201150-00023

29. Liu W, Flanders JA, Wang LH, et al. A safe, fibrosis-mitigating, and scalable encapsulation device supports long-term function of insulin-producing cells. Small Weinh Bergstr Ger. 2022;18(8):e2104899. doi:10.1002/smll.202104899

30. Barra JM, Kozlovskaya V, Kepple JD, et al. Xenotransplantation of tannic acid-encapsulated neonatal porcine islets decreases proinflammatory innate immune responses. Xenotransplantation. 2021;28(6):e12706. doi:10.1111/xen.12706

31. Zhi ZL, Khan F, Pickup JC. Multilayer nanoencapsulation: A nanomedicine technology for diabetes research and management. Diabetes Res Clin Pract. 2013;100(2):162-169. doi:10.1016/j.diabres.2012.11.027

32. Groot Nibbelink M, Skrzypek K, Karbaat L, et al. An important step towards a prevascularized islet microencapsulation device: in vivo prevascularization by combination of mesenchymal stem cells on micropatterned membranes. J Mater Sci Mater Med. 2018;29(11):174. doi:10.1007/s10856-018-6178-6

33. Vaithilingam V, Evans MDM, Lewy DM, Bean PA, Bal S, Tuch BE. Co-encapsulation and co-transplantation of mesenchymal stem cells reduces pericapsular fibrosis and improves encapsulated islet survival and function when allografted. Sci Rep. 2017;7(1):1-13. doi:10.1038/s41598-017-10359-1

34. Figliuzzi M, Cornolti R, Perico N, et al. Bone Marrow–Derived Mesenchymal Stem Cells Improve Islet Graft Function in Diabetic Rats. Transplant Proc. 2009;41(5):1797-1800. doi:10.1016/j.transproceed.2008.11.015

35. Barkai U, Rotem A, de Vos P. Survival of encapsulated islets: More than a membrane story. World J Transplant. 2016;6(1):69-90. doi:10.5500/wjt.v6.i1.69

36. Komatsu H, Rawson J, Barriga A, et al. Posttransplant oxygen inhalation improves the outcome of subcutaneous islet transplantation: A promising clinical alternative to the conventional intrahepatic site. Am J Transplant. 2018;18:832-842. doi:10.1111/ajt.14497

37. Colton CK. Oxygen supply to encapsulated therapeutic cells. Adv Drug Deliv Rev. 2014;67-68:93-110. doi:10.1016/j.addr.2014.02.007

38. Meng X, Xing Y, Li J, et al. Rebuilding the Vascular Network: In vivo and in vitro Approaches. Front Cell Dev Biol. 2021;9. doi:10.3389/fcell.2021.639299

39. Conkling N, Tang Q, Faleo G, Stock P, WIsel S, Desai T. Prevascularization of the Subcutaneous Space Improves Survival of Transplanted Mouse Islets. Transplantation. 2018;10(7S):372. doi:10.1097/01.tp.0000543124.81125.ef

40. MACGILLIVARY AS, TOLEIKIS PM, MAZZUCA DM. 205-LB: Clinical Validation of the Implanted Prevascularized Cell Pouch as a Viable, Safe Site for Diabetes Cell Therapy. Diabetes. 2020;69(Supplement_1). doi:10.2337/db20-205-LB

41. Zhu H, Li W, Liu Z, et al. Selection of implantation sites for transplantation of encapsulated pancreatic islets. Tissue Eng Part B Rev. 2017;00(00):ten.TEB.2017.0311. doi:10.1089/ten.TEB.2017.0311

42. Magisson J, Sassi A, Xhema D, et al. Safety and function of a new pre-vascularized bioartificial pancreas in an allogeneic rat model. J Tissue Eng. 2020;11:204173142092481. doi:10.1177/2041731420924818

43. Pepper AR, Pawlick R, Bruni A, et al. Transplantation of Human Pancreatic Endoderm Cells Reverses Diabetes Post Transplantation in a Prevascularized Subcutaneous Site. Stem Cell Rep. 2017;8(6):1689-1700. doi:10.1016/j.stemcr.2017.05.004

44. Smink AM, de Haan BJ, Lakey JRT, de Vos P. Polymer scaffolds for pancreatic islet transplantation — Progress and challenges. Am J Transplant. 2018;18(9):2113-2119. doi:10.1111/ajt.14942

45. Chang R, Faleo G, Russ HA, et al. Nanoporous Immunoprotective Device for Stem-Cell-Derived β-Cell Replacement Therapy. ACS Nano. 2017;11(8):7747-7757. doi:10.1021/acsnano.7b01239

46. Nyitray CE, Chang R, Faleo G, et al. Polycaprolactone Thin-Film Micro- and Nanoporous Cell-Encapsulation Devices. ACS Nano. 2015;9(6):5675-5682. doi:10.1021/acsnano.5b00679

47. Russ HA, Parent AV, Ringler JJ, et al. Controlled induction of human pancreatic progenitors produces functional beta-like cells in vitro.-sup. EMBO J. 2015;34(13):1759-1772. doi:10.15252/embj.201591058

48. Nair GG, Liu JS, Russ HA, et al. Recapitulating endocrine cell clustering in culture promotes maturation of human stem-cell-derived β cells. Nat Cell Biol. 2019;21:263-274. doi:10.1038/s41556-018-0271-4

49. Granlund L, Hedin A, Korsgren O, Skog O, Lundberg M. Altered microvasculature in pancreatic islets from subjects with type 1 diabetes. Okada H, ed. PLOS ONE. 2022;17(10):e0276942. doi:10.1371/journal.pone.0276942

50. Burganova G, Bridges C, Thorn P, Landsman L. The Role of Vascular Cells in Pancreatic Beta-Cell Function. Front Endocrinol. 2021;12. doi:10.3389/fendo.2021.667170

51. Sneddon JB, Tang Q, Stock P, et al. Stem Cell Therapies for Treating Diabetes: Progress and Remaining Challenges. Cell Stem Cell. 2018;22(6):810-823. doi:10.1016/j.stem.2018.05.016

52. Carlsson PO, Palm F, Andersson A, Liss P. Markedly decreased oxygen tension in transplanted rat pancreatic islets irrespective of the implantation site. Diabetes. 2001;50(3):489-495. doi:10.2337/diabetes.50.3.489

53. An D, Chiu A, Flanders JA, et al. Designing a retrievable and scalable cell encapsulation device for potential treatment of type 1 diabetes. Proc Natl Acad Sci. 2018;115(2). doi:10.1073/pnas.1708806115

Chapter 4. Modulating the Immune Microenvironment around Implants to Promote Implant Integration

4.1 Introduction

Inflammation is a complex biological response to tissue injury or infection, involving the activation of immune cells and the release of various cytokines and chemokines.[11–13] This process is mediated by immune cells such as macrophages, which are activated upon contact with the biomaterials used in the encapsulation devices. Macrophages play a key role in initiating inflammation and directing the subsequent immune response.[8,14–17] When macrophages come in contact with the implant, they are activated to their inflammatory phenotype, creating a toxic local microenvironment. The activation of macrophages depends on the properties of the biomaterial used in the device, such as surface chemistry, topography, stiffness, and degradation products. These properties will eventually cause macrophages to either amplify their inflammatory response or to polarize to their anti-inflammatory phenotype to activate the tissue repair process.[8,16–18] Moreover, as these macrophages polarize, they also exhibit different cell shapes: inflammatory macrophages have a rounded cell shape while reparative macrophages have an elongated cell shape.[19–21]

Therefore, the choice of biomaterial is critical in designing effective encapsulation devices.[3,16,17] Ideally, biomaterials should promote the polarization of macrophages to their anti-inflammatory phenotype, which is associated with tissue repair and regeneration. Recent studies have shown that the surface topography of biomaterials can modulate macrophage phenotype, with nanoscale and microscale features leading to different polarization outcomes. Nanotopography has been shown to promote the M2

phenotype,[22–25] while microtopography has been shown to promote the M1 phenotype.[20,23,26,27] Additionally, promoting an elongated cell shape by patterning the physical cues or decreasing perceived stiffness of substrate can also induce the reparative M2 phenotype.[20,21,23,28] Therefore, tailoring the surface topography of biomaterials can serve as a powerful tool in modulating macrophage polarization to its reparative phenotype, thus controlling the immune response and accelerating engraftment of the device and increasing its efficacy in treating T1D.

In this chapter, we investigate the effects of surface topography on macrophage polarization in response to PCL-based biomaterials for cell encapsulation in T1D. We first fabricate and characterize mineralized PCL thin films with nanoscale topography and micron-scaled topographic PCL thin films. We then evaluate the changes in gene expression levels of TNFα and Arg1, which are markers for the M1 inflammatory phenotype and M2 reparative phenotype, respectively, in macrophages cultured on these biomaterials. Our results provide insights into how the surface topography of biomaterials can be tailored to modulate macrophage phenotype and improve the success of cell encapsulation for treating type 1 diabetes.

4.2 Materials & Methods

4.2.1 Nano-scale topographic thin-film fabrication

PCL thin films were fabricated according to previously published literature.[29–31] The PCL thin films were incubated in 10 mL of modified simulated body buffer with low (10 mM) and high (100 mM) concentration of HCO3 for period of 7 days, according to established literature.[32] The mSBF solution contained 141mM NaCl, 4.0 mM KCl, 0.5 mM

MgSO4, 1.0 mM MgCl2, 4.2 mM or 100mM NaHCO3, 20.0 mM HEPES, 5.0 mM CaCl2, and 2.0 mM KH2PO4 in ddH2O. Prior to incubation in mSBF, some of the PCL thin films were hydrolyzed in 0.5M NaOH solution for 5h at 37°C.

4.2.2 Micron-scale topographic thin-film fabrication

SU-8 10 negative photoresist (MicroChem) was used to create microstructures designed to be 10 μm in height. Microstructures were fabricated on plasma-treated 3-inch silicon wafers. A spin-coater was used to coat SU-8 10 photoresist. The coating conditions were 5 second spin speed of 500 rpm at 100 rpm/second acceleration, after which the ramp was increased to 3000 rpm spin speed at an acceleration of 300 rpm/second and hold for a total of 30 seconds. After the SU-8 10 10 μm thick coating was applied, the wafer was soft baked for 2 minutes at 65°C, followed by 5-7 minutes at 95°C. The wafer was then patterned using a Karl Suss MJB3 mask aligner by exposing the wafer through a photomask to a 365 nm UV light source. Following exposure, post expose bake was performed for 1 minute at 65°C, followed by 2 minutes at 95°C.

Elastomeric stamp using polydimethylsiloxane (PDMS) was generated from the silicon wafer. 10 parts of Sylgard 184 pre-polymer and 1 part of curing agent was combined and poured over the silicon wafer, after which the PDMS mold was left in a vacuum oven to cure at 70°C overnight. The resulting PDMS mold was then used to spin-coat 150 mg/mL PCL thin films. Resulting thin films were ~10 μm in thickness containing pillars of height 10 μm.

4.2.3 Characterization using scanning electron microscopy

Nano- and micro-topographic PCL thin films with and without cells were fixed after 48h of culture and the sample was dehydrated and dried using HMDS. These samples were mounted on a flat SEM mount with colloidal graphite (Ted Pella). Using the Carl Zeis Ultra 55 field emission electron microscope at University of California San Francisco, the samples were imaged.

4.2.4 Cell culture of RAW264.7, mouse BMDM, and human-derived macrophages

The RAW264.7 cell line was used to culture immortalized macrophages in vitro. The cells were maintained in DMEM medium supplemented with 10% FBS and 1% PenStrep at 37°C in a humidified atmosphere containing 5% CO_2.

Mouse BMDMs were obtained from adult mice, which were euthanized using CO2 inhalation according to a protocol approved by the Institutional Animal Care Use Committee of University of California San Francisco. Bone marrow of the dissected femurs were flushed with 5 mL DMEM and the bone marrow was centrifuged for 5 minutes and then cultured for five days in 6-well tissue culture plates. To promote macrophage differentiation, cells were stimulated with 20 ng/mL of monocyte colony stimulation factor (M-CSF) every other day.

Human tissue macrophages were derived from peripheral blood monocytes. 5 mL of human blood was collected and density gradient separation method using Polymorphprep solution (Sigma) was used to isolate human monocytes. The tubes were centrifuged at 500RCF for 40 min at room temperature. The peripheral blood mononuclear cells (PBMCs) were collected, diluted in PBS, and centrifuged at 350RCF

for 10 minutes. The supernatant was removed and re-suspended in red cell lysis buffer, after which the cells were centrifuged at 250 RCF for 5 minutes. The cells were then resuspended in medium and cultured in 24 well plates for 6 days at a seeding density of 500,000 cells/well. To promote macrophage differentiation, cells were stimulated with human M-CSF every 2-3 days.

4.2.5 Macrophage polarization using RTqPCR

All cells were seeded on TCP or PCL films glued to 24 well plates at a seeding density of 50,000 cells/mL. Control conditions included M0 cells on TCP, M1-polarized cells on TCP (stimulation of 100 ng/mL of LPS), and M2-polarized cells on TCP (stimulation of 40 ng/mL of IL-4). After 24- or 48-h of culture, RNA was harvested using RNEasy Mini Kit (Qiagen) and converted to cDNA using iScript cDNA synthesis kit (Bio-Rad Laboratories). The Viia7 qPCR machine was used to perform qPCR and relative gene expression levels were calculated using the $\Delta\Delta$Ct method and normalized against the housekeeping gene. To conduct these experiments, custom-made DNA primers (Integrated DNA Technologies) were utilized, which can be found in **Table 4.1**.

4.3. Results

4.3.1 Fabrication and characterization of mineralized PCL thin films

PCL thin films were fabricated according to previously established protocols.[29–31] Subsequent incubation of hydrolyzed PCL films in modified simulated body fluid (mSBF) resulted in a significant growth of a mineral layer on the surface of the material (**Figure 1A**).[32] A qualitative analysis of the non-hydrolyzed and hydrolyzed surface incubated for

7 days in mSBF with varying concentrations of bicarbonate ion (HCO3) confirmed the formation of mineral coatings on the hydrolyzed surfaces. Scanning electron microscopy (SEM) images revealed that non-hydrolyzed PCL films incubated with mSBF resulted in little to no formation of minerals, demonstrating that pre-treatment of PCL was crucial for the mineral nucleation process (**Figure 1B**). The SEM images also show distinct morphological differences resulting from the use of mSBF solutions with HCO3 concentrations of 10mM (low) and 100mM (high). The mineral layer formed at lower HCO3 concentrations exhibited more dispersed spherical nanostructures. Some of the spherical nanostructures aggregated to form larger spheres that were less than 500 nm in diameter. At high concentrations of HCO3, the entire surface of the PCL film was covered with plate-like structures of minerals. These plate-like structures are composed of aggregated spherical nanostructures, similar to the ones that were formed in the low mSBF concentration.

Furthermore, FTIR spectra of non-hydrolyzed and hydrolyzed PCL with mSBF incubation further confirms the data seen in SEM (**Figure 1C**). The non-hydrolyzed PCL showed similar absorption bands as untreated PCL, despite being incubated in mSBF solution. However, when the PCL films were hydrolyzed and incubated with mSBF, the absorption bands corresponded to those shown by hydroxyapatite. Additionally, increasing concentration of HCO3 in the mSBF solution also corresponded with increasing relative intensity of the phosphate peaks at 564 and 1032 cm^{-1} and of the hydroxyl peaks ranging from 330 to 3650 cm^{-1}.

4.3.2 Macrophage polarization on nanostructured PCL films

To evaluate the effect of nanoscale topography created through mineralized PCL on macrophages, changes in gene expression levels of TNFα (a marker for the M1 inflammatory phenotype) and Arg1 (a marker for the M2 reparative phenotype) were quantified after 24- and 48-hour cultures (**Figure 2**).[19,33] After 24 hours of culture, immortalized macrophages cultured on flat and mineralized PCL showed no significant changes in TNFα expression compared to tissue culture plastic (TCP). However, significant changes were seen after 48 hours of culture. RAW264.7 cells cultured on flat PCL showed increased TNFα expression compared to TCP, while the macrophages cultured on 10mM mineralized PCL showed a significantly lower TNFα expression level (**Figure 2**). However, although the 100 mM mineralized PCL film did show a decreased level of TNFα expression as compared to flat PCL, this change was similar to expression level of macrophages cultured on TCP. While the M1 expression levels decreased, M2 expression of macrophages cultured on 10mM mSBF significantly increased after 24 hours of culture. Additionally, a similar trend was observed, where an increase in mSBF concentration led to decreased increase in M2 expression (**Figure 2**). This indicates that there is a concentration-dependent nanotopography that can lead to decreased M1 and increased M2 phenotype in immortalized macrophages.

This topography-driven change in phenotype was also tested in primary murine BMDMs. Despite the changes observed in the immortalized macrophages, murine BMDMs did not show any change in expression levels of TNFα and Arg1 at 24- and 48-hours (**Figure 3**). These findings suggest that the topography-driven phenotype

modulation observed in immortalized macrophages may not be directly applicable to primary murine BMDMs.

4.3.3 Fabrication and characterization of micron-scaled topographic PCL thin films

Micron-scaled PDMS topographic molds were fabricated using SU-8 photolithography, after which the PDMS molds were used to generate four unique micron-structured patterns on PCL thin films. SEM images of topographic thin films confirms pillars of that are 10μm in height and 25 μm in diameter (**Figure 4**). The spacing between the pillars was varied to create various patterns that can affect macrophage attachment pattern and shape. All films will be referred by their horizontal width space and vertical width space (e.g., H70_V10 means pillars that are 70 μm apart horizontally and 10 μm apart vertically).

4.3.4 Macrophage polarization on micron-scaled topographic PCL films

To understand the effect of patterned micron-scaled topography on macrophage polarization, immortalized and primary murine and human macrophages were cultured on the various topographic patterns. SEM imaging was used to assess the impact of pillar spacing on macrophage morphology. The results revealed distinct differences in macrophage shape based on the spacing between the pillars (**Figure 4**). When cultured on H10_V10 pillars, macrophages exhibited an elongated morphology, with some cells extending and attaching to different pillars. Similarly, the H20_V20 topographies, which have greater inter-pillar distances, still promoted an elongated macrophage cell shape.

However, when macrophages were cultured on H20_V10 and H70_V10 topographies, a different morphology was observed. In contrast to the elongated shape seen on H10_V10 and H20_V20 topographies, macrophages cultured on H20_V10 and H70_V10 topographies exhibited a more rounded cell shape (**Figure 4**). Notably, macrophages did not interact with the pillars on the H70_V10 topography, likely due to the large horizontal distance between the pillars (**Figure 4**). These observations indicate that the spacing between the pillars can significantly impact macrophage morphology and suggest that topographical cues could play a crucial role in directing macrophage behavior.

Changes in gene expression of macrophages cultured on the microtopography were quantified for immortalized and primary macrophages. RAW264.7 cells cultured on topographic and flat PCL films showed no changes in expression levels of CXCL5, a M1 marker, and Arg1 after 24h of culture (**Figure 5**). However, a longer culture period of 48h showed some changes in macrophage gene expression. Macrophages on H20_V10 pillars showed a 2-fold increase in expression levels of CXCL5, and macrophages on H70_V10 and H20_V20 showed 0.5-fold decrease in CXCL5 expression levels (**Figure 5**). Although there were changes observed on the M1 macrophage spectrum, the M2 marker, Arg1, showed no change in gene expression level after 48h (**Figure 5**). These findings indicate that microtopography selectively affects M1 macrophage gene expression without altering M2 marker expression.

When murine BMDMs were cultured on the micron-scaled topographies, a different response was observed. The study found that the topographies, apart from H20_V10, exhibited a significant increase in CXCL5 expression levels of at least two-fold after 48

hours of culture (**Figure 6**). Additionally, the macrophages showed an almost three-fold increase in Arg1 expression levels across all topographies (**Figure 6**). Interestingly, the results showed that macrophages cultured on flat PCL films exhibited an unexpected outcome of an eight-fold increase in Arg1 expression levels (**Figure 6**). This suggests that PCL may promote the reparative phenotype in macrophages. These findings highlight the distinct responses of murine BMDMs to micron-scaled topographies, in contrast to the observations made in immortalized macrophages.

To validate the findings from the murine BMDM study, a similar experiment was conducted using human macrophages. Human macrophages were cultured on the same micron-scaled topographies for a period of 48 hours. The results of this study showed a similar pattern of gene expression as the murine study, with all topographies, except H20_V10 and H70_V10, exhibiting at least a two-fold increase in the M1 expression levels, indicated by IL-1β (**Figure 7**). However, unlike the murine BMDM, human macrophages showed no change in M2 expression levels, indicated by CD206 (**Figure 7**). These findings reveal a similar pattern of M1 marker expression in human macrophages as observed in murine BMDMs, while highlighting distinct species-specific differences in M2 marker expression in response to the tested topographies.

4.4 Discussion

In the present study, we investigated the impact of mineralized and topographically patterned PCL thin films on macrophage polarization. Our findings demonstrate that nanoscale topography generated through mineralization of PCL films significantly affects the macrophage phenotype. Furthermore, we provide evidence that micron-scaled

topographical features on PCL thin films can modulate macrophage morphology and gene expression, which may have implications for the design of biomaterials for tissue engineering and regenerative medicine applications.

The successful fabrication of mineralized PCL films with distinct morphological differences resulting from varying HCO3 concentrations highlights the importance of pre-treatment and incubation conditions in controlling the mineral nucleation process (**Figure 1**). Our SEM and FTIR analysis confirmed the formation and composition of mineral coatings on hydrolyzed PCL surfaces, emphasizing the need for hydrolysis in promoting mineral formation (**Figure 1B,C**). The observed differences in mineral layer morphology due to HCO3 concentrations suggest that the control over the mineralization process could enable the fine-tuning of nanoscale topography for specific applications.

Our study shows that nanoscale topography created through mineralized PCL can modulate macrophage polarization. Immortalized macrophages exhibited a decrease in inflammatory M1 markers and an increase in reparative M2 markers in a concentration-dependent manner (**Figure 2**). This indicates that nanotopography can play a significant role in directing macrophage behavior. Interestingly, primary murine BMDMs did not exhibit the same response to nanoscale topography, suggesting that immortalized cell lines may not accurately represent the behavior of primary cells (**Figure 3**). Further investigation using primary cells is warranted to better understand the impact of nanotopography on macrophage polarization.

The fabrication of micron-scaled topographic PCL thin films with distinct pillar patterns allowed us to explore the effect of microscale topography on macrophage polarization. Our findings demonstrate that the spacing between the pillars can

significantly impact macrophage morphology, with cells exhibiting either elongated or rounded shapes depending on the pillar arrangement (**Figure 4**). This suggests that topographical cues can play a crucial role in directing macrophage behavior.

Gene expression analysis of macrophages cultured on microtopographic PCL films revealed some changes in M1 marker expression levels, but no change in M2 markers in immortalized macrophages (**Figure 5**). On the other hand, primary murine BMDMs showed changes in both M1 and M2 marker expression levels. The observed increase in Arg1 expression levels for macrophages cultured on flat PCL films was unexpected and suggests that PCL may promote the reparative phenotype in macrophages (**Figure 6**). Human-derived macrophages exhibited a similar pattern of M1 marker expression but showed no change in M2 markers (**Figure 7**). This discrepancy emphasizes the need for further investigation using human cells to better understand the translational potential of topography-mediated macrophage polarization.

In conclusion, our study demonstrates that both nanoscale and microscale topographies on PCL thin films can modulate macrophage polarization. These findings provide valuable insights into the role of topography in directing macrophage behavior and could have important implications for the design of biomaterials for tissue engineering and regenerative medicine applications.

While our study provides valuable insights into the impact of topography on macrophage polarization, it is important to acknowledge the need for further validation and investigation. To ensure the reliability and reproducibility of our findings, the experiments should be repeated with various macrophage sources and across different experimental setups. To enhance the understanding of the observed effects on cell

phenotype, future studies should consider the simultaneous changes in both topography and composition while working with mineralized PCL experiments. Quantifiable characterizations of roughness and topography for the samples, in addition to SEM images, would provide more accurate insights into the effects of varying bicarbonate concentrations on mineral composition and surface mineral coverage. Moreover, additional *in vitro* assays, such as immunofluorescence staining and flow cytometry, could be employed to comprehensively assess the changes in gene expression profiles and protein levels following exposure to different topographical features. Furthermore, linking the nano and micro aspects of this study would benefit from addressing the compositional differences between nano- and micro-PCL surfaces. By conducting experiments that investigate the impact of these compositional differences, future research can provide a more comprehensive understanding of the interplay between topography and composition in influencing cell behavior. It is also crucial to recognize that macrophages exist on a continuum of activation states, and thus, a more comprehensive analysis of gene expression changes is required to uncover the complex interplay between topography and macrophage polarization. By employing a multifaceted approach, we can gain a deeper understanding of the topography-mediated modulation of macrophage behavior, which can ultimately lead to the development of more effective biomaterials for tissue engineering and regenerative medicine applications. Additionally, future studies should focus on elucidating the mechanisms underlying topography-mediated macrophage polarization and exploring the potential of three-dimensional biomaterials with topographical cues to modulate macrophage function and wound healing response.

Table 4.1. Primers used for qPCR

Cell Type	Gene	Sequence
RAW264.7	GAPDH	Forward: TGTCGTGGAGTCTACTGGTGTCTTC
		Reverse: CGTGGTTCACACCCATCACAA
RAW264.7	TNFα	Forward: TGGAACTGGCAGAAGAGG
		Reverse: AGACAGAAGAGCGTGGTG
RAW264.7	Arg1	Forward: TTGGGTGGATGCTCACACTG
		Reverse: TTGCCCATGCAGATTCCC
RAW264.7	CCL5	Forward: GCCCACGTCAAGGAGTATTTC
		Reverse: ACACACTTGGCGGTTCCTTC
Murine BMDM	GAPDH	Forward: TGTCGTGGAGTCTACTGGTGTCTTC
		Reverse: CGTGGTTCACACCCATCACAA
Murine BMDM	TNFα	Forward: TGGAACTGGCAGAAGAGG
		Reverse: AGACAGAAGAGCGTGGTG
Murine BMDM	Arg1	Forward: TTGGGTGGATGCTCACACTG
		Reverse: TTGCCCATGCAGATTCCC
Murine BMDM	CCL5	Forward: GCCCACGTCAAGGAGTATTTC
		Reverse: ACACACTTGGCGGTTCCTTC
Human-Derived macrophages	GAPDH	Forward: ACAACTTTGGTATCGTGGAAGG
		Reverse: GCCATCACGCCACAGTTTC
Human-Derived macrophages	IL1β	Forward: ATGATGGCTTATTACAGTGGCAA
		Reverse: GTCGGAGATTCGTAGCTGGA
Human-Derived macrophages	CD206	Forward: AAGGCGGTGACCTCACAAG
		Reverse: AAAGTCCAATTCCTCGATGGTG

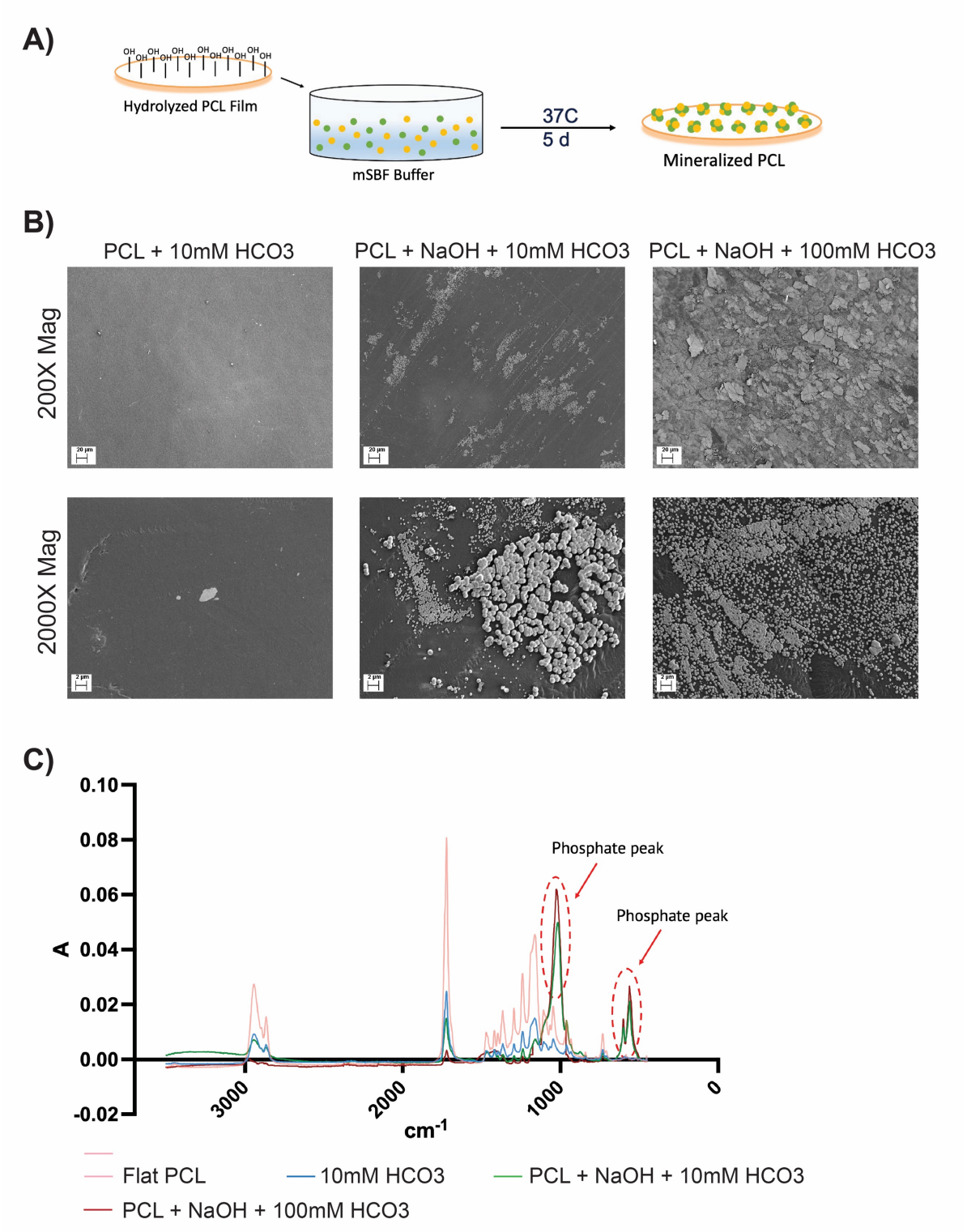

Figure 4.1. Characterization of mineralized PCL thin films fabricated using modified simulated body fluid (mSBF) with varying bicarbonate ion (HCO3) concentrations. (**A**) Hydrolyzed PCL films incubated in mSBF exhibit significant mineral layer growth on the

surface. (**B**) SEM images display minimal mineral formation on non-hydrolyzed PCL films, highlighting the importance of pre-treatment for mineral nucleation. Distinct morphological differences are observed based on mSBF HCO3 concentrations: 10 mM (low) exhibits dispersed spherical nanostructures, while 100 mM (high) shows complete surface coverage with plate-like structures composed of aggregated spherical nanostructures. (**C**) FTIR spectra confirm the SEM findings, with hydrolyzed PCL films incubated in mSBF exhibiting absorption bands corresponding to hydroxyapatite. The relative intensity of phosphate peaks at 564 and 1032 cm-1 and hydroxyl peaks ranging from 330 to 3650 cm-1 increase with higher HCO3 concentrations.

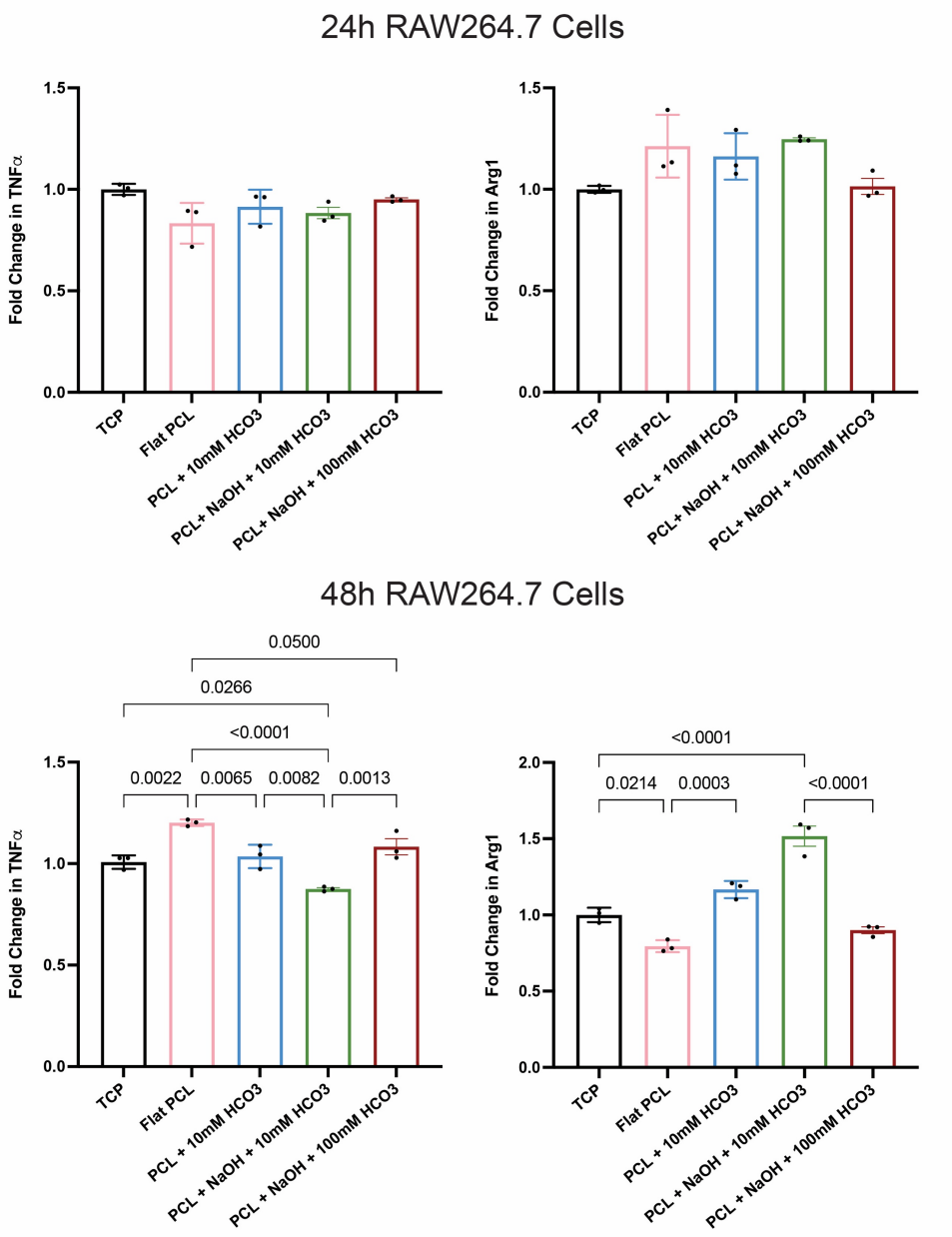

Figure 4.2. Evaluation of M1 and M2 macrophage marker expression on flat, 10 mM, and 100 mM mineralized PCL surfaces. TNFα (M1 marker) and Arg1 (M2 marker) expression

levels were assessed after 24 and 48 hours of culture. At the 24-hour time point, flat and mineralized PCL surfaces exhibited no notable differences in TNFα expression compared to TCP. However, after 48 hours, flat PCL surfaces displayed increased TNFα levels relative to TCP, whereas 10 mM mineralized PCL presented significantly reduced expression. Interestingly, 100 mM mineralized PCL showed decreased TNFα levels compared to flat PCL, aligning with TCP expression. Arg1 (M2 marker) expression significantly rose after 24 hours on 10 mM mSBF, exhibiting an inverse correlation between mSBF concentration and M2 expression increase.

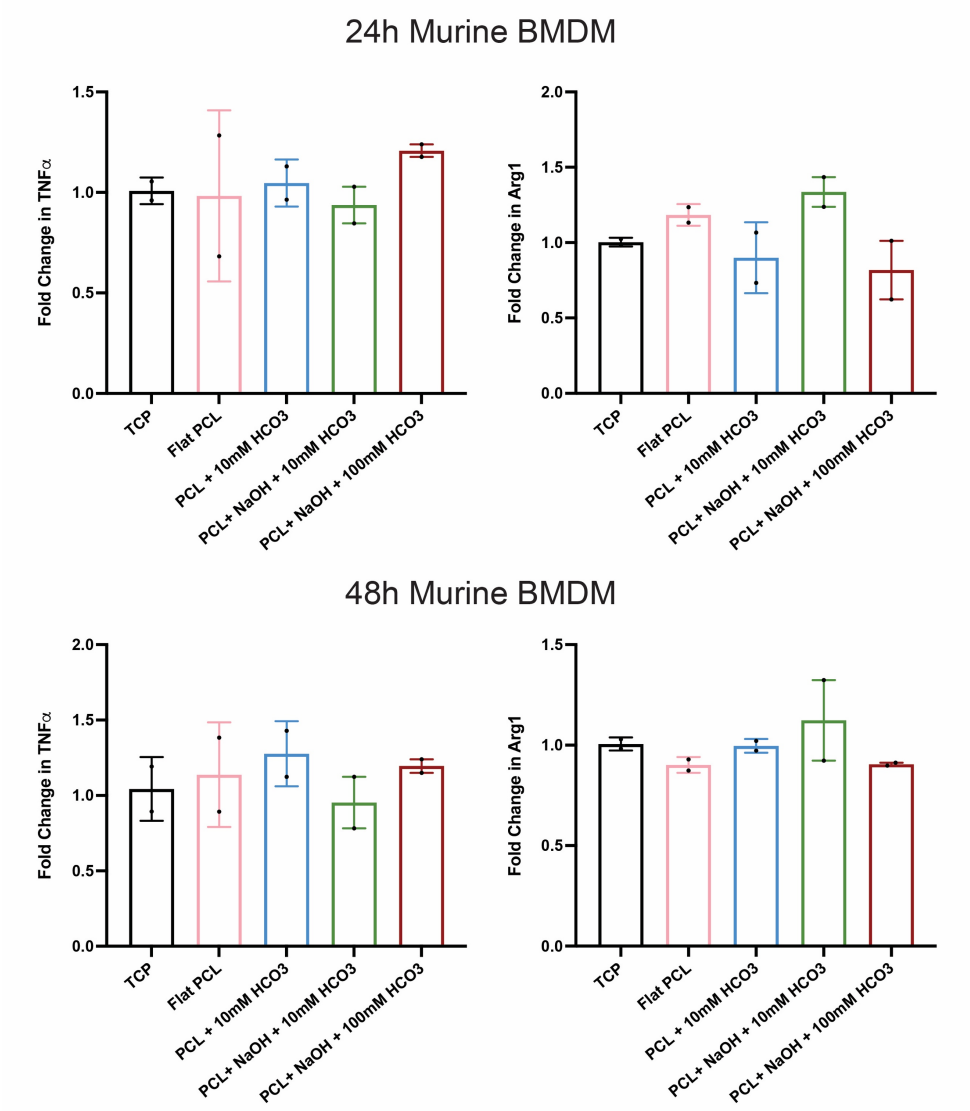

Figure 4.3. Changes in TNFα and Arg1 gene expression levels were quantified after 24- and 48-hour cultures of primary murine BMDMs on flat and mineralized PCL films. No significant changes were observed in TNFα and Arg1 expression levels, suggesting that the response to nanotopography may be cell type-dependent.

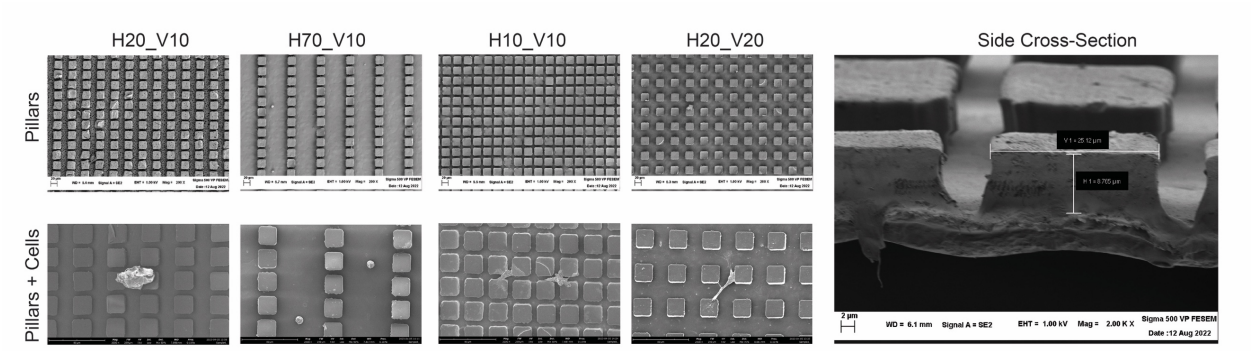

Figure 4.4. SEM imaging of topographic thin films and their effect on macrophage morphology. SEM images confirming the dimensions of the 10µm height and 25 µm diameter pillars with varying spacing between them. Macrophages cultured on H10_V10 and H20_V20 topographies exhibited an elongated morphology, with some cells extending and attaching to different pillars, as observed by SEM imaging. These results demonstrate the ability of pillar spacing to influence macrophage attachment and shape.

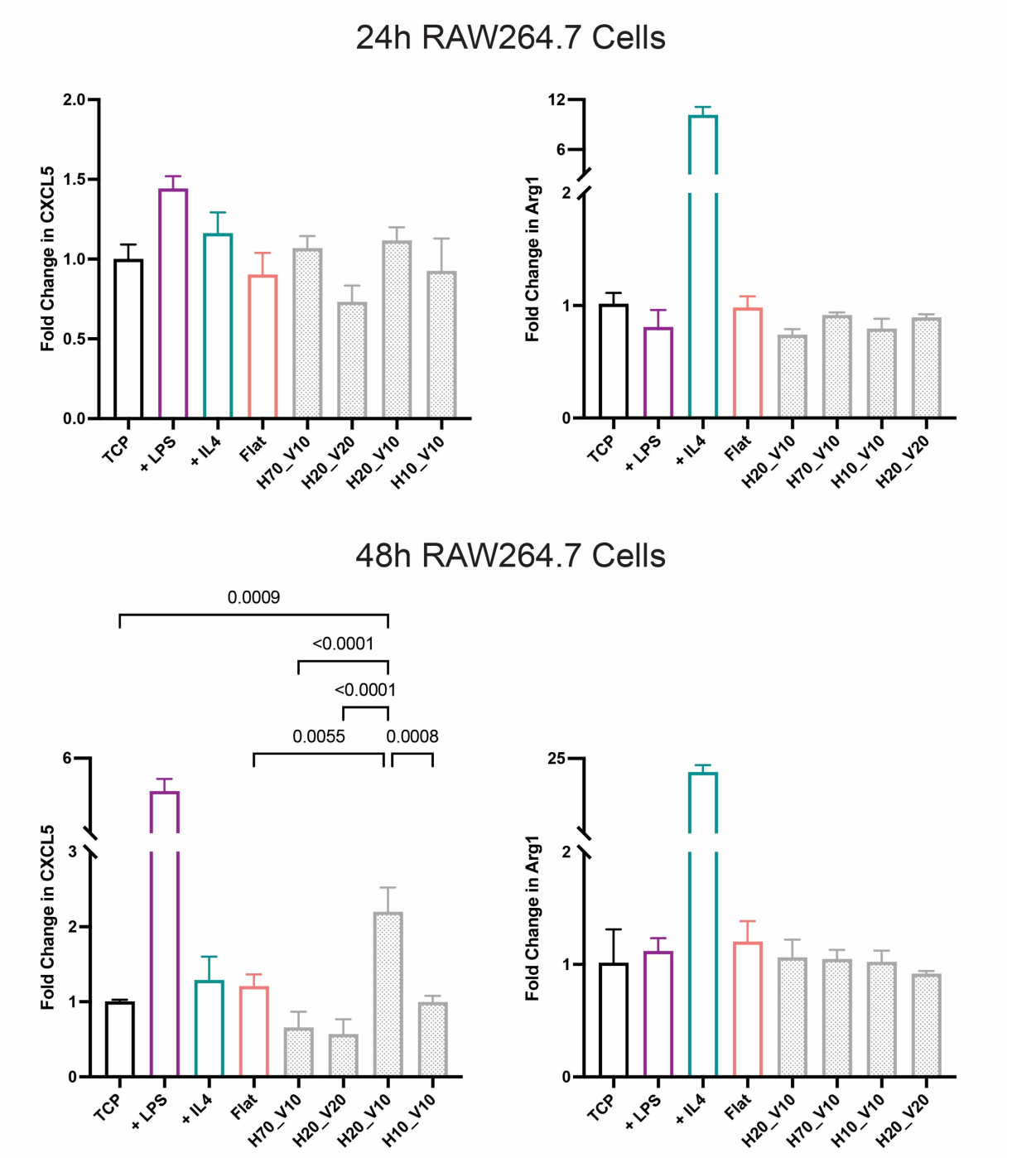

Figure 4.5. Impact of microtopographic PCL films on gene expression profiles in immortalized and primary macrophages. No alterations in CXCL5 (M1 marker) and Arg1 (M2 marker) expression levels were observed for RAW264.7 cells cultured on topographic and flat PCL films after a 24-hour incubation period. Following 48 hours of culture, a 2-fold upregulation of CXCL5 expression was detected in macrophages grown on H20_V10 pillars, while a 0.5-fold reduction was noted for H70_V10 and H20_V20 conditions. Arg1 expression remained unchanged across all experimental conditions after 48 hours.

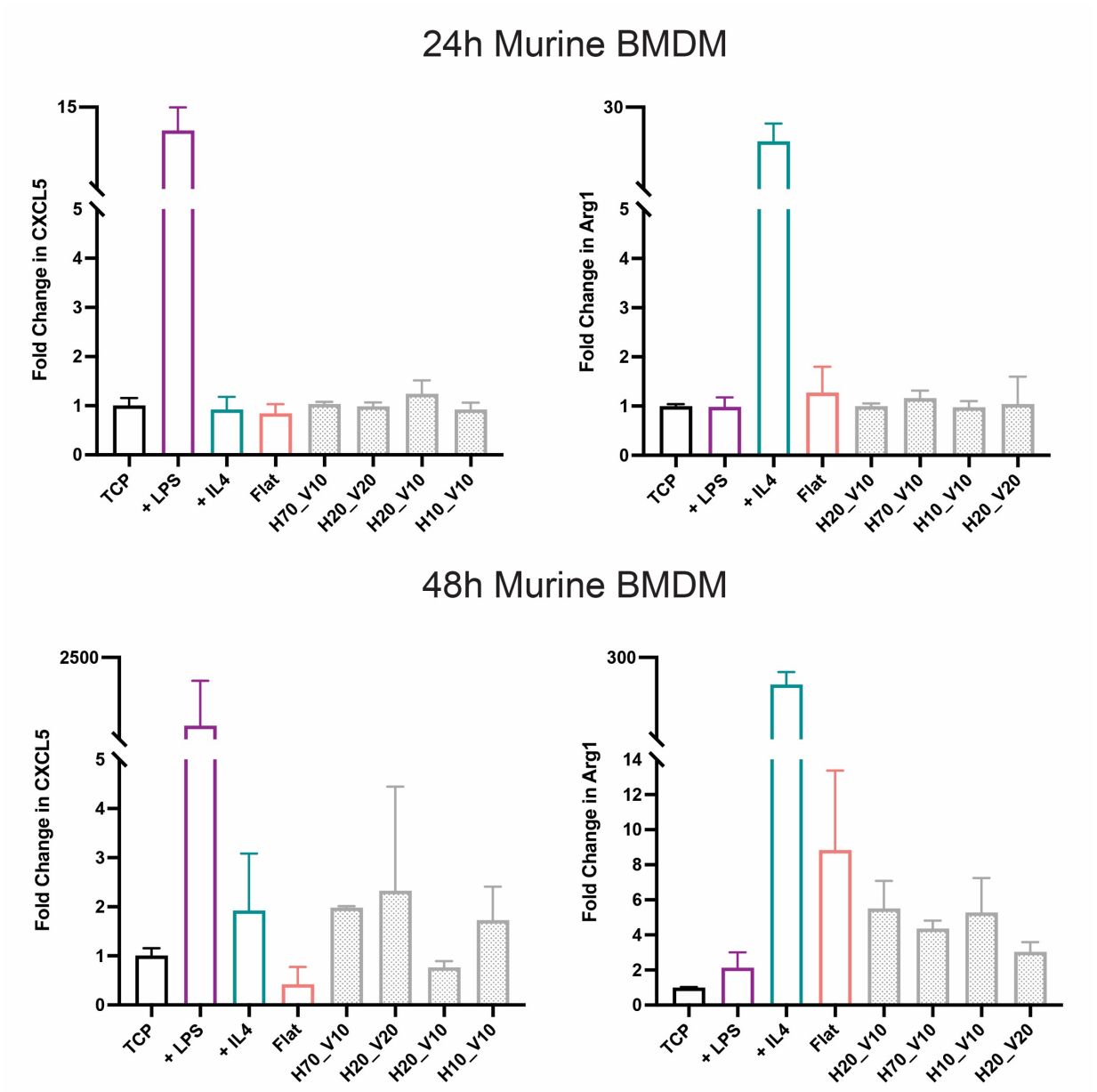

Figure 4.6. Differential gene expression profiles of murine BMDMs cultured on micron-scaled topographies. After 48 hours, all topographies, except H20_V10, demonstrated a significant increase in CXCL5 (M1 marker) expression, with levels elevated by at least two-fold. A nearly three-fold upregulation of Arg1 (M2 marker) expression was observed across all topographies. Remarkably, an eight-fold increase in Arg1 expression levels was found for macrophages cultured on flat PCL films, suggesting a potential role of PCL in promoting the reparative macrophage phenotype.

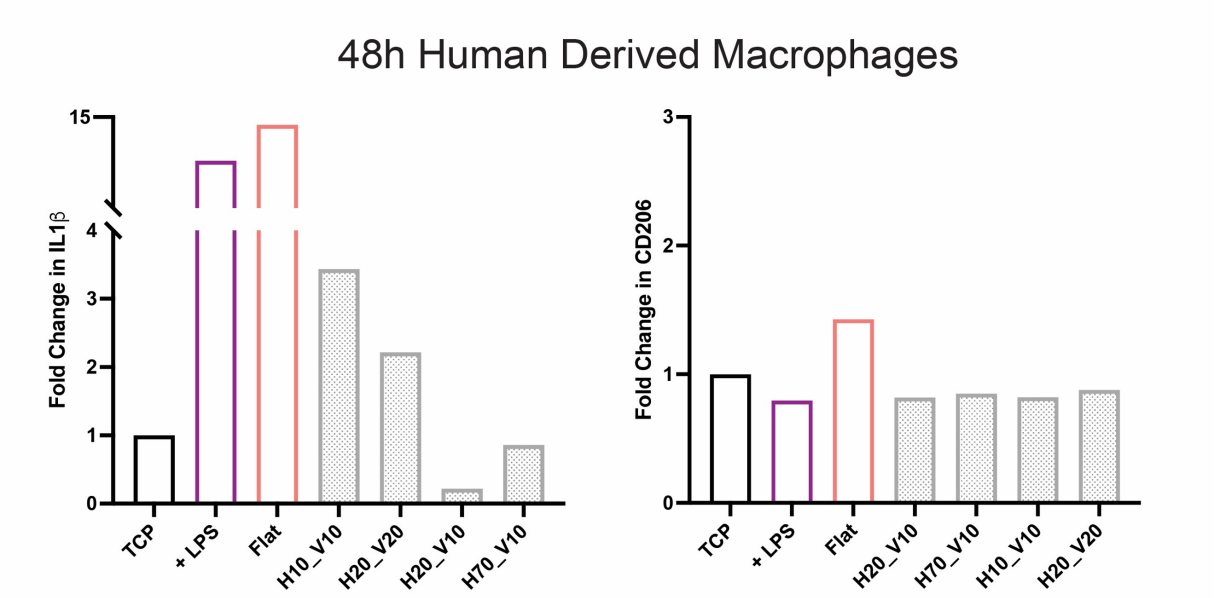

Figure 4.7. Comparative gene expression analysis of human-derived macrophages cultured on micron-scaled topographies. Following a 48-hour incubation period, all topographies, excluding H20_V10 and H70_V10, displayed a minimum two-fold upregulation in M1 expression levels, as evidenced by IL-1β. In contrast to murine BMDMs, human macrophages exhibited no alterations in M2 expression levels, denoted by CD206.

4.5 References

1. Atkinson MA, Eisenbarth GS, Michels AW. Type 1 diabetes. Lancet. Published online 2014. doi:10.1016/S0140-6736(13)60591-7.
2. Katsarou A, Gudbjörnsdottir S, Rawshani A, et al. Type 1 diabetes mellitus. Nat Rev Prim. Published online 2017. doi:10.1038/nrdp.2017.16.
3. Desai T, Shea LD. Advances in islet encapsulation technologies. Nat Rev Drug Discov. 2017;16(5):338-350. doi:10.1038/nrd.2016.232
4. Krishnan R, Alexander M, Robles L, Foster CE, Lakey JRT. Islet and stem cell encapsulation for clinical transplantation, Rev. Diabet Stud. 2014;11:84-101. doi:10.1900/RDS.2014.11.84.
5. An D, Chiu A, Flanders JA, et al. Designing a retrievable and scalable cell encapsulation device for potential treatment of type 1 diabetes. Proc Natl Acad Sci. 2018;115(2). doi:10.1073/pnas.1708806115
6. Goswami D, Domingo-Lopez DA, Ward NA, et al. Design Considerations for Macroencapsulation Devices for Stem Cell Derived Islets for the Treatment of Type 1 Diabetes. Adv Sci. 2021;8(16):2100820. doi:10.1002/advs.202100820
7. Farina M, Alexander JF, Thekkedath U, Ferrari M, Grattoni A. Cell encapsulation: Overcoming barriers in cell transplantation in diabetes and beyond, Adv. Drug Deliv Rev. 2019;139:92-115. doi:10.1016/j.addr.2018.04.018.
8. Kharbikar BN, Chendke GS, Desai TA. Modulating the foreign body response of implants for diabetes treatment. Adv Drug Deliv Rev. 2021;174:87-113. doi:10.1016/j.addr.2021.01.011

9. Desai TA, Tang Q. Islet encapsulation therapy — racing towards the finish line? Nat Rev Endocrinol. 2018;14(11):630-632. doi:10.1038/s41574-018-0100-7
10. Kharbikar BN, Mohindra P, Desai TA. Biomaterials to enhance stem cell transplantation. Cell Stem Cell. 2022;29(5):692-721. doi:10.1016/j.stem.2022.04.002
11. Anderson JM, Jiang S. Implications of the acute and chronic inflammatory response and the foreign body reaction to the immune response of implanted biomaterials. In: Immune Response to Implant. Mater. Devices Impact Immune Syst. Success an Implant. Springer International Publishing; 2016:15-36. doi:10.1007/978-3-319-45433-7_2.
12. Chung L, Maestas DR, Housseau F, Elisseeff JH. Key players in the immune response to biomaterial scaffolds for regenerative medicine, Adv. Drug Deliv Rev. 2017;114:184-192. doi:10.1016/j.addr.2017.07.006.
13. Franz S, Rammelt S, Scharnweber D, Simon JC. Immune responses to implants - A review of the implications for the design of immunomodulatory biomaterials, Biomaterials. Published online 2011. doi:10.1016/j.biomaterials.2011.05.078.
14. Ward WK. A review of the foreign-body response to subcutaneously-implanted devices: The role of Macrophages and cytokines in biofouling and fibrosis. J Diabetes Sci Technol. 2008;2:768-777. doi:10.1177/193229680800200504.
15. Chandorkar Y, Ravikumar K, Basu B. The Foreign Body Response Demystified. ACS Biomater Sci Eng. 2019;5:19-44. doi:10.1021/acsbiomaterials.8b00252.
16. Darnell M, Mooney DJ. Leveraging advances in biology to design biomaterials. Nat Mater. 2017;16(12):1178-1184. doi:10.1038/nmat4991

17. Stabler CL, Li Y, Stewart JM, Keselowsky BG. Engineering immunomodulatory biomaterials for type 1 diabetes. Nat Rev Mater. doi:10.1038/s41578-019-0112-5.
18. Carver W, Esch AM, Fowlkes V, Goldsmith EC. The biomechanical environment and impact on tissue fibrosis. In: The Immune Response to Implanted Materials and Devices: The Impact of the Immune System on the Success of an Implant. Springer International Publishing; :169-188. doi:10.1007/978-3-319-45433-7_9.
19. McWhorter FY, Davis CT, Liu WF. Physical and mechanical regulation of macrophage phenotype and function. Cell Mol Life Sci CMLS. 2015;72(7):1303-1316. doi:10.1007/s00018-014-1796-8
20. McWhorter FY, Wang T, Nguyen P, Chung T, Liu WF. Modulation of macrophage phenotype by cell shape. Proc Natl Acad Sci. 2013;110(43):17253-17258. doi:10.1073/pnas.1308887110
21. Chen S, Jones JA, Xu Y, Low HY, Anderson JM, Leong KW. Characterization of topographical effects on macrophage behavior in a foreign body response model. Biomaterials. 2010;31(13):3479-3491. doi:10.1016/j.biomaterials.2010.01.074
22. Kam KR, Walsh LA, Bock SM, Ollerenshaw JD, Ross RF, Desai TA. The effect of nanotopography on modulating protein adsorption and the fibrotic response. Tissue Eng Part A. 2014;20(1-2):130-138. doi:10.1089/ten.TEA.2012.0772
23. Luu TU, Gott SC, Woo BWK, Rao MP, Liu WF. Micro and Nano-patterned Topographical Cues for Regulating Macrophage Cell Shape and Phenotype. ACS Appl Mater Interfaces. 2015;7(51):28665-28672. doi:10.1021/acsami.5b10589

24. Schmitz T, Jannasch M, Weigel T, et al. Nanotopographical Coatings Induce an Early Phenotype-Specific Response of Primary Material-Resident M1 and M2 Macrophages. Materials. 2020;13(5):1142. doi:10.3390/ma13051142
25. Bachhuka A, Madathiparambil Visalakshan R, Law CS, et al. Modulation of Macrophages Differentiation by Nanoscale-Engineered Geometric and Chemical Features. ACS Appl Bio Mater. 2020;3(3):1496-1505. doi:10.1021/acsabm.9b01125
26. Robotti F, Bottan S, Fraschetti F, et al. A micron-scale surface topography design reducing cell adhesion to implanted materials. Sci Rep. 8:10887. doi:10.1038/s41598-018-29167-2.
27. Bartneck M, Schulte VA, Paul NE, Diez M, Lensen MC, Zwadlo-Klarwasser G. Induction of specific macrophage subtypes by defined micro-patterned structures. Acta Biomater. 2010;6(10):3864-3872. doi:10.1016/j.actbio.2010.04.025
28. Bota PCS, Collie AMB, Puolakkainen P, et al. Biomaterial topography alters healing in vivo and monocyte/macrophage activation in vitro. J Biomed Mater Res A. 2010;95(2):649-657. doi:10.1002/jbm.a.32893
29. Nyitray CE, Chang R, Faleo G, et al. Polycaprolactone Thin-Film Micro- and Nanoporous Cell-Encapsulation Devices. ACS Nano. 2015;9(6):5675-5682. doi:10.1021/acsnano.5b00679
30. Chang R, Faleo G, Russ HA, et al. Nanoporous Immunoprotective Device for Stem-Cell-Derived β-Cell Replacement Therapy. ACS Nano. 2017;11(8):7747-7757. doi:10.1021/acsnano.7b01239

31. Chendke GS, Faleo G, Juang C, et al. Supporting Survival of Transplanted Stem-Cell-Derived Insulin-Producing Cells in an Encapsulation Device Augmented with Controlled Release of Amino Acids. Adv Biosyst. 2019;3(9):1900086. doi:10.1002/adbi.201900086
32. Suárez-González D, Barnhart K, Migneco F, Flanagan C, Hollister SJ, Murphy WL. Controllable mineral coatings on PCL scaffolds as carriers for growth factor release. Biomaterials. 2012;33(2):713-721. doi:10.1016/j.biomaterials.2011.09.095
33. Mosser DM, Edwards JP. Exploring the full spectrum of macrophage activation. Nat Rev Immunol. 2008;8(12):958-969. doi:10.1038/nri2448

Chapter 5. Conclusions and Perspectives

This thesis provides a comprehensive analysis of the challenges faced by cell encapsulation devices for T1D treatment, particularly focusing on the FBR and its subsequent effects on cell survival, vasculature, and inflammation. Through the development of nutrient-supplementing devices, pre-vascularization techniques, and tailoring biomaterial properties, we demonstrate significant progress in enhancing the performance and long-term success of cell encapsulation devices for T1D management.

This work demonstrates two significant advancements in improving the survival of encapsulated cells within the subcutaneous space. The nutrient-releasing reservoir, as described in Chapter 2, effectively increases cell survival by 30% in the poorly vascularized subcutaneous space by providing a steady supply of essential nutrients to the encapsulated cells. Furthermore, the novel RPVIM approach presented in Chapter 3 demonstrates a remarkable increase in cell survival, reaching up to 75% after 28 days of implantation. These results highlight the potential of combining innovative strategies to enhance the performance of cell encapsulation devices.

However, there is still room for improvement in achieving near-complete cell survival. As discussed in Chapter 4, the impact of surface topography on macrophage polarization and the immune response can be further explored to optimize the design of encapsulation devices. Future studies should investigate the integration of topographic features into the encapsulation devices to modulate the immune response and promote reparative macrophage phenotypes, potentially bringing cell survival closer to 100%. By combining the successful approaches of nutrient-releasing reservoirs, pre-vascularization techniques, and topographic modifications, a path can be paved towards highly effective

cell encapsulation devices that ensure optimal engraftment and function in the treatment of T1D.

While the results presented in this thesis are encouraging, some areas require further investigation and development for the successful translation of these findings into clinical practice. Future research should be directed towards the following aspects:

1. Long-term studies and *in vivo* testing with immunocompetent mice: It is crucial to conduct long-term *in vivo* studies to evaluate the durability and performance of the developed encapsulation devices, focusing on their ability to maintain functionality and prevent adverse immune responses over extended periods. Since all the studies have been performed with NSG mice, it is essential to test the devices in immunocompetent mice to assess their performance in a more clinically relevant setting.
2. Diabetic mouse model testing: To better understand the immune response and subsequent device engraftment in the disease state, it would be beneficial to test the devices long-term in a diabetic mouse model. This approach will help determine the potential impact of the disease on the encapsulation devices and identify any unforeseen challenges that may arise in a diabetic environment.
3. Integration with other therapeutic approaches: As mentioned previously, combining cell encapsulation devices with other treatment strategies, such as immunomodulatory therapies, tailoring surface topography of biomaterials, and pre-vascularization techniques, could potentially enhance the overall efficacy of T1D management.

4. Scalability and manufacturing: To bring these devices to clinical use, it is essential to establish efficient, scalable, and cost-effective manufacturing processes that can produce consistent and reliable encapsulation devices. However, challenges exist in fabricating large-scale topographic devices, manufacturing stem-cell derived insulin-producing cells, and executing a two-step approach for prevascularizing, like RPVIM, in patients. Addressing these challenges will be crucial in translating the research findings into practical applications for T1D treatment.

In conclusion, this thesis contributes to addressing the challenges associated with cell encapsulation devices for T1D treatment, particularly focusing on the foreign body response and fibrosis. By investigating and modulating these factors, a foundation has been laid for the development of more effective and durable encapsulation devices. As knowledge advances and these technologies are refined, progress toward providing a transformative solution for individuals living with T1D can be achieved.

By addressing the aforementioned areas and fostering interdisciplinary collaboration and innovation, the groundwork is established for a future where cell encapsulation devices become a standard, effective, and long-lasting treatment option for T1D patients, ultimately improving their quality of life and disease management.

Publishing Agreement

It is the policy of the University to encourage open access and broad distribution of all theses, dissertations, and manuscripts. The Graduate Division will facilitate the distribution of UCSF theses, dissertations, and manuscripts to the UCSF Library for open access and distribution. UCSF will make such theses, dissertations, and manuscripts accessible to the public and will take reasonable steps to preserve these works in perpetuity.

I hereby grant the non-exclusive, perpetual right to The Regents of the University of California to reproduce, publicly display, distribute, preserve, and publish copies of my thesis, dissertation, or manuscript in any form or media, now existing or later derived, including access online for teaching, research, and public service purposes.

DocuSigned by:
Gaurie Chandke
951C971689AE4EF...
Author Signature

5/11/2023
Date